CONTENTS

Abbreviations

AFU	**:**	**Arbitrary fluorescent unit**
CBB	**:**	**Coomassie brilliant blue**
cDNA	**:**	**Complimentary DNA**
CNBr	**:**	**Cyanogen bromide**
DAB	**:**	**3′,3′-Diaminobenzidine**
DAPI	**:**	**4′,6-diamino-2-phenylindole**
dsRNA	**:**	**Double stranded RNA**
EDTA	**:**	**Ethylenediaminetetraacetic acid**
EGTA	**:**	**Ethylene glycol tetraacetic acid**
EST	**:**	**Expressed sequence tag**
E64d	**:**	***trans*-epoxysuccinyl-L-leucinamido-(4-guanidino) butane**
EVGS	**:**	**Elastica-van Gieson stain**
FCA	**:**	**Freund's Complete Adjuvant**
FIA	**:**	**Freund's Incomplete Adjuvant**
H & E	**:**	**Hematoxylin and eosin**
IgG	**:**	**Immunoglobulin G**

IPTG	**:**	**Isopropyl-β-D-thiogalactopyranoside**
LongEFd	**:**	**EF-hand domain of longistatin**
mRNA	**:**	**Messenger RNA**
MBR	**:**	**Molar binding ratio**
MCA	**:**	**Amidomethylcoumarin**
ORF	**:**	**Open reading frame**
PA	**:**	**Plasminogen activator**
PAI	**:**	**Plasminogen activator inhibitor**
PBS	**:**	**Phosphate buffered saline**
PCR	**:**	**Polymerase chain reaction**
RT-PCR	**:**	**Reverse transcription-polymerase chain reaction**
qRT-PCR	**:**	**Quantitative RT-PCR**
PMSF	**:**	**Phenylmethanesulfonyl fluoride**
PPP	**:**	**Platelet-poor plasma**
PRP	**:**	**Platelet-rich plasma**
RNAi	**:**	**RNA interference**
dsRNA	**:**	**Double stranded RNA**
Serpin	**:**	**Serine protease inhibitor**
SDS-PAGE	**:**	**Sodium dodecyl sulfate polyacrylamide gel electrophoresis**
TBS-T	**:**	**Tris buffer saline-Tween20**
t-PA	**:**	**Tissue-type plasminogen activator**
u-PA	**:**	**Urokinase-type plasminogen activator**
tcu-PA	**:**	**Two chain u-PA**

Unit abbreviations

h	**:**	**hour(s)**
M	**:**	**mol**
mM	**:**	**millimol**
µM	**:**	**micromol**
nM	**:**	**nanomol**
ml	**:**	**milliliter**
µl	**:**	**microliter**
mg	**:**	**milligram**
µg	**:**	**microgram**
ng	**:**	**nanogram**
Da	**:**	**dalton**
kDa	**:**	**kilodalton**
bp	**:**	**base pair**

General introduction

Ticks are eight-legged arthropods belonging to the order Ixodida and superfamily Ixodoidea. They are broadly classified into three families such as Ixodidae (hard ticks), Argasidae (soft ticks) and Nuttalliellidae. Among them, ixodid ticks or hard ticks comprise nearly 80% of the known tick's species (683 species of hard ticks) of the world. Ticks are distributed throughout the world from sub-arctic through equatorial zones to Antarctic regions, and their habitats range from desert to rainforest. Although totally there are about 907 tick species but their economic importance is variable, and different tick species are dominant in different parts of the globe (1−4). The most important genera of hard ticks are *Amblyomma*, *Dermacentor*, *Haemaphysalis*, *Hyalomma*, *Ixodes* and *Rhipicephalus* (5). Recently, the genus *Boophilus* has been placed into the genus *Rhipicephalus*. In Asia, *Rhipichephalus* (*Boophilus*) *microplus* is a common tick fauna especially throughout the tropical areas. Also, ticks of the genera *Hyalomma, Amblyomma, Ixodes* and *Haemaphysalis* are prevalent in this continent (6−8). Among *Haemaphysalis* ticks, *H. bispinosa* is prevalent in Indian subcontinent, and *H. longicornis* is widely distributed in many countries from the Far East to Australia (6, 7). In Japan, *H. longicornis* is the most commonly occurring tick but *H. flava*, *H. hystricis*, *H. campanulata*, *H. japonica*, *H. ias*, *R. sanguineus*, *I. persulcatus*, *I. nipponensis* and *A. testudinarium* have also been recorded (8). Of the ticks recorded in Japan, *H. longicornis* is very important since it acts as a vector of many bacterial, viral, protozoan and rickettsial diseases (9). Among the diseases babesiosis, anaplasmosis, theileriosis

and Q fever have both veterinary and medical importance. These maladies are associated with human suffering, and are a major constraint to animal production as they may cause morbidity or mortality in affected animals (10, 11). *H. longicornis* is now used as a leading model tick in the field of tick research.

Ticks themselves are very harmful, and have a great economic importance simply due to the damages and problems directly induced by them. Ticks can cause severe irritation and allergy; thus, deteriorate health and reduce productivity. Damages caused by tick bites, especially during massive infestation, also diminish the value of hides and skins. Additionally, the saliva of certain tick species can induce paralysis, tick toxicosis or sweating sickness in various animals including humans (5, 12−14). Moreover, another dimension of tick related problem is the severe bovine dermatophilosis, which is induced by the presence of adult *A. varieganum*, however, the causative pathogen is not transmitted by the tick (5). It has been estimated that about 80% cattle of the world are infested with ticks; thus, ticks are the most economically important ectoparasites for global livestock production (5, 15). In addition to the direct adverse effects on health and productivity, ticks serve as unique vectors of many important diseases inflicting humans and animals. Ticks are prevalent from the ancient period of time and their existence has been recorded in an Egyptian papyrus scroll dated 1550 B.C. Although early scholars were familiar with ticks and damages caused by ticks but the vector potential of ticks and the magnitude of the tick-related problems were well understood at the end of the nineteenth century with the historic discovery of Smith and Kilborne (1893) that the Cattle tick (*Boophilus*) transmits babesiosis, a protozoan disease, which is also known as Texas fever/tick fever/red water fever. In fact, the Cattle tick was identified as a vector of the infectious disease before the malarial vector mosquito. This historic work was followed by a series of discoveries that ticks also transmit many deadly pathogens such as bacteria, viruses, rickettsiae, protozoa and even helminths (16−20). Now, it is well established that ticks serve as an important vector of various diseases, such as Lyme disease, tick-borne encephalitis,

Rocky Mountain spotted fever, babesiosis, theileriosis, anaplasmosis, Heartwater (cowdriosis), Crimean-Congo Hemorrhagic fever, Omsk Hemorrhagic fever, Colorado tick fever, Kyasanur forest disease, African swine fever, Nairobi sheep disease, tick-borne relapsing fever and Tularaemia. Indeed, ticks are only second to mosquitoes as vectors of diseases of humans and animals (10, 11, 21−24). It has been estimated that ticks cause about US$ 200 and 175 million loss per year in USA and Australia, respectively, and an estimated loss of about US$ 7000 million/year globally. In Australia, tick is considered as the "number one" problem in livestock production (5). Therefore, sustainable livestock production for the fulfillment of protein requirements is not possible without active tick and tick-borne disease control programs.

People have been trying to control ticks since long before to minimize the losses caused directly by ticks themselves and the diseases transmitted by them. Many tick control programs have been launched to counteract the adverse effects of ticks and also to eradicate tick-borne diseases. Those programs were mainly conducted on the basis of the use of chemical acaricides. Among the chemical acaricides, arsenic compounds were used in the early 1900s. Organo-chlorine compounds were introduced during the years of 1945−55 when *Boophilus* ticks developed resistance to arsenicals in different countries. Therefore, organo-phosphorous compounds and carbamate were incorporated into the tick control programs in the 1955−70 period followed by the use of formamidines and related chemicals after 1970. However, due to repeated use of acaricides, resistance develops frequently in ticks (25−27). Additionally, chemical acaricides are very hazardous for human and animal health as they have direct toxic effect. Besides, because of their residual effects, they are not environmentally friendly and also cause contamination of foods, especially, milk and meat (5). These obstacles in controlling ticks with chemical acaricides have created an acute need for the development of a sustainable alternative method of control. Alternative approaches include genetic control, by developing tick resistant cattle bread; biological control, by using natural enemies or pathogens of ticks (eg. parasitoid, bacteria and fungi), and

anti-tick vaccines (28, 29). Development of tick resistant bread preserving other desirable production characteristics is difficult since ticks, although have some host preference, are not strictly host specific and a single animal is susceptible to different species of ticks. On the other hand, biological means alone, although may be used as a part of integrated pest managements, is not potent enough to control ticks because lifecycle of ticks is very complex. Ticks can affect a wide array of animals from small, wild rodents to livestock and even humans. Also, ticks of many species can pass a long period of time off the host without blood-meals (30−33). In contrast, anti-tick vaccine (immunization of host with antigens derived from ticks, when ticks imbibe blood from immunized host then the antibody is expected to exert its function; thus, the anti-tick vaccine affects feeding, breading and survival of ticks) has the potential to be a non-contaminating, sustainable, cost-effective and environmentally sound technique, which is potentially applicable to a wide variety of hosts. In fact, partial to strong immunity to tick can be induced by vaccinating animals with a variety of antigenic materials, including whole tick homogenates, salivary gland extracts, ticks internal organs (mainly gut materials as a cocktail of concealed antigens), cement materials and so on (34−38). Although the idea of controlling ticks by vaccination has been conceived about 80 years ago but progress in the development of effective anti-tick vaccines is very slow. Yet today, only *Rhipicephalus* (*Boophilus*) *microplus*-86 kDa protein (Bm86, a midgut antigen) based vaccines (TickGARD® and Gavac®) have been developed and commercially available, and are being successfully used in controlling *R. microplus* ticks but these vaccines are not effective against all ticks. Besides, these vaccines are primarily effective against adult stage, and efficacy is also variable (85.2−99.6%) against *R. microplus* from different geographical locations (29, 39−42). Virtually, this area of tick control is still in an initial step and warrant a lot of research efforts. Therefore, identification and characterization of potential bioactive molecules from ticks, which are essential for their feeding and survival strategies, are of considerable interest.

Blood-feeding is an essential biologic phenomenon for the survival of hard ticks. Ticks

live entirely on the nutrients derived from host's blood (43−45). These ectoparasites firmly attach to hosts' skin using their deeply penetrating mouthparts, and suck blood. Ticks are pool feeder and their blood-feeding mechanism is very complex and quite different from that of vessel feeder hematophagous insects. Hematophagous insects like mosquitoes suck blood directly from the blood vessels within a couple of seconds but the hard ticks feed on blood-meals for a long time (5−10 days or more depending on the species of tick) making a large blood pool beneath the host's skin. In fact, their mouthparts are adapted for grasping, holding, tearing and crushing. Extensive laceration of tissues is the characteristic of tick's feeding. Ticks can not canulate individual blood vessels (22). Thus, development of blood pool is a prerequisite to the feeding of blood-meal by ticks. Although size of the blood pool produced by different species of ticks varies but it is an essential feature in the feeding mechanism of ticks (44, 45). Blood pools contain copious unclotted blood and exudates, especially in the rapid phase of feeding (45, 47). However, fact is that, when a hematophagous animal probes to ingest blood then tissue is damaged, which induces activation of platelets and causes vasoconstriction leading to the initiation of clotting cascades. This type of host's response occurs within seconds (46). To battle against the hemostatic effects of hosts, hematophagous animals, like ticks (46, 47), tsetse flies (48), mosquitoes (49), black flies (50), kissing bugs (51), leeches (52), and vampire bats (53) secret anticoagulant with their saliva. Since hard ticks (eg. *H. longicornis*) feed blood for several days; they have to combat continuously for a long time against host's hemostatic mechanism at the site of wound as well as within the gut. It is of current interest to look at the molecular scenario inside the blood pool that maintains a large volume of unclotted blood underneath the skin. Prior studies suggest that hard ticks, the smart pharmacologists, produce a vast array of pharmacologically active biomolecules that are injected into the feeding lesions during persistent blood-feeding processes, which play crucial modulatory roles in their feeding success, especially to keep the blood in a fluid state (47, 54−57). Saliva of ticks is a complex mixture of different types of enzymes, inhibitors and other proteins or

nonproteinaceous substances. Several proteases have been identified and characterized from tick sialome (47, 54, 56, 58). However, the key molecule(s) that specifically prevents blood coagulation and initiates fibrinolysis in the blood pool to facilitate successful acquisition of blood-meals is yet to be identified.

Proteases are a group of enzymes, which cause hydrolysis of proteins and peptides. Functionally, proteases are classified into four classes: serine, cysteine, aspartic and metallo-proteases (59). Among them, serine proteases comprise nearly one-third of all known proteases (60). Classical serine proteases use the canonical Ser/His/Asp catalytic triad to hydrolyze substrates (61), and the members of the triad are located in well-conserved regions. The consensus sequence for Ser is 'GX**S**XG' and those of His and Asp are 'LSAS**H**C' and 'SXLL**D**DGLX(2-3)D', respectively (62). However, in unconventional serine proteases, this general architecture is absent. In addition to their own functional motif/domain, proteases contain different types of accessory structures or motifs, such as Ca^{2+}-binding motifs (63), Zn^{2+}-binding motifs (64) or motifs specific for interacting with inhibitors or other molecules (65, 66).

EF-hand motif (motif composed of two helices known as E and F joined by a loop), the main Ca^{2+}-binding motif, was first discovered by R. H. Kretsinger over three decades ago through the structural analysis of parvalbumin, a tiny Ca^{2+}-binding protein isolated first from carp muscle (67). EF-hand motif is also known as a helix-loop-helix motif. The calcium-incorporating loop region of a canonical EF-hand consists of 12 residues that usually starts with an aspartic acid and essentially ends with a glutamic acid (67, 68). However, in unconventional EF-hands, the number of amino acids in the loop region may vary from 11−14 residues. Although EF-hand motif usually occurs in pairs, alpha and beta parvalbumin have three EF-hands, while grancalcin, calpain and ALG-2 have five EF-hands (68) and, more exceptionally, a few Ca^{2+}-binding proteins have one EF-hand (69). A group of EF-hand proteins contain 4 EF-hand motifs (calmodulin and troponin C) but some Ca^{2+}-binding proteins contain six, eight or even 12 EF-hand motifs (68). On the other hand,

smaller EF-hand proteins, such as S100 proteins, osteonectin and multiple coagulation factor deficiency 2 like protein (MCFD2), possess two EF-hand motifs (68, 70). Generally, EF-hand Ca^{2+}-binding motifs act as calcium signaling molecules and/or buffers in the cytosol of the cell (63, 71, 72). However, some Ca^{2+}-binding proteins such as S100A2, S100A6 and S100B are present in the nucleus, where they control gene expression (70, 73). In a few exceptional cases, EF-hand Ca^{2+}-binding proteins are secreted from the cells and exert critical roles extracellularly (63, 70, 74).

In the present study, I have identified and characterized a novel protein from salivary glands of *H. longicornis* and named this protein longistatin. Longistatin is a 17.8-kDa soluble protein. It contains two calmodulin-like functional EF-hand domains at the C-terminus. Longistatin is secreted from salivary glands and injected into the host tissues. Longistatin is upregulated with the feeding process of blood-meal from host animals. Longistatin does not contain any conserved canonical catalytic triad specific for serine proteases but still it hydrolyzes several serine protease specific synthetic substrates showing affinity towards the amide bonds derived from Arg. Longistatin is inhibited by various commercially available serine protease inhibitors and Zinc (Zn^{2+}). Longistatin degrades fibrinogen and activates plasminogen; thus, exerts pivotal roles in the feeding mechanisms of ticks by maintaining the fluidity of blood during the acquisition of blood-meals from hosts. Another novelty is that longistatin is resistant to the inhibitory effects of the plasminogen activator inhibitor-1 (PAI-1). Longistatin is the first plasminogen activator identified and characterized from ticks.

Chapter 1

Identification of an EF-hand protein from the salivary glands of the ixodid tick, *Haemaphysalis longicornis*

1. Introduction

The EF-hand Ca^{2+}-binding motif, the helix-loop-helix motif, is one of the most common motifs found in the animal genome. EF-hand proteins, the proteins with EF-hand Ca^{2+}-binding motifs, are widely distributed throughout the cells. EF-hand proteins and calcium (Ca^{2+}) are essential for life since they control substantial parts of cell functions, starting from the cell's birth, through mitosis to its end with apoptosis (75, 76). Almost every function of our body, such as heartbeat, breathing, vision, locomotion, thinking and memory processing, is controlled by Ca^{2+} (70, 75, 76). Calcium is the major secondary messenger involved in many cellular and extracellular functions. Cells respond to extra-cellular stimuli through the transient change in Ca^{2+} concentration. This signal transduction is sensed by Ca^{2+}-binding proteins. Usually, EF-hand proteins play their critical roles as calcium signaling molecules and/or buffers within the cell (63, 71, 72) but some EF-hand Ca^{2+}-binding proteins also play critical functions extracellularly such as extracellular matrix remodeling and neuronal plasticity at the synaptic junctions (63, 70). Extracellular Ca^{2+}-binding proteins are present in the extracellular space in their Ca^{2+}-bound form;

thus, the proteins are protected against proteolytic cleavage (72). Usually EF-hand proteins do not contain (except osteonectin, so far studied) disulfide bridges. Therefore, EF-hand domains are very important in stabilizing structure and right conformation of the proteins. In addition, extracellular EF-hand proteins, especially extracellular S100 proteins, bind with RAGE (receptor for advanced glycation end products) and regulate synthesis of pro-inflammatory cytokines and mediate metastasis of tumor cells (71, 72). EF-hand proteins have been reported from a wide spectrum of organisms from unicellular, simple prokaryotes to multi-cellular, complex mammals (71), and more than 600 Ca^{2+}-binding proteins have been discovered (73).

Here, I have identified and cloned a full-length cDNA from salivary glands of the ixodid tick, *H. longicornis*, which encodes a protein containing two functional EF-hand Ca^{2+}-binding domains. The protein has been named as longistatin. I show that longistatin is secreted from the salivary glands and injected into host tissues during acquisition of blood-meal. Longistatin is able to bind calcium. In this chapter, I also demonstrate that longistatin may function in the feeding processes of blood-meals from host animals since the expression of *longistatin*-specific transcript is upregulated with the feeding of ixodid ticks. Longistatin is the first characterized EF-hand protein isolated from the salivary glands of ticks.

2. Materials and Methods

2.1. Ticks and animals

Parthenogenetic Okayama strain of *Haemaphysalis longicornis* were propagated at the Laboratory of Parasitic Diseases, National Institute of Animal Health (NIAH), Tsukuba, Japan, by feeding on the ear of the tick-naïve, specific pathogen-free (SPF) Japanese White rabbits according to the methods described previously (77) to obtain different lifecycle stages of ticks at different feeding intervals. Briefly, the ears of rabbits were cleaned by hair clipping; ticks were placed on the ears and given support with ear bags and an Elizabethan collar. Ear bags were changed at 24 h

intervals. Ticks were collected after detachment following full engorgement or after the indicated period of feeding. Rabbits used in these experiments were acclimatized to the experimental laboratory conditions for 2 weeks prior to the commencement of the experiments. Animal care was conducted according to the protocols approved by the Animal Care and Use Committee, NIAH (Permit Numbers: 09-017, 09-018, 10-008, 10-010). All surgeries were performed under sodium pentobarbital anesthesia, and all efforts were made to minimize the animals' suffering.

2.2. Cloning and sequencing of longistatin cDNA

The gene coding for longistatin was identified from the expressed sequence tags (ESTs) constructed from the salivary gland cDNA libraries of *H. longicornis* following the methods described previously (78). Briefly, the plasmid containing the gene coding for longistatin was extracted using the Qiagen DNA Purification kit (QIAGEN Science, Germantown, MA, USA). The nucleotide sequences of the cDNA were determined using the big dye terminator method on an ABI PRISM 3100 automated sequencer (Applied Biosystem, Foster City, CA, USA). The GENETYX-WIN DNA analysis software system (Software Inc, Tokyo, Japan) was used to deduce the amino acid sequence of longistatin. Sequence similarity searches were performed using the BLAST program (79). Alignment with the previously reported similar protein sequences, available in GenBank (80), were done using CLUSTALW. The putative signal sequence was analyzed using the prediction server SignalP V2.0.b2 (http://www.cbs.dtu.dk/services/SignalP) (81). Theoretical molecular weight (mol. Wt) and pI were determined using PeptideMass (http://us.expasy.org/tools/peptidemass.html) (82). Domains were searched using ExPASy-PROSITE (http://au.expasy.org/prosite/). N-linked glycosylation sites were searched using NetNGlyc 1.0 (http://www.cbs.dtu.dk/services/NetNGlyc).

2.3. Production of recombinant longistatin

The open reading frame (ORF) of longistatin was amplified by PCR from PBS/longistatin

using a set of primers, 5′CCG CTC GAG CGG GCA GGC CGG CGA CCA GCA G 3′ and 5′GGA ATT CCC TAA ATT TGG TTG GTC AGG TC 3′, which contained *Xho*I and *Eco*RI restriction sites, respectively. PCR was performed for 3 min at 95 °C followed by 35 cycles of 30 s at 95 °C, for 30 s at 57 °C and 1.5 min at 72 °C with a final elongation at 72 °C for 5 min. Both the PCR product and the vector pTrcHisB (Invitrogen, Carlsbad, CA, USA) were digested by *Xho*I and *Eco*RI restriction enzymes. The purified PCR product was inserted into the *Xho*I and *Eco*RI sites of the vector pTrcHisB (Invitrogen). The resultant plasmid was transformed into competent cells of *Escherichia coli* Top10F′ strain (Invitrogen) following the conventional method. The expression of longistatin in *E. coli* with a polyhistidine-tag was performed according to the procedure described by Tsuji et al (83). Briefly, the transfected cells were allowed to grow in SOB medium (Tryptone 20.0 mg, Yeast extract 5.0 mg, Sodium chloride 0.5 mg, Magnesium sulfate anhydrous 2.4 mg and Potassium chloride 0.186 mg per ml) containing 50 µg ampicillin/ml at 37 °C under vigorous shaking (200 rpm) until the OD of 1 at 600 nm (OD_{600}) was achieved. To induce recombinant protein expression, isopropyl-β-D thiogalactopyranoside (IPTG) was added to 1 mM concentration and the culture was grown for an additional 4 h at 37 °C on a shaking incubator. The culture was then centrifuged at 10,000 × *g* and 4 °C for 20 min and the pellet was resuspended in 10 ml of lysis buffer (20 mM sodium phosphate and 500 mM sodium chloride, pH 7.8). Egg white lysozyme (100 µg/ml) was added to the cell suspension and incubated in ice for 15 min. The suspension was sonicated for 2 min on ice with an ultrasonic processor (VP-15S, TAITEC, Saitama, Japan) followed by immediate freezing at –80 °C and then thawing at 37 °C for 15 min in each case. After three cycles of sonication, freezing and thawing, the *E. coli* lysate was centrifuged at 23,900 × *g* and 4 °C for 30 min and supernatant was collected. The recombinant protein was purified using ProBond™ resin (Invitrogen) under native conditions as described by the manufacturer and subsequently eluted with a stepwise gradient of imidazole (25–500 mM). The eluted recombinant protein was concentrated using Centrisart® (Sartorius, Goettingen, Germany) having a mol. wt cut-

off of 10 kDa. The concentrated protein was dialyzed extensively at 4 °C with successive changes of 20 mM Tris-HCl (pH 7) and a decreasing concentration of NaCl (500–250 mM) using a Slide-A-Lyser® Dialysis Cassette (Pierce, Rockford, IL, USA) with a mol. wt cut-off of 10 kDa. Purified recombinant longistatin was electrophoresed on a 12.5% SDS-PAGE gel under reducing conditions. The gel was treated with 50% methanol in 10% acetic acid for 10 min at room temperature. The protein was subjected to silver staining (Daiichi Pure Chemicals, Tokyo, Japan) following the manufacturer's instructions. Finally, protein concentration was determined using micro-BCA reagent (Pierce) and stored at –20 °C until further use.

2.4. Western blot analysis

Crude *E. coli* lysate was electrophoresed through a 12.5% SDS-PAGE gel under reducing conditions and the proteins were transferred onto nitrocellulose membrane. The membrane was incubated with 5% skim milk for 30 min at room temperature. Polyhistidine-tagged longistatin was probed with the anti-His monoclonal antibody (1: 1,000) (Anti-6 × His (Mouse IgG1-*K*), Monoclonal (HI192) AS, Nacalai Tesque Inc., Kyoto, Japan). The membrane was washed with Tris-buffered saline-Tween-20 (TBS-T) and incubated with alkaline phosphatase-conjugated goat anti-mouse IgG (H+L) (ZYMED, San Francisco, CA, USA) as a secondary antibody for 1 h. The membrane was washed again with TBS-T and the bound protein was visualized with nitroblue tetrazolium/5-bromo-4-chloro-3-indolyl phosphate (BCIP/NBT, Promega, Medison, WI, USA).

2.5. N-terminal sequencing of longistatin

Purified recombinant protein was subjected to electrophoresis on a 12.5% SDS-PAGE gel under reducing conditions. After electrophoresis, the protein was electro-blotted onto a polyvinylidene difluoride (PVDF) membrane (Millipore, Bedford, MA, USA) in 10 mM 3-(cyclohexylamino)-1-propanesulfonic acid (CAPS) buffer (pH 11) containing 10% methanol. The blotted protein was stained with coomassie brilliant blue (CBB), followed by distaining with 50%

methanol. The target protein band was excised from the blot and was subjected to N-terminal sequencing using the Procise 494 cLC Protein Sequencing System (Applied Biosystem) (84).

2.6. Generation of mouse polyclonal antibody

BALB/c mice were immunized by s.c. injection of 50 μg of recombinant protein emulsified with Freund's Complete Adjuvant (FCA, DIFCO, Detroit, MI, USA) followed by booster immunizations 2 weeks apart using Freund's Incomplete Adjuvant (FIA, DIFCO) through the same route. The immunized mice were sacrificed 1 week after the last booster and sera were collected and stored at –20 °C for further use.

2.7. Reverse transcription-PCR (RT-PCR) analysis

Unfed and fed adult ticks (24 h, 48 h, 72 h, 96 h and engorged (120 h)), and post-engorged ticks (day 0, day 1 and day 2) were washed with 70% ethanol and rinsed in PBS. Then ticks were dissected under a dissecting microscope (SZX7 Olympus, Tokyo, Japan) using ice-cool PBS and different organs were collected. Shortly after collection, the tissues were submerged in RNA*later*®, a RNA Stabilization Reagent (QIAGEN). The total RNA was isolated by using an RNeasy Mini Kit (QIAGEN) according to the manufacturer's protocol. Total RNA was also collected from other lifecycle stages (egg, larva and nymph) of *H. longicornis*. Five hundred nanogram of total RNA was used for RT before PCR. Single stranded cDNA was prepared using a Takara RNA PCR Kit (AMV) Ver.3.0 (Takara, Shiga, Japan) following the manufacturer's instructions. A series of PCRs were carried out using 500 ng of cDNA from each sample and *longistatin*-specific oligonucleotides (5′GCT ATC TCG GCT CCT GTG TC 3′ and 5′ATC TTC GCC AGG TCC TTC TT 3′) or oligonucleotides specific for a control cDNA encoding β-actin in a final volume of 20 μl. PCR was performed for 5 min at 95 °C followed by 35 cycles of 30 s at 95 °C, 30 s at 54 °C and 1.5 min at 72 °C and finally elongation at 72 °C for 5 min. The PCR product was subjected to electrophoresis in a 1% agarose gel.

2.8. Immunohistochemistry

Immunohistochemistry was performed as previously described (85). Briefly, ticks were fixed overnight in 4% paraformaldehyde in 0.1 M phosphate buffer (pH 7.2) and embedded in paraffin. Thin transverse sections were cut from paraffin-embedded well-fixed ticks. Sections were fixed on glass slides and deparaffinized with xylene. The sections were rehydrated with graded series of alcohol washes, followed by inactivation of endogenous peroxidase with 1% H_2O_2 in PBS containing 10% ethanol for 1 h and blocked with 10% goat serum (Wako, Osaka, Japan) in PBS. They were then incubated overnight at 4 °C with mouse anti-longistatin serum (1: 100). Sections treated with pre-immune mouse sera (1: 100) were used as a control. Slides were rinsed thoroughly with ice-cool PBS by placing on a rotator (40 rpm). The sections were then reacted with the peroxidase-labeled anti-mouse IgG secondary antibody and the substrate 3′, 3′diaminobenzidine tetrahydrochloride (Fast™ DAB set, Sigma, St. Luis, MO, USA). After color development, the slides were dehydrated with graded series of alcohol washes, cleared in xylene and then covered with cover slips and examined under a microscope (Leica Microsystem, Wetzlar, Germany).

2.9. Cell separation and immunocytochemistry

Salivary gland cells were collected from partially fed (96 h) adult ticks by teasing the freshly collected salivary glands through a stainless steel mesh in PBS containing complete protease inhibitors. The cells were washed in PBS to remove cellular debris and centrifuged at 4,400 × *g* for 10 min at room temperature. Finally, 200 µl of PBS were added and sediments were resuspended. A thin smear was prepared on a glass slide using 10 µl of cell-suspension. Cells were then fixed with 4% paraformaldehyde in PBS (0.1 M, pH 7.4) for 20 min at room temperature and were treated with 0.1% Triton × 100 in PBS for 20 min under the same conditions. The slides were washed with PBS and blocked with 10% goat serum (Wako) for 30 min at room temperature and

then incubated overnight with mouse anti-longistatin sera (1: 100) at 4 °C. The cells were washed in PBS and reacted with a green fluorescent-labeled secondary antibody (Alexa Flour® 488 goat anti-mouse IgG (H+L), Invitrogen) for 1 h at room temperature. The slides were then washed thoroughly with PBS and mounted with VECTASHIELD® mounting medium containing DAPI (Vector Laboratories, Burlingame, CA, USA) and examined under a fluorescent microscope (Leica).

2.10. Detection of longistatin in secretory pathways of salivary glands and in host tissues

Immunofluorescent staining was performed using thin (5 μM) sections from partially fed (72 h) adult ticks following the methods as described previously (86). Briefly, sections were treated with mouse anti-longistatin sera (1: 100) and bound antibodies were detected using a green fluorescent-labeled secondary antibody (Alexa Flour® 488 goat anti-mouse IgG (H+L), Invitrogen). Slides were mounted with VECTASHIELD® mounting medium containing DAPI (Vector Laboratories) and examined under a fluorescent microscope (Leica). I also employed immunofluorescent staining for the detection of longistatin in the feeding lesions of ticks on the host. To do this, thin sections were prepared from tissue samples collected from the feeding lesions developed on a rabbit ear at the site of attachment of the tick following the procedures as previously described (87). Immunofluorescent staining was performed using mouse anti-longistatin sera as described above. Additionally, larvae of *H. longicornis* were fed on the tick-naïve rabbit ears for 72 h as described above and ear tissues were collected with attached larvae. Thin sections were prepared and subjected to immunofluorescence staining using mouse anti-longistatin sera (1: 200) as described above. Sections were also subjected to hematoxylin and eosin (H & E) staining following the standard protocol.

2.11. Ca^{2+}-binding assays

Purified longistatin was electrophoresed using 10% SDS-PAGE gels in the presence of 3 mM $CaCl_2$ or 3 mM EDTA under reducing conditions. BSA was used as a control. Gels were

stained with CBB. Additionally, both the endogenous and recombinant proteins were transferred onto nitrocellulose membranes and were stained with 25 mg/L ruthenium red (Calbiochem, Darmstadt, Germany) in a buffer containing 60 mM KCl, 5 mM $MgCl_2$ and 10 mM Tris-HCl (pH 7) for 15 min at room temperature.

3. Results

3.1. Molecular characteristics of longistatin

Sequence analysis revealed that the full-length longistatin cDNA consisted of 750 bases which included the complete coding region together with 5′ and 3′ non-coding regions. The in-frame start codon is located at nucleotides 133–135 and the stop codon is at 601–603. The ORF consisting of 471 nucleotides, extends from residues 133–603 which codes for a protein of 156 amino acid residues having a calculated molecular mass of 17,788 Da and a pI of 4.84. From the analysis of the N-terminus of the polypeptide with the SignalP program (http://www.cbs.dtu.dk/services/SignalP), it was determined that the molecule has a signal peptide and is predicted to be cleaved at Ala^{21}–Gln^{22}. The mature protein has a predicted molecular mass of 15,541 Da with a theoretical pI of 4.59 and longistatin is not stabilized by disulfide bonds. No potential site for N-glycosylation was predicted in the putative polypeptide encoded by the *longistatin* cDNA. Longistatin contains two EF-hand Ca^{2+}-binding domains (http://au.expasy.org/prosite/) at residues 83–94 and 135–146 (Figure 1 and 2A). Alignment of longistatin EF-hand domains -I and -II (LongEFd-I and -II) with the EF-hand domains from diversified sources revealed that LongEFd-I and -II have conserved canonical structures. The loop region of each domain consists of 12 amino acid residues and is arranged in the pattern of X•Y•Z•–Y•–X••–Z, where X, Y, Z, –X, –Y and –Z are the Ca^{2+} coordinating ligands and the dot represents the intervening residues. In both domains, LongEFd-I and -II, X and –Z positions are occupied by aspartic acid and glutamic acid, respectively (Figure 2B). Despite a few radical departures from

the general liganding rule, the loop region of the most common canonical EF-hands usually consists of 12 amino acid residues which starts with an aspartic acid and ends with a glutamic acid (67). These negatively charged amino acids play important roles in the binding of positively charged Ca^{2+}. In conjunction, the bidentate glutamic acid at the –Z position is indispensible for the formation of pentagonal bipyramid coordination geometry (68). Furthermore, LongEFd-I and LongEFd-II contain several bulky hydrophobic residues (Figure 2B), and are predicted to form a hydrophobic core, which is a salient characteristic of helix-loop-helix proteins (68, 88). The amino acid sequence of LongEFd-II represents the conserved glycine residue at position 6 in the loop, which plays an important role in the proper folding of ligands around the metal ion (88). In the LongEFd-I, the glycine residue has been substituted by asparagine. The substitution of glycine at position 6 with other amino acid residues is not unexpected and has been detected in some well-recognized Ca^{2+}-binding proteins like, carp parvalbumin, rabbit parvalbumin, S-100A, S-100B, porcine intestinal Ca^{2+}-binding protein (PICBP), bovine intestinal Ca^{2+}-binding protein (BICBP) and rabbit skeletal muscle alkali light chain (88). Results of BLAST (NCBI, National Institute of Animal Health, http://www.ncbi.nlm.nih.gov/BLAST) searches revealed that longistatin has the highest identity with multiple coagulation factor deficiency 2-like protein of *Ixodes scapularis* (51% identity).

3.2. Migration of purified recombinant longistatin on SDS-PAGE

To determine the biochemical properties, longistatin was expressed in *E. coli*, strain TOP10F', using a pTrcHisB™ vector, and was harvested as a soluble protein from bacterial cultures. Expression of recombinant longistatin was detected with anti-His monoclonal antibody (Nacalai Tesque, Inc.) (Figure 3B). One liter of bacterial culture, on an average, yielded 3.15 mg purified longistatin. The purity of recombinant longistatin was confirmed by SDS-PAGE analysis followed by silver staining, and a single band was detected (Figure 3A). The calculated molecular

mass of longistatin is 15.54 kDa (excluding signal peptide). Longistatin migrated on SDS-PAGE gels as a 24 kDa fusion protein with a polyhistidine tag (Figure 3A, B). This unexpected mobility of prokariotically expressed longistatin to 24 kDa instead of its calculated molecular mass of 15.54 kDa on SDS-PAGE analysis was not due to *N*-linked glycosylation, as longistatin does not contain any potential *N*-glycosylation sites. However, this type of mobility of the recombinant protein over the expected size has been observed in other cases. Thrombostasin, a thrombin inhibitor isolated from horn fly saliva, showed a significantly higher molecular mass (16.7 kDa) on SDS-PAGE instead of its calculated molecular mass of 9.2 kDa, which was predicted to be due to its acidic characteristics (89). Longistatin is also acidic in nature (pI 4.59) and it is assumed that the higher molecular mass band of longistatin on SDS-PAGE is due to its acidic characteristics. Sequence analysis of the purified recombinant longistatin (24 kDa protein) was performed. The representative first 10 amino acid residues were QAGDQQQMQP which exactly corresponds to the 22−31 amino acid residues of longistatin (GenBank accession number AB 519820), confirming that the 24 kDa protein is true longistatin.

3.3. Longistatin is upregulated with the blood-feeding processes

For transcription profiling of longistatin, total RNA was extracted from the unfed and fed different lifecycle stages and organs of ticks, and was subjected to RT-PCR analysis. Longistatin-specific transcripts were expressed at a level which corresponded well to its expected size (246 bp). The transcript was detected in all lifecycle stages including eggs but its expression was highly up-regulated after feeding (Figure 4A). Furthermore, the gene was specifically expressed in salivary glands and completely absent in other organs (Figure 4B), suggesting its salivary gland specificity. RT-PCR data also revealed that the gene was dramatically up-regulated with the feeding process of ticks. The highest expression was detected at 96 h of feeding and in fully engorged (120 h) adult ticks (Figure 4C). Expression of the longistatin-specific gene decreased abruptly after spontaneous

detachment of ticks from the host following full engorgement (Figure 4D), implying that longistatin may have some potential roles in the blood-feeding processes of hard ticks.

3.4. Longistatin is produced in salivary glands and injected into hosts' tissues

To detect the endogenous form of longistatin, both immunohistochemistry and immunofluorescent staining were performed using thin sections of partially fed (72 h) adult *H. longicornis*. Immunohistochemical examination showed that the endogenous longistatin, which reacted with mouse anti-longistatin sera, was localized only in the salivary glands, further indicating its salivary gland-specific expression. No positive reaction was detected in either the internal or external tissues of ticks treated with pre-immune mouse sera (Figure 5A). Using immunofluorescent staining, longistatin was detected within the cells as well as in the lumen of the functional acini of salivary glands (Figure 5A, arrow), suggesting that longistatin is synthesized and secreted by the salivary gland cells.

To determine the intracellular localization of the endogenous protein, salivary gland cells from partially fed (96 h) adult ticks were isolated and were subjected to immunofluorescent staining. Cells treated with mouse anti-longistatin sera showed intense reactivity with the entire cytoplasm, however, the longistatin-specific reaction was little bit more intense near the periphery of the cell (Figure 5A). These results suggest that endogenous longistatin is distributed throughout the cytoplasm of the salivary gland cells.

To ensure the presence of longistatin in the feeding lesions, thin histological sections prepared from rabbit ear tissues containing blood pools following a successful blood-feeding by adult ticks were also subjected to immunofluorescent staining. Intense longistatin-specific reactions were detected by using mouse anti-longistatin sera (1: 100) in the feeding lesions (Figure 5Bc), especially in the areas where massive hemorrhages were observed by H & E staining (Figure 5Bb), implying that longistatin is secreted and is injected through saliva into the blood pools. To

further validate the results regarding the site of synthesis, secretion and injection of longistatin into host tissues during the acquisition of blood-meals, immunofluorescent study were conducted using rabbit ear tissues with attached *H. longicornis* larvae. Longistatin-specific reactions were observed within the tick's salivary glands, ducts, mouthparts and also at the biting sites, clearly indicating that longistatin is synthesized in the salivary glands and injected into the host's tissues during feeding (Figure 6).

3.5. Longistatin binds with Ca^{2+}

To verify the Ca^{2+}-binding affinity of longistatin, the gel mobility shift assay was performed using 10% SDS-PAGE gels under reducing condition in the presence of 3 mM Ca^{2+} or 3 mM EDTA. Data showed that migration of longistatin was relatively faster in the presence of 3 mM Ca^{2+} than that in the presence of a metal chelator, EDTA, under the same conditions, suggesting that longistatin is capable of binding with Ca^{2+}. Longistatin appeared at the level of 21 kDa on SDS-PAGE containing 3 mM Ca^{2+}. But the longistatin band was observed at the level of about 24 kDa in the presence of 3 mM EDTA while the control protein BSA appeared at the same level in both of the gels (Figure 7A). I hypothesized that the binding of Ca^{2+} with longistatin induces some significant conformational changes rendering the molecule to migrate rapidly during electrophoresis. A similar pattern of electrophoretic mobility was observed in several other well-studied Ca^{2+}-binding proteins such as Calmodulin, Calcineurin B and Troponin C (90). For further confirmation of Ca^{2+}-binding affinity, both endogenous and recombinant proteins were electrophoretically transferred onto nitrocellulose membranes and stained with ruthenium red (Figure 7B), which is a specific stain for Ca^{2+}-binding proteins. Ruthenium red inhibits the binding of Ca^{2+} with the Ca^{2+}-binding proteins, and specifically stains them. The interaction between ruthenium red and Ca^{2+}-binding sites is extremely specific and sensitive (91). Ruthinium red staining is, therefore, widely used for the detection of Ca^{2+}-binding proteins. The results suggest

the specific interaction of ruthenium red with the Ca^{2+}-binding sites of longistatin.

4. Discussion

Tick saliva contains a wide array of pharmacologically active biomolecules having diversified functions which help ticks to feed blood-meal persistently (35, 54, 87, 92, 93). Here, I describe that longistatin, a novel EF-hand protein isolated from the salivary glands of *H. longicornis*, binds with calcium and is thought to be closely linked to the feeding processes of ticks.

Sequence alignment reveals that both of the Ca^{2+}-binding sites of longistatin conserve the general rules of arrangement of ligands of standard EF-hand domains. The most noteworthy, within the Ca^{2+}-binding loop region, position 8 and 10 are occupied by hydrophobic amino acid residues. This ligand pattern is identical to the classical arrangement of amino acids in the historical consensus sequence of EF-hand first described by Kretsinger and Nockolds (67), which is also seen in the Ca^{2+}-binding sites of other well-known standard EF-hand proteins such as bovine brain calmodulin (94), *Tetrahymena* calmodulin (95) and in rabbit skeletal troponin C (96). In the LongEFd-I, positions 8 and 10 of the loop are occupied by leucine and glycine, respectively, but in the LongEFd-II leucine has been replaced with isoleucine, and glycine with tyrosine. Although position 8 and to a lesser extent position 10 of the EF-hand loop region are conserved hydrophobic sites, but more precisely, position 8 is most frequently occupied by the residue isoleucine, leucine or valine (68). These two well-conserved sites of the loop region, together with the C- and N-terminal hydrophobic surface, are involved in the metal dehydration process (88).

Localization studies strongly support the salivary gland-specific expression of longistatin. It is suggested that longistatin is synthesized and accumulated in the cytoplasm, finally secreted out from the salivary gland cells and takes part in the feeding process after reaching the blood pools, the essential feeding lesions on the host. Usually EF-hand Ca^{2+}-binding domains are prevalent among the cytoplasmic proteins (63) and act as a calcium sensor or buffer in the cytosol of the cell

(72) engaging in various biological functions such as ciliary beating, muscle contraction, membrane excitability, cell proliferation and cell death through signaling of multiple physiobiochemical pathways (76, 97). However, in some rare cases EF-hand Ca^{2+}-binding proteins are secreted from the cells and exert their function in extracellular spaces (63, 74). RT-PCR data demonstrate that the gene coding for longistatin is expressed in all lifecycle stages, including eggs. Notably, the longistatin-specific gene is dramatically up-regulated in pre-engorged (96 h) and engorged (120 h) adult ticks but declines sharply in the post-feeding period, suggesting its vital roles in the blood-feeding processes of ixodid ticks. Feeding patterns of ixodid ticks are not alike the vessel feeder hematophagous insects that suck blood directly and rapidly from the blood vessel. Ixodid ticks usually take blood over a long period (98), making a large blood pool under the skin. During the process of piercing the skin of mammalian hosts, ticks tear the dermis, lacerate the surrounding tissues and disrupt the continuity of the smaller blood vessels with their specialized mouthparts. Thus, they produce a blood pool under the skin from which they suck blood and fluid that are drained into the resulting wound (54). Tick-feeding lesions on a non-immune host, are characterized by cavities filled with unclotted blood (99). While feeding, ixodid ticks inject large amounts of fluid into the host at the site of attachment which is a mixture of salivary cocktail and the regurgitated fluid component of the ingested blood. In ixodid ticks, the total blood-feeding period is distinctly divided into two phases such as the slow feeding period (up to 3 days post-attachment) and the rapid feeding period (further 2−3 days). During the slow feeding period, the size of the blood pool is relatively smaller, contains scanty blood and exudates and the tick imbibes very little amount of blood. On the contrary, during the rapid feeding period, the blood pool becomes voluminous, contains a considerable amount of blood and exudates, and the tick takes the blood-meal very rapidly (45). Therefore, the high level of expression of the longistatin-specific gene in the pre-engorged (96 h) and engorged ticks together with the sharp declination of expression after detachment of ticks following full engorgement, clearly indicates that longistatin

modulates the feeding processes of blood from host animals.

Taken together, longistatin, an EF-hand protein, is synthesized in the salivary glands of *H. longicornis* and secreted with the saliva, and injected into the blood pool developed on hosts' tissues. Longistatin is able to bind with calcium. Furthermore, transcriptional data strongly suggest that longistatin contributes to the feeding success of blood-meals from host animals by ixodid ticks throughout the entire feeding period.

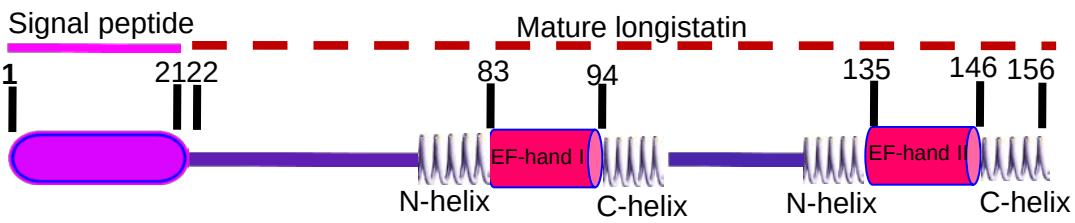

Figure 1. Schematic diagram of the protein structure of longistatin. Longistatin is composed of 156 amino acid residues and contains a signal peptide, which is predicted to be cleaved at Ala^{21}–Gln^{22}. Longistatin has two canonical EF-hand domains at the C-terminus.

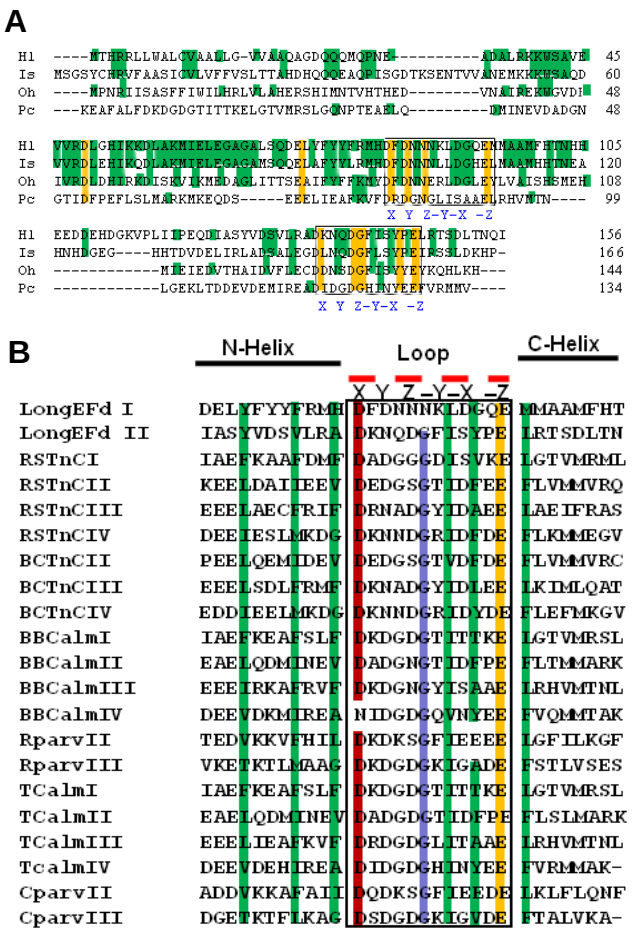

Figure 2. Sequence alignment of longistatin. (A) Comparison of the deduced amino acid sequence of longistatin (Hl) with the amino acid sequences of homologous molecules. Sequences were selected from (GenBank accession numbers are indicated in parentheses): Is, *Ixodes scapularis* (**AAY66924**), Oh, *Ornithoctonus huwena* (**ACH48184**) and Pc, *Paramacium* calmodulin (100). Loop regions of EF-hand domains are boxed. Amino acid residues in yellow are conserved in all sequences and those in green, are identical to longistatin only. X, Y, Z, –Y, –X and –Z represent calcium coordinating positions of the loop. (B) Alignment of longistatin EF-hand domains -I and -II with EF-hand domains of proteins with known structures such as rabbit skeletal troponin C (RSTnC I, II, III and IV), bovine cardiac troponin C (BCTnC II, III and IV), bovine brain calmodulin (BBCalm I, II, III and IV), rabbit parvalbumin (Rparv II and III), *Tetrahymena* calmodulin (TCalm I, II, III and IV) and carp parvalbumin (Cparv II and III) (88). Yellow denotes the omnipresence of glutamic acid in –Z position and dark red indicates commonly occurring aspartic acid in the X position of canonical EF-hands. Amino acid residues in green are involved in the formation of the hydrophobic core of the EF-hand domain. Violet indicates the frequently occurring glycine residue at position 6 of the loop region of standard EF-hands.

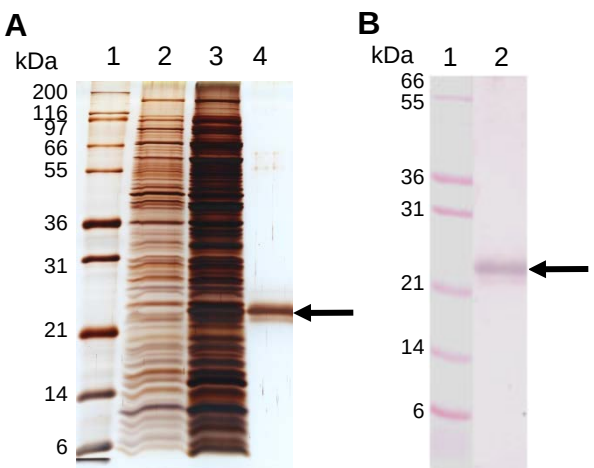

Figure 3. Detection and purification of recombinant longistatin. (A) Detection of purity of longistatin by SDS-PAGE analysis. Purified longistatin together with *Escherichia coli* lysate was electrophoresed through 12.5% SDS-PAGE gel under reducing conditions. The gel was stained with silver stain. Lane 1, molecular weight marker; lane 2, *E. coli* lysate before induction; lane 3, *E. coli* lysate 3 h after induction with isopropyl-β-D thiogalactopyranoside (IPTG) and lane 4, purified longistatin. (B) Western blot analysis to detect the His-tagged recombinant longistatin using anti-His monoclonal antibody. Crude *E. coli* lysate was electrophoresed through a 12.5% SDS-PAGE gel under reducing conditions and proteins were transferred onto nitrocellulose membrane. The membrane was treated with anti-His monoclonal antibody as described in the Materials and Methods. Lane 1, molecular weight marker and lane 2, recombinant longistatin.

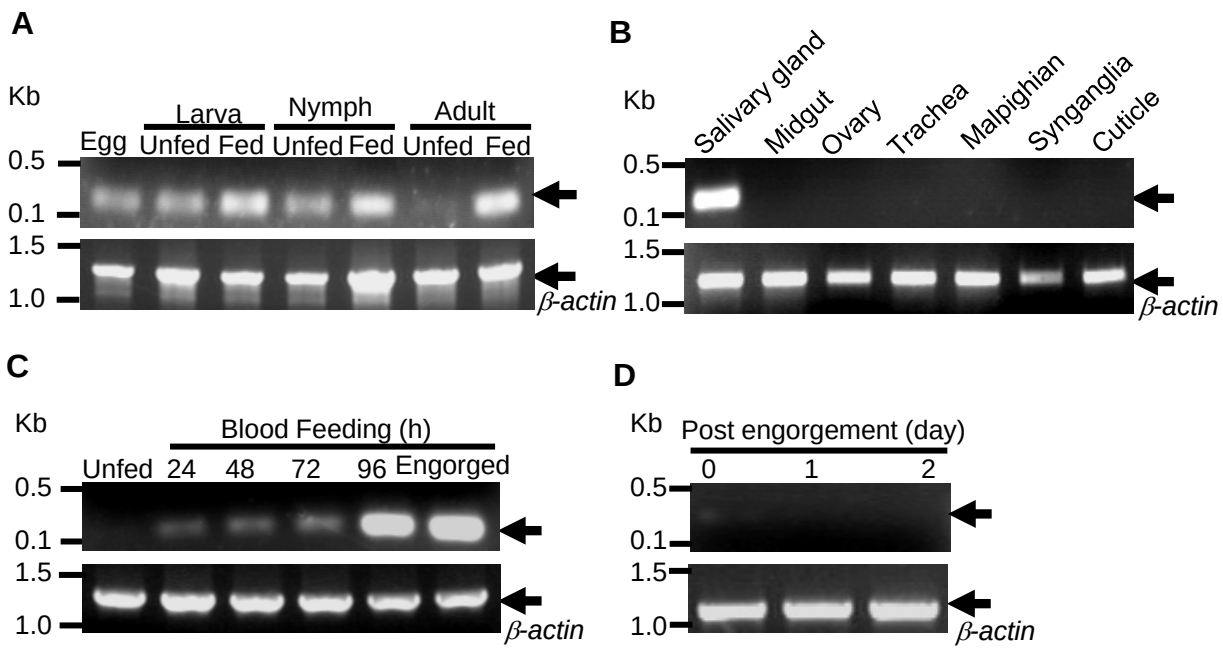

Figure 4. Transcription profiling of longistatin in *Haemaphysalis longicornis*. (A) Expression of the longistatin-specific gene in all lifecycle stages of *H. longicornis* (arrow). Reverse transcription-PCR (RT-PCR) was performed using total mRNA extracted from all developmental stages, including eggs. (B) Organ-specific expression of *longistatin* gene (arrow). Total mRNA was collected from various organs of partially fed (72 h) adult ticks and subjected to RT-PCR analysis. (C) Expression profile of the gene in salivary glands of adult ticks at different blood feeding stages (arrow). RT-PCR analysis was performed using total mRNA collected from salivary glands of adult *H. longicornis* at different blood feeding stages. (D) Expression of the longistatin-specific gene in the post-engorgement period (arrow). Total mRNA was collected from salivary glands of adult ticks at the different post-engorgement period (day 0, day 1 and day 2) and was subjected to RT-PCR analysis. *β-actin* was shown as an internal control.

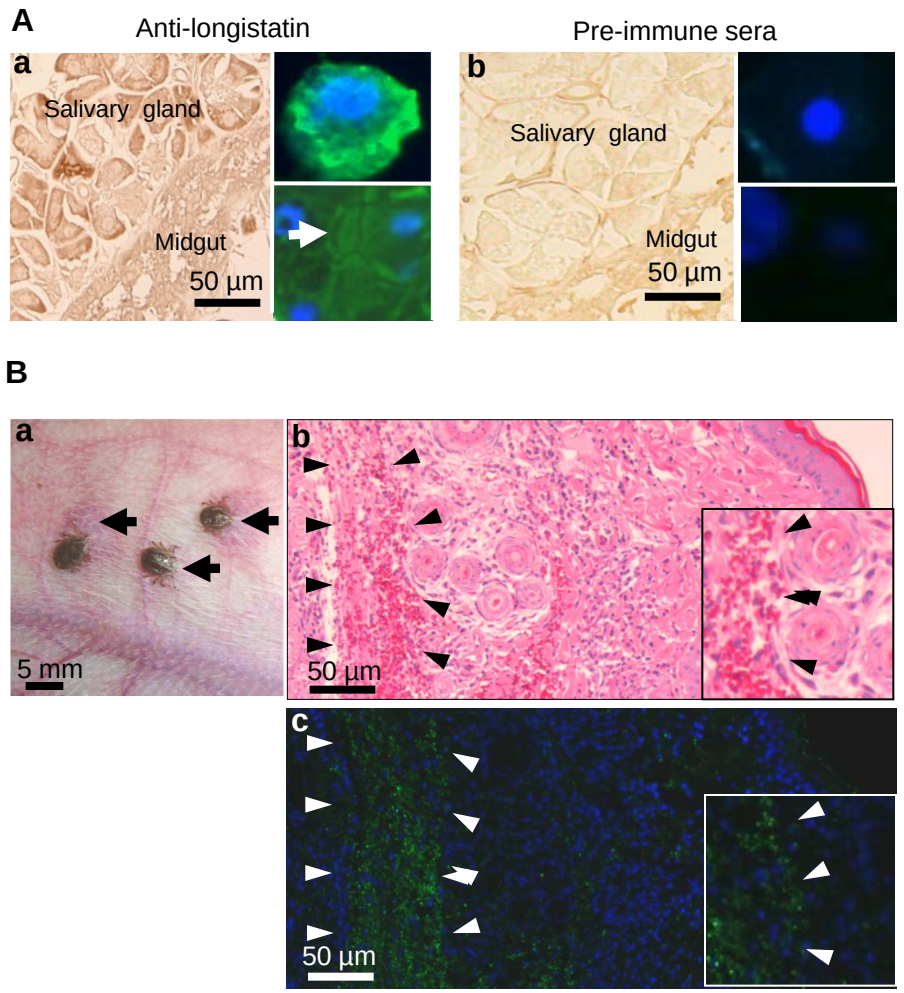

Figure. 5. Endogenous longistatin detected in the tick *Haemaphysalis longicornis*, and in host tissues. (A) Localization of endogenous longistatin in partially fed (72 h) adult ticks. Ticks were fixed in paraformaldehyde and embedded in paraffin. Sections were prepared and treated with either immune (1: 100, Aa) or pre-immune mouse sera (1: 100, Ab). The longistatin-specific reaction was detected in the salivary glands and in the lumen of the functional acini (arrow). Salivary gland cells were collected from partially fed (96 h) adult ticks and reacted with mouse anti-longistatin (1: 100, Aa)/preimmune sera (1: 100, Ab) followed by the treatment with a green fluorescent-labeled secondary antibody (Alexa Flour® 488 goat anti-mouse IgG (H+L), Invitrogen). (B) Longistatin detected in the feeding lesions *in vivo*. A rabbit's ear showing blood pools at the site of attachment of ticks (arrows; Ba). The area of hemorrhage in the blood pool stained by H & E (arrowheads; Bb, 10x objective). Detection of longistatin in the feeding lesions of a rabbit's ear (arrowheads; Bc, 10x objective). Rabbit's ear tissues were collected from a euthanized rabbit as described in the Materials and Methods and were fixed in 4% paraformaldehyde and embedded in paraffin. Sections were prepared and treated with mouse anti-longistatin sera (1: 100) followed by the treatment with a green fluorescent-labeled secondary antibody (Alexa Flour® 488 goat anti-mouse IgG (H+L), Invitrogen). The area marked by the square is at 40x objective.

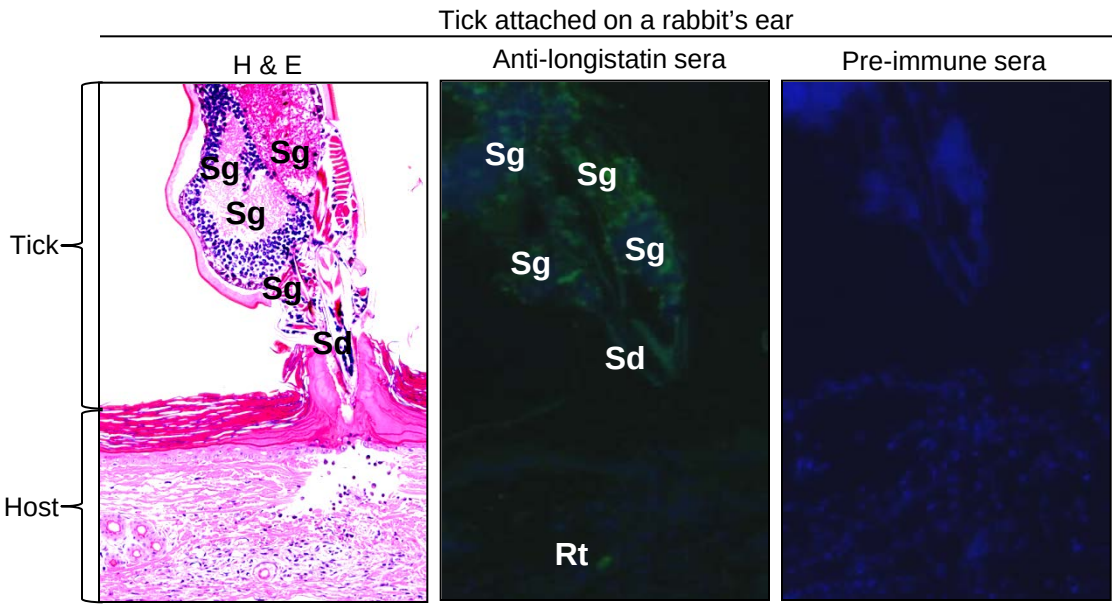

Figure 6. Longistatin was secreted from salivary glands and injected into the feeding sites. Larvae of *Haemaphysalis longicornis* were fed on the tick-naïve rabbits' ear. Ear tissues were collected from euthanized rabbits with partially fed (72 h) attached larvae, and were fixed in 4% paraformaldehyde. Sections were prepared and subjected to H & E staining and immunofluorescence using mouse anti-longistatin sera (1: 200) or pre-immune sera as described in the Materials and Methods.

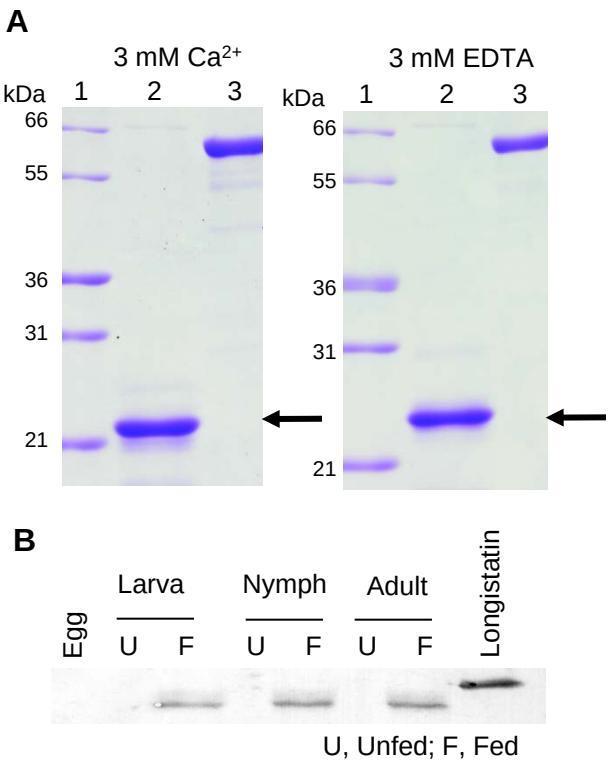

Figure 7. Ca^{2+}-binding affinity of longistatin. (A) Gel mobility shift assay. Purified recombinant longistatin was electrophoresed in the presence of 3 mM Ca^{2+} or 3 mM EDTA through 10% SDS-PAGE gels. Lane 1, molecular weight marker; lane 2, longistatin (arrow); lane 3, BSA (control). Longistatin migrated rapidly in the presence of Ca^{2+}. (B) Ruthenium red staining of longistatin. Endogenous longistatin from different lifecycle stages and purified recombinant longistatin were subjected to SDS-PAGE analysis followed by blotting onto nitrocellulose membranes. Nitrocellulose membranes were then stained with ruthenium red for 15 min at room temperature. U, unfed; F, fed. The right most lane recombinant longistatin.

Chapter 2

Enzyme kinetics of longistatin

1. Introduction

Proteases are key players in all physio-chemical functions of living cells. They hydrolyze amide bonds that link amino acids to one another, making peptides or proteins. This hydrolytic process requires concentrated efforts of the key residues located in the enzyme's active site (101, 102). Among the four functional groups of enzymes such as serine, cysteine, aspartic and metallo-proteases (59), serine proteases are more common (60) and control numerous biological processes, such as cytogenesis, apoptosis, angiogenesis, neuronal plasticity, zymogen processing, matrix remodeling, immune response, inflammation, blood coagulation and fibrinolysis (103−106). On the basis of structure, serine proteases are categorized into two groups such as classical/conventional/typical serine proteases and unconventional/atypical serine proteases. Classical serine proteases use conserved Ser/His/Asp catalytic triad during hydrolysis of substrates (61). Here, Ser is the nucleophile, His is the general base and Asp neutralizes charges developed on His (105, 107). In contrast, unconventional serine proteases do not contain canonical conserved catalytic triad. In the unconventional serine proteases, several types of catalytic machineries with different compositions and configurations have been detected. Indeed, variations are observed in each residue of the triad. His can be replaced by Glu/Lys (108), Asp by Glu/His (109−112) and

even Ser can be substituted by Thr (60, 113). In a few cases, the catalytic machinery has been proposed to consist of 4 residues, forming a tetrad (110), while in other atypical serine proteases, one or even two members of the triad have been eliminated forming "dyad" (59, 105) or "Ser-only" configuration active sites (60, 114). Furthermore, in a very few exceptional serine proteases, all three members of the triad have been eliminated together (60, 62, 105, 115).

Here, I demonstrate that, despite the vast sequence dissimilarity with traditional serine proteases, longistatin functions as a serine protease. Longistatin is the first unconventional serine protease identified and characterized from arthropods.

2. Materials and Methods

2.1. Removal of metal contaminants from recombinant longistatin

Recombinant longistatin was produced, purified and concentrated following the procedures as described in the Chapter 1. His-tag was removed from longistatin by incubating with enterokinase (EKMax™, Invitrogen), and purified using the enterokinase-eleminating column (Ek-Away™ Resin, Invitrogen) following the manufacturer's protocol. His-tag removed longistatin was used in enzyme assays. Metal contaminants were removed by dialyzing longistatin against 10 mM EDTA, when needed. Briefly, purified protein was loaded into Slide-A-Lyser® Dialysis Cassette (Pierce) with a mol. wt cut-off of 10 kDa and dialyzed extensively at 4 °C with several changes of 10 mM EDTA for 6 h.

2.2. Determination of substrate specificity

Longistatin (6 μg) was incubated with synthetic substrates specific for proteases of different groups, such as Boc-VPR-MCA (α-thrombin), Pyr-GR-MCA (t-PA/u-PA), Boc-QAR-MCA (trypsin), Suc-AAPF-MCA (chymotrypsin), Boc-EKK-MCA (plasmin), Suc-AAA-MCA (elastase), Suc(OME)-AAPV-MCA (elastase), Z-AAN-MCA (legumain) or Ac-DNLD-MCA

(Cathepsin D), at different concentrations (0–800 μM, final concentration) in a total reaction volume of 100 μl in buffer A (50 mM Tris-HCl, 100 mM NaCl and 5 mM $CaCl_2$) at 37 °C and pH 7 up to 1 h. Substrate hydrolysis was monitored by measuring excitation and emission wavelengths of 360 nm and 460 nm, respectively, using a Spectra Fluor fluorometer (TECAN, Mannedorf, Switzerland). Catalytic constants were calculated by Lineweaver-Burk plot as described previously (116).

2.3. Determination of the temperature and pH optima of longistatin

Temperature and pH optima were determined following the procedures as described previously (116). Briefly, to determine the temperature specificity, longistatin (6 μg) was incubated with Boc-VPR-MCA, an α-thrombin specific substrate, (200 μM, final concentration) in a total reaction volume of 100 μl of buffer A at different temperature (20–45 °C) and pH 7. Substrate hydrolysis was monitored by measuring excitation and emission wavelengths of 360 nm and 460 nm, respectively, using a Spectra Fluor fluorometer (TECAN). On the other hand, to determine the optimum pH, longistatin (6 μg) was incubated with the same substrate at different pH (6−9.5) and at the temperature 37 °C using 1 M sodium citrate buffer at pH 6–6.5 and buffer A at pH 7–9.5 up to 1 h. Substrate hydrolysis was monitored using a Spectra Fluor fluorometer (TECAN) as mentioned above.

2.4. Inhibition assays

Longistatin (2.5 μg) was pre-incubated in the absence or presence of PMSF (0–5 mM, final concentration), aprotinin (0–3 μM, final concentration), antipain (0–100 μM, final concentration), leupeptin (0–750 μM, final concentration), chymostatin (0−1 mM, final concentration), E-64d (0–500 μM, final concentration), iodoacetamide (0–4 mM, final concentration), pepstatin (0–500 μM, final concentration) or EGTA (0–10 mM, final concentration) in 100 μl of buffer (25 mM Hepes, pH 7.2, and 25 mM NaCl) at 37 °C for 1 h. Then, fibrinogen (7.5 mM, final concentration) was

added and incubated for 48 h in the same conditions as mentioned above. Aliquots were separated by 12.5% SDS-PAGE under reducing conditions and gels were stained with CBB. Additionally, the effects of various inhibitors on longistatin activity were determined using Boc-VPR-MCA (200 μM, final concentration) and IC_{50} was calculated as described previously (87). Briefly, longistatin (6 μg) was pre-incubated in the absence or presence of various inhibitors as mentioned above at the indicated concentrations for 1 h at 37 °C and diluted immediately with buffer A. Boc-VPR-MCA (200 μM, final concentration) was added in each well and substrate hydrolysis was monitored using a Spectra Fluor fluorometer (TECAN) as mentioned above.

2.5. Effects of metal ions

Effects of metal ions on longistatin were determined as described previously (117). Briefly, longistatin (6 μg, metal contaminant-free) was pre-incubated in the absence or presence (0−5 mM, final concentration) of $CaCl_2$, $MgCl_2$, $MnCl_2$, $ZnCl_2$, NaCl or KCl in a total volume of 100 μl of 50 mM Tris-HCl (pH 7) at 37 °C for 15 min. Synthetic substrate BOC-VPR-MCA (200 μM, final concentration) was added in each well and residual activity was judged using a Spectra Fluor fluorometer (TECAN) as described above.

2.6. Reversal of Zn^{2+} inhibition by EDTA

Longistatin (6 μg, metal contaminant-free) was pre-incubated in the absence or presence of $ZnCl_2$ (10 mM, final concentration) at 37 °C for 15 min in a total volume of 100 μl of 50 mM Tris-HCl (pH 7) and then EDTA (50 mM, final concentration) was added and incubated further for 15 min under the same conditions. Synthetic substrate Boc-VPR-MCA (200 μM, final concentration) was added in each well and substrate hydrolysis was monitored using a Spectra Fluor fluorometer (TECAN) as described above.

3. Results

3.1. Longistatin hydrolyzes serine protease-specific substrates

To explore the enzymatic activity, longistatin was incubated with synthetic fluorogenic substrates specific for different groups of proteases. Longistatin hydrolyzed several serine protease-specific substrates but did not affect the substrates specific for other proteases. Among the serine protease-specific substrates, longistatin potently hydrolyzed those containing Arg at the P1 site, indicating its specific affinity for the amide bond of Arg. Catalytic rate was relatively high during hydrolysis of the α-thrombin-specific substrate (k_{Cat}/K_m 2.97 $M^{-1}s^{-1}$) followed by that of t-PA/u-PA (k_{Cat}/K_m 2 $M^{-1}s^{-1}$) and the trypsin-specific substrate (k_{Cat}/K_m 0.88 $M^{-1}s^{-1}$) (Table 1).

3.2. Longistatin functions at a wide range of temperature and pH

Longistatin hydrolyzed substrates at a wide range of temperature from 20−45 °C. The catalytic rate was very low at 20 °C but increased rapidly with the increase of temperature and peaked at 37 °C, and beyond that the activity decreased (Figure 8A). Longistatin also hydrolyzed substrates at a wide range of pH (pH 6−9.5). At pH 6−6.5, activity was very low but dramatically increased at pH 7 and then decreased gradually with the further increase of pH (Figure 8B), indicating that longistatin is active at neutral to slightly alkaline conditions.

3.3. Longistatin is inhibited by serine protease inhibitors

Serine protease inhibitors such as PMSF, aprotinin, antipain and leupeptin efficiently inhibited the hydrolyzing activity of longistatin. Aprotinin (IC_{50} 0.35 μM) exerted the most potent inhibitory effects followed by antipain (IC_{50} 41.56 μM), leupeptin (IC_{50} 198.86 μM) and PMSF (IC_{50} 278.57 μM). Longistatin was not affected by chymostatin, pepstatin, iodoacetamide and E-64d. EDTA and EGTA, even at the highest recommended concentration (10 mM), reduced its activity up to 7.35−13.65% (Table 2), indicating that longistatin is not a metallo-protease.

However, slight attenuation of catalysis may be due to the chelation of bound Ca^{2+}, resulting in a change in the right configuration necessary for the optimum activity. Divalent cation binding is also critical for proper folding of acetylcholinesterase and α, β hydrolases (63). Furthermore, PMSF, aprotinin, antipain and leupeptin efficiently inhibited the fibrinogenolytic activity of longistatin at 5 mM, 3 μM, 100 μM and 750 μM concentrations, respectively. In contrast, pepstatin, iodoacetamide, E-64d and EGTA had almost no effect on the fibrinogenolytic activity of longistatin (Figure 9), indicating that the fibrinogenolytic activity of longistatin is dependent on the serine protease-like functional capability. However, in the presence of EGTA, γ-band digestion was partially inhibited.

3.4. Zn^{2+} is a regulatory switch of longistatin

Longistatin was reacted with several cations; among them, $Ca^{2+}$and Mg^{2+} slightly increased the enzymatic activity of longistatin but Na^{+} and K^{+} had no effect (data not shown). However, Zn^{2+} potently inhibited longistatin in a concentration-dependent manner with an IC_{50} value of 275 μM. Mn^{2+} also attenuated its functions but to a much smaller extent (Figure 10A). The inhibitory effect of Zn^{2+} was completely revived by EDTA (Figure 10B). Surprisingly, upon mixing with longistatin, Zn^{2+} produced milky white turbidity and addition of EDTA cleared it within a few minutes (data not shown), suggesting that Zn^{2+} led to the precipitation of longistatin resulting in reversible inhibition of the protein.

4. Discussion

The main machinery in the catalytic mechanisms of typical serine proteases is the conserved catalytic triad (60, 105). In addition to the typical serine proteases, there are some unconventional serine proteases that use catalytic residue arrangements other than the canonical triad. The number of unconventional serine proteases with different compositions and

configurations of catalytic machinery is expanding day by day. Recently, Ekici et al (60) summarized as many as 23 atypical serine proteases with different novel triads or dyads or proteases in which the nucleophilic hydroxyl is derived from Thr rather than Ser. Here, I report on longistatin from *H. longicornis*, which does not possess any conserved canonical serine protease triad [Chapter 1]. Despite that fact, longistatin catalyzes serine protease-specific substrates and is potently inhibited by various commercially available serine protease inhibitors.

Longistatin hydrolyzed several fluorogenic substrates specific for serine proteases, and enzymatic activity of longistatin was efficiently inhibited by commercially available common serine protease inhibitors. Importantly, longistatin was inhibited by PMSF, which is a well-known irreversible and specific inhibitor of serine proteases. PMSF inhibits serine proteases through sulfonylation of the active-site Ser of serine proteases. Active-site Ser of a serine protease, but not other Ser residues, is affected by PMSF owing to hyperactivity of the Ser located at the catalytic machinery of the enzyme (115). In addition, longistatin is potently inhibited by aprotinin, which inhibits many serine proteases by binding to the active site of the serine proteases, forming a tight complex. Although longistatin does not contain any conserved catalytic triad of serine proteases, the enzyme may have hyperactive residues that function in a similar fashion to those of typical serine proteases.

Longistatin displays trypsin-like substrate specificity. Among the serine proteases, chymotrypsin or chymotrypsin-like enzymes cleave substrates with bulky, hydrophobic residues (Phe, Tyr, Trp, Leu and Ile) at the P1 position and elastases attack on Ala and Val. However, trypsin or trypsin-like enzymes accommodate P1 basic residues, like Arg and Lys (118). Longistatin has specificity for P1-Arg. Furthermore, longistatin was efficiently inhibited by broad spectrum serine protease inhibitors (eg. PMSF, aprotinin and leupeptin) and/or by inhibitors specific for trypsin or trypsin-like serine proteases (eg. antipain). In contrast, longistatin was not affected by chymostatin even at a very high concentration (1 mM). Chymostatin specifically

inhibits chymotrypsin or chymotrypsin-like serine proteases and several cysteine proteases. This result reinforces the assertion that longistatin is a trypsin-like serine protease. Of the P1-Arg substrates, catalytic efficiency of longistatin was also variable, for example, hydrolysis of Boc-VPR-MCA was ~4 times higher than that of Boc-QAR-MCA. This variation is possibly due to the residues at other sites.

I demonstrate that Zn^{2+} inhibits longistatin. Since hydrolysis of peptide bonds is irreversible, proteases are controlled by several regulatory machineries to prevent unnecessary enzymatic activities. Indeed, various endogenous protease inhibitors, activators and ions participate to regulate precisely and timely the hydrolysis of peptide bonds by proteases (119). Possibly, Zn^{2+} acts as a regulatory switch of longistatin, consistent with extracellular S100 EF-hand proteins that display an unusually high affinity for Zn^{2+}, and Zn^{2+} plays regulatory roles (71, 73). However, Zn^{2+} also inhibits a few serine proteases such as kallikreins (118, 120). Collectively, the substrate and inhibitor specificities of longistatin strongly suggest that longistatin behaves like a serine protease. Longistatin may have non-conserved catalytic machinery that functions in a similar fashion to the conserved catalytic triad of traditional serine proteases.

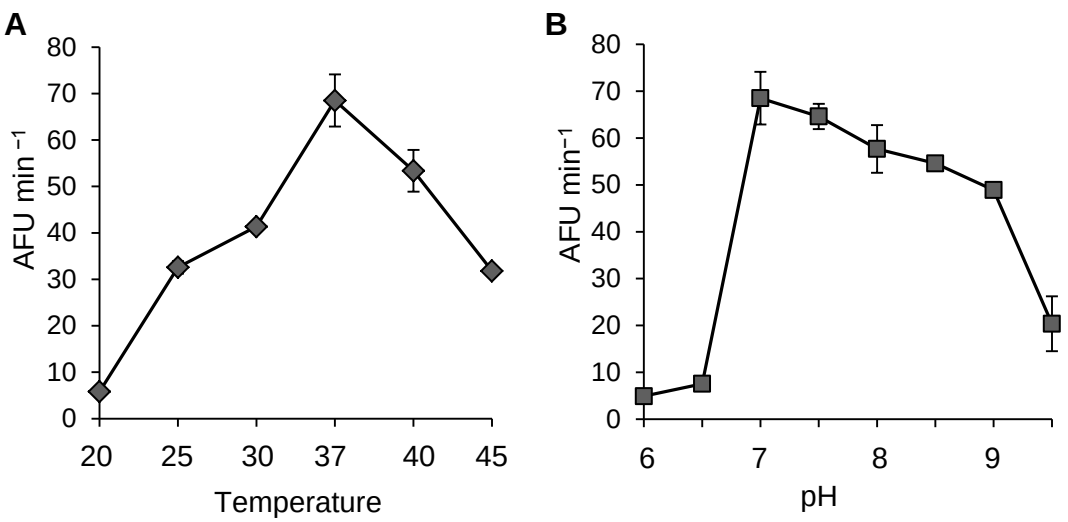

Figure 8. Effects of temperature and pH on the enzymatic activity of longistatin. (A) Effect of temperature. Longistatin (6 µg) and Boc-VPR-MCA, an α-thrombin specific substrate, (200 µM, final concentration) were incubated at different temperature (20−45 ºC) and pH 7 in buffer A and substrate hydrolysis was monitored by measuring excitation and emission wavelengths of 360 nm and 460 nm, respectively, as described in the Materials and Methods. Catalytic activity was maximum at 37 ºC. (B) Influence of pH. Longistatin (6 µg) and Boc-VPR-MCA (200 µM) were incubated at different pH (6−9.5) and at 37 ºC in an appropriate buffer and substrate hydrolysis was monitored as mentioned above. Catalytic activity of longistatin was maximum at pH 7. Data were presented as mean±SD, n=3. AFU, arbitrary fluorescent unit.

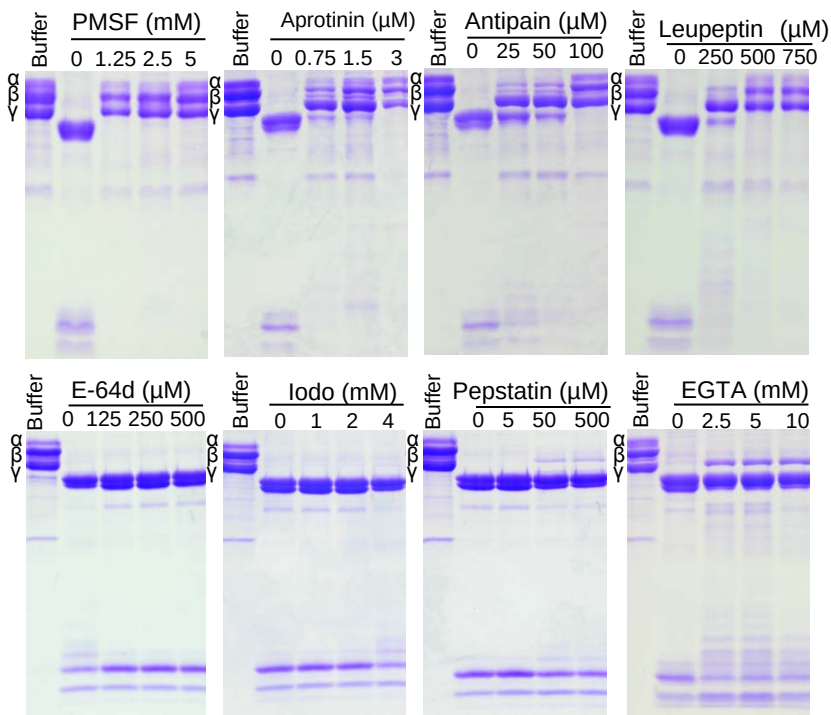

Figure 9. Effects of protease inhibitors on longistatin. Longistatin (2.5 μg) was pre-incubated with various protease inhibitors at indicated concentrations at 37 ºC for 1 h and then fibrinogen was added (7.5 mM, final concentration) and incubated further for 48 h as described in the Materials and Methods. Aliquots were collected and separated by 12.5% SDS-PAGE gels under reducing conditions. Gels were stained with CBB. Fibrinogenolytic activity was efficiently inhibited by serine protease inhibitors.

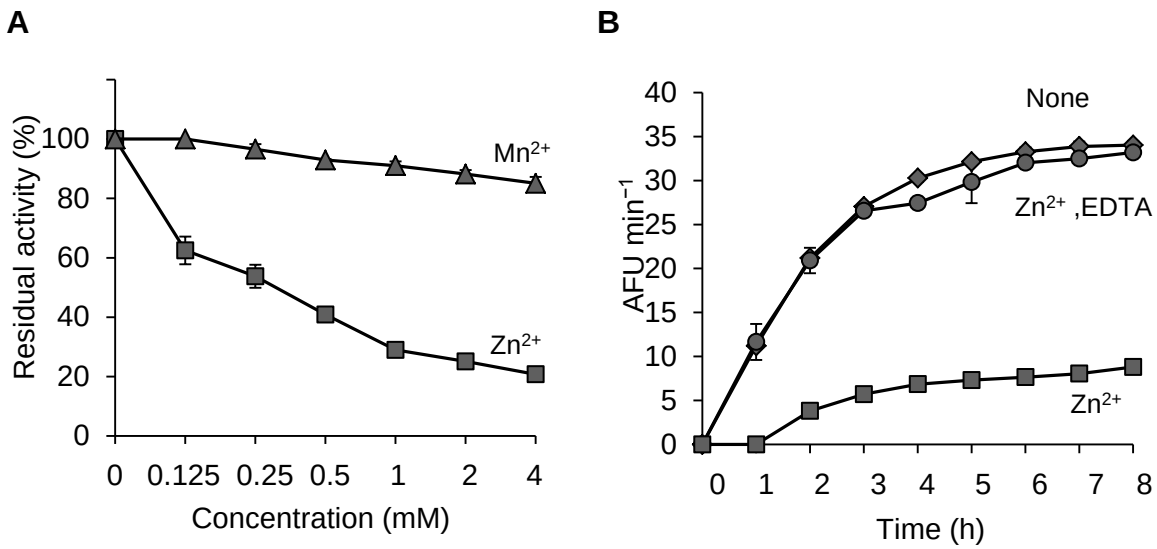

Figure 10. Effects of Zn^{2+} and Mn^{2+} on longistatin, and reversal by EDTA. (A) Longistatin was inhibited by Zn^{2+} and Mn^{2+}. Longistatin (6 µg, metal contaminant free) was pre-incubated in the absence or presence of $ZnCl_2$ (0−4 mM) and $MnCl_2$ (0−4 mM) in 100 µl of 50 mM Tris-HCl (pH 7) at 37 ºC for 15 min and residual activity was judged using Boc-VPR-MCA, an α-thrombin specific substrate (200 µM, final concentration) by measuring excitation and emission wavelengths of 360 nm and 460 nm, respectively, as described in the Materials and Methods. (B) Inhibitory effect of Zn^{2+} was reversed by EDTA. Longistatin (6 µg, metal contaminant free) was pre-incubated in the absence or presence of $ZnCl_2$ (10 mM) at 37 ºC for 15 min and then EDTA (50 mM, final concentration) was added and incubated further for 15 min under the same conditions. Residual activity was judged using Boc-VPR-MCA (200 µM) as mentioned above. Data are presented as mean±SD, n=3. AFU, arbitrary fluorescent unit.

Table 1. Hydrolysis of synthetic substrate

Substrates	**Specific enzyme**	**Enzyme group**	V_{max} **(μM/min)**	K_m **(μM)**	k_{Cat} **(S^{-1})**	k_{Cat}/K_m **(M^{-1} S^{-1})**
Boc-VPR-MCA	α-Thrombin	Serine protease	5.3×10^{-2}	58.35	1.7×10^{-4}	2.97
Pyr-GR-MCA	t-PA/u-PA		9.5×10^{-2}	155.23	3.1×10^{-4}	2
Boc-QAR-MCA	Trypsin		5.4×10^{-2}	133.35	1.18×10^{-4}	0.88
Suc-AAPF-MCA	Chymotrypsin		NH	ND	ND	ND
Boc-EKK-MCA	Plasmin		NH	ND	ND	ND
Suc-AAA-MCA	Elastase		NH	ND	ND	ND
Suc(OME)-AAPV-MCA	Elastase		NH	ND	ND	ND
Z-AAN-MCA	Legumain	Cysteine protease	NH	ND	ND	ND
Ac-DNLD-MCA	Cathepsin D	Aspartic protease	NH	ND	ND	ND

Substrates were incubated in the absence or presence of longistatin (6 μg) in a total volume of 100 μl in buffer A. Substrate hydrolysis was monitored by measuring excitation and emission wavelengths of 360 nm and 460 nm, respectively, using a Spectra Fluor fluorometer (TECAN) as described in Materials and Methods. Catalytic constants were calculated by Lineweaver-Burk plot. NH, not hydrolyzed; ND, not done. Three independent experiments with three replicates were performed in each assay.

Table 2. Interaction of longistatin with various inhibitors

Inhibitors	**Types of inhibitor**	**Concentration**	**Inhibition (%)**	**IC_{50} (μM)**
Aprotinin	Serine protease	3 μM	94.52	0.35
Antipain		100 μM	79.2	41.56
Leupeptin		1 mM	82.8	198.86
PMSF		5 mM	100	278.57
Chymostatin		1 mM	1.06	-
Iodoacetamide	Cysteine protease	4 mM	5.0	-
E6-4d		500 μM	0	-
Pepstatin	Aspartic protease	500 μM	4.5	-
EDTA	Metalloprotease	10 mM	7.35	-
EGTA		10 mM	13.65	-

Longistatin (6 μg) was pre-incubated in the absence or presence of various inhibitors at the indicated concentrations for 1 h at 37 °C and diluted immediately with buffer A (50 mM Tris-HCl, 100 mM NaCl and 5 mM $CaCl_2$). Boc-VPR-MCA, an α-thrombin specific substrate, (200 μM, final concentration) was added in each well, and substrate hydrolysis was monitored using a Spectra Fluor flurometer (TECAN) as mentioned in the Materials and Methods section. Three independent experiments with three replicates were performed in each assay.

Chapter 3

Longistatin activates plasminogen and degrades fibrinogen of hosts

1. Introduction

Blood coagulation is a very complex but a well-synchronized biochemical process by which blood forms a clot and the damaged blood vessel is sealed by a platelet-rich fibrin plug leading to hemostasis. Any damage to the vascular beds due to laceration of tissues exposes tissue factor from the endothelium to the circulating blood, which initiates coagulation cascades. Once coagulation is initiated, the process leads to the generation of thrombin, which converts fibrinogen to fibrin, the building block of a hemostatic plug (46, 121−124). In contrast, fibrinolysis is an enzymatic process wherein a fibrin clot is dissolved. Normally, in the body, both coagulation and fibrinolytic processes are precisely regulated by the measured participation of zymogens, activators, inhibitors, cofactors and receptors. Plasmin is the major fibrinolytic enzyme and is derived from the limited proteolytic cleavage of plasminogen, the circulating plasma zymogen, by its physiological activators such as tissue-type plasminogen activator (t-PA) and urokinase-type plasminogen activator (u-PA) (104, 123, 125, 126). Homeostasis in blood fluidity is not only vital for humans but also for hematophagous animals, which have to counteract their hosts' hemostatic mechanisms and/or facilitate the fibrinolytic processes to keep the blood in a fluid state during acquisition and digestion of blood-meals. Therefore, it is believed that blood sucking-animals

require an extensive spectrum of anticoagulantion and/or fibrinolytic mechanisms to maximize their feeding as part of their diverse survival strategies. Thus, hematophagous animals are thought to possess anticoagulant and/or fibrinolytic proteins that have been acquired during their evolution (46, 49, 53).

Previous literatures regarding blood-feeding physiology suggest that ixodid ticks produce a diverse group of bioactive molecules that are injected into the feeding lesions during persistent feeding processes. These molecules are thought to play crucial modulatory roles in their feeding success, especially to keep the blood in a fluid state in the blood pool and within the gut as well (47, 54−57). However, the key molecule that prevents blood coagulation as well as initiates fibrinolysis in the blood pool; thus, facilitate successful acquisition of blood-meals is still unclear. In the Chapter 1, I have shown that longistatin, an ixodid tick salivary gland-derived bioactive molecule, is functionally linked to the blood-feeding processes. The molecule was shown to be secreted into the blood pool created by ticks while they attach on a robust mammalian host and suck blood to engorge.

Here, I demonstrate that longistatin binds with fibrin and specifically catalyzes the activation of plasminogen into plasmin, and hydrolyzes fibrinogen *in vitro*; the latter is known to be a major component of cross-linked fibrin polymer. Longistatin is the first plasminogen activator isolated and characterized from ticks.

2. Materials and Methods

2.1. Anticoagulation and fibrinogenolytic assays

Fibrinogen (7.5 mM, final concentration, Sigma) was pre-incubated in a total volume of 397 µl of buffer containing 25 mM Hepes (pH 7.2) and 25 mM NaCl in the absence or presence of longistatin (0.1, 0.2, 0.4, 0.8 and 1.6 µM) or plasmin (1.6 µM, Sigma) at 25 °C for 3 h. Fibrin clot formation was initiated by the addition of 3 µl of thrombin (0.10 NIH unit/µl, Sigma). Fibrin clot

formation was detected visually and also by determining changes in turbidity at OD_{450} using a spectrophotometer (Beckman Coulter) at 15 min intervals. To detect the fibrinogenolytic activity of longistatin, fibrinogen (7.5 mM , final concentration) was incubated in a total volume of 100 µl of buffer (25 mM Hepes, pH 7.2, and 25 mM NaCl) in the absence or presence of longistatin (0.4, 0.8 and 1.6 µM) or plasmin (1.6 µM) at 25 °C for 48 h. Aliquots were collected and separated by 12.5% SDS-PAGE under reducing condition.

2.2. Plasminogen activation assays

Longistatin at various concentrations (40, 80, 160, 320 and 640 nM, final concentration) was incubated in a 96-well cell culture plate without or with plasminogen (0.24 units, Calbiochem) in the absence or presence of fibrin CNBr fragments (0.25, 1 and 4 µg, Technoclone) in a total volume of 200 µl of buffer A (50 mM Tris-HCl, pH 7.5; 100 mM NaCl and 5 mM $CaCl_2$) at 25 °C for 2 h. Then, 2 µl (100 µM, final concentration) of plasmin-specific fluorogenic substrate (Boc-Glu-Lys-Lys-MCA, Peptide Institude) was added. Substrate hydrolysis was monitored by measuring excitation and emission wavelengths of 360 nm and 460 nm, respectively, at 15 min intervals using a Spectra Fluor fluorometer (TECAN). All assays were performed in triplicate and activity of activated plasminogen was expressed in an arbitrary fluorescent unit per min (AFU/min).

2.3. Fibrinolytic assays

Fibrin clot was incubated in the presence or absence of longistatin. An initial fibrin clot was produced by incubating 10 µl of fibrinogen (7.5 mM, final concentration) and 5 µl of thrombin (0.10 NIH unit/µl) in a total volume of 400 µl of buffer A (50 mM Tris-HCl, pH 7.5; 100 mM NaCl and 5 mM $CaCl_2$) at 25 °C for 1 h. An equal volume of plasminogen (2.4 units), t-PA (154 nM, Calbiochem) or longistatin at various concentrations (40, 80, 160, 320 and 640 nM) in a total volume of 100 µl of buffer, as mentioned above, was added to the fibrin clot and incubated at 25 °C for 24 h. Lysis of fibrin clot was detected visually and also by measuring changes in turbidity at

OD_{450} using a spectrophotometer (Beckman Coulter) at different time intervals (0, 6, 12 and 24 h). Furthermore, to verify the plasminogen activation potential of longistatin, 20 µl of digested products of clots corresponding to each concentration were collected and subjected to 12.5% SDS-PAGE analysis under reducing conditions.

2.4. Fibrin clot binding assays

Fibrin binding assays were conducted with the modifications of procedures described previously (120). Briefly, purified fibrinogen (3.75, 7.5, 15, 30 and 60 mM; final concentration) was mixed in the absence or presence of longistatin (10 µg) or an equal amount of t-PA (Calbiochem) or u-PA (Cosmo Bio Co. LTD, CA, USA) in a total volume of 200 µl of buffer A (50 mM Tris-HCl, pH 7.5; 100 mM NaCl and 5 mM $CaCl_2$). Fibrin clot formation was initiated by adding 3 µl of thrombin (0.10 NIH unit/µl) immediately and was incubated at 25 °C for 1 h. The clot was centrifuged at 10,000 × *g* for 10 min and supernatant was collected. The remaining clot was extensively washed in PBS and treated with anti-longistatin (1: 100), anti-t-PA (1: 100, Calbiochem), anti-u-PA (1: 20, Acris Antibodies GmBH, CA, USA) or pre-immune sera (1: 100) overnight at 4 °C. Bound antibodies were detected using a green fluorescent-labeled secondary antibody. Supernatant was analyzed by 12.5% SDS-PAGE under reducing conditions. The target protein band was excised and protein was extracted from the gel using a negative zinc staining kit following the manufacturer's instructions (Bio-Rad, CA, USA). Double volume of cold (−20 °C) acetone was mixed thoroughly with the extracted protein, incubated at −20 °C for 1 h and centrifuged at 10,000 × *g* for 30 min. The pellet was air-dried and dissolved with distilled water. The concentration of the extracted protein was determined using micro-BCA reagents (Pierce). To determine the binding parameters, longistatin (2−10 µg) or an equal amount of t-PA was incorporated into the fibrin clot. Residual longistatin/t-PA was extracted from the supernatant and the concentration of the relevant protein was determined following the same methods as mentioned

above. K_d, B_{max} and molar binding ratio (MBR) were calculated according to the procedures as previously described (128).

2.5. Ex vivo thrombolysis assays

Platelet-rich thrombi were produced by incubating 0.2 ml of fresh dog blood in a 96-well flat-bottom cell culture plate for 15 min. Thrombi were removed and washed gently with normal saline and weighed using a digital balance (Sartorius). The thrombi were then treated with t-PA (154 nM) or longistatin at various concentrations (40, 80, 160, 320 and 640 nM) in a total volume of 0.5 ml of fresh dog plasma at 37 °C for 12 h and weighed at 3 h intervals. Furthermore, fibrin clot was produced by incubating purified, commercially available fibrinogen (7.5 mM) and thrombin (0.10 NIH unit/µl) as mentioned above and was treated with t-PA (154 nM) or longistatin (640 nM) in fresh dog-plasma following the same experimental procedures and conditions.

2.6. Statistical analysis

Data were presented as mean±SD, where appropriate. Statistical significance was determined using the Student's *t* test with unequal variance.

3. Results

3.1. Longistatin degrades fibrinogen and delays fibrin clot formation

To judge the anticoagulant activity, longistatin was reacted with several coagulation factors (viz., fibrinogen, thrombin, factors VIIa and Xa) using different approaches but none of them was affected by longistatin except fibrinogen. Interestingly, longistatin was found to delay fibrin clot formation, degrade fibrinogen and efficiently activate plasminogen into its active form, plasmin; a terminal protease of the fibrinolytic pathways. To evaluate the anticoagulation potential of longistatin, fibrinogen (7.5 mM) was pre-incubated in the absence or presence of longistatin (0.1, 0.2, 0.4, 0.8 and 1.6 µM) or plasmin (1.6 µM) and then thrombin (0.10 NIH unit/µl) was added as

described in the Materials and Methods. Longistatin significantly ($p<0.01$) interrupted the normal fibrin clot formation in a concentration-dependent manner. In the absence of longistatin, fibrin clot was formed within 15 min, but in the presence of longistatin (1.6 μM) or plasmin (1.6 μM), no visible clot was developed within this time (Figure 11A). Longistatin was shown to delay the formation of a visible fibrin clot. Fibrin clotting time was significantly extended (up to 90 min) at a concentration of 1.6 μM longistatin (Figure 11B), indicating potent anticoagulant activity of longistatin. To explore the fibrinogenolytic potential, fibrinogen was incubated in the absence or presence of longistatin (0.4, 0.8 and 1.6 μM) or plasmin (1.6 μM) and was subjected to SDS-PAGE analysis. Longistatin potently degraded the α, β and γ chains of fibrinogen in a concentration-dependent manner. Longistatin completely hydrolyzed all three chains of fibrinogen at 1.6 μM concentration, as it was done by 1.6 μM plasmin (Figure 11C), implying that longistatin is an efficient fibrinogenolytic protease of ixodid ticks.

3.2. Longistatin activates plasminogen in the presence of soluble fibrin

Initially, I determined the plasminogen activation potential of longistatin by measuring the amidolytic activity of activated plasminogen on the plasmin-specific fluorogenic substrate. Data revealed that the initial rate of plasminogen activation was proportional to the concentration of longistatin. Hydrolysis of the plasmin-specific substrate sharply increased with the increase of concentration of longistatin. However, longistatin alone, even at a higher concentration (640 nM), was not able to induce hydrolysis of plasmin-specific fluorogenic synthetic substrate (Figure 12A), indicating that longistatin activated plasminogen into its active form, plasmin, which hydrolyzed the synthetic substrate releasing MCA. Most interestingly, plasminogen activation potential of longistatin was significantly increased in the presence of soluble fibrin (firbin CNBr fragments) and induced robust amidolytic activity. Addition of fibrin CNBr fragments (4 μg) to the assay mixture caused an increase of plasminogen activation rate up to 4 times higher than that in the

absence of fibrin CNBr fragments (Figure 12B). CNBr fragments of fibrin, the soluble fibrin, is usually regarded as a t-PA stimulator and increases the rate of plasminogen activation about 5 times (129, 130). Plasminogen was sparingly affected by longistatin in the absence of soluble fibrin (Figure 12B), indicating the extraordinary specificity of longistatin towards fibrin-bound plasminogen rather than free circulating plasminogen.

3.3. Longistatin is able to lyse fibrin clot by activating plasminogen

Although plasmin has an enzymatic activity towards a broad spectrum of substrates, but the fibrin clot is considered as its main native substrate (131). To further evaluate the plasminogen activation efficiency of longistatin, fibrin polymer was incubated with plasminogen-longistatin/-t-PA mixture or with buffer only at 25 °C for 24 h. Data revealed that, in the presence of either longistatin or t-PA, plasminogen was able to induce lysis of fibrin clot. Visual observation and spectrometric analysis at 450 nm (OD_{450}) revealed that the fibrinolytic potential of plasminogen, in the presence of longistatin, was directly proportional to the concentration of the recombinant protein used. These results firmly suggest that longistatin activates plasminogen to an active form, plasmin in a concentration-dependent manner, which in turn lyses the visible fibrin clot. Longistatin caused complete lysis of fibrin clot in the nanomolar range (Figures 13A and B). SDS-PAGE analysis showed that longistatin efficiently cleaved plasminogen into its heavy and light chains. These results are comparable to those of purified, active and commercially available t-PA (Figure 13C). Here, it was also observed that longistatin activated a sufficient amount of plasminogen only in the presence of fibrin clot and induced profound fibrinolysis (data not shown).

3.4. Longistatin binds with fibrin

To explore the fibrin-binding capability of longistatin, I conducted fibrin-binding assays. Longistatin-specific green fluorescence was detected in the fibrin meshwork when purified recombinant longistatin was incorporated with fibrin and reacted with anti-longistatin sera.

However, longistatin-specific fluorescent reaction was completely absent in the absence of longistatin in the reaction mixture or when longistatin-impregnated fibrin meshwork was treated with pre-immune sera (1: 100), indicating that longistatin is able to bind with fibrin clot. To compare the fibrin binding of longistatin, I used t-PA as a positive control because t-PA is known to bind with fibrin (127). Here, t-PA-specific fluorescence was only detected when t-PA added fibrin was treated with anti-t-PA mouse monoclonal antibody (1: 100), but no such reaction was visible in the presence of pre-immune sera (normal sera) at the same concentration. To evaluate the specificity of the fibrin-binding assays, I used u-PA as a negative control because u-PA does not bind with fibrin (103). u-PA-specific reaction was not detected in the fibrin meshwork even in the presence of a relatively high concentration (1: 20) of anti-u-PA antibody (Figure 14A). SDS-PAGE analysis also revealed that the concentration of residual longistatin was markedly reduced after fibrin clot formation (Figure 14B), which reinforced the assertion that longistatin was bound with the fibrin clot. Furthermore, I determined the concentration of longistatin/t-PA in the supernatant obtained from the fibrin-binding assay mixer and data showed that the percentage of binding of longistatin/t-PA with fibrin meshwork was directly proportional to the amount of fibrin. Longistatin binding was 97.93%±1.68% when 60 mM fibrinogen was used to produce fibrin clot and, under the same conditions, binding of t-PA was 90.6%±1.2%. Specificity of the binding was evidenced by the absence of u-PA binding (Figure 14C). To evaluate the fibrin-binding potentials of longistatin, I determined the fibrin-binding parameters of longistatin and compared them with those of t-PA. Longistatin was shown to bind with fibrin with the estimated K_d, B_{max} and MBR of 145.5±3.3 nmol/L, 3.1±0.6 μmol/L and 42.3±7.4, whereas those of t-PA were 159.2±7.4 nmol/L, 1.4±0.4 μmol/L and 19.3±4.7, respectively (Table 3), suggesting that longistatin potently binds with fibrin. Fibrin binding is an essential feature for the plasminogen activators that specifically activate fibrin clot-bound plasminogen. For example, t-PA is a very weak activator of plasminogen in the absence of fibrin. The affinity between t-PA and plasminogen is significantly increased in

the presence of fibrin of blood clot (104, 132). Fibrin binding was also assumed as critical in the activation process of plasminogen by longistatin.

3.5. Longistatin activates plasminogen present in plasma milieu and induces thrombolysis

To demonstrate the thrombolytic capability of longistatin, I treated freshly prepared platelet-rich thrombi kept in fresh plasma. Longistatin was able to cause lysis of platelet-rich thrombi in the presence of fresh plasma in a concentration-dependent manner and efficiently lysed thrombi at 640 nM concentration (Figure 15A). Longistatin induced more than 50% lysis of thrombi within 2 h at 640 nM concentration (data not shown). In the same experimental setup, longistatin (640 nM) and t-PA (154 nm) induced 93.62%±2.33% and 98.78%±2.11% lysis of thrombi, respectively, by 12 h (Figure 15B). Moreover, like t-PA, longistatin efficiently digested fibrin clot produced from purified, commercially available fibrinogen and thrombin in the presence of plasma (data not shown). Taken together, the results suggest that longistatin is capable of causing thrombolysis and subsequent recanalization of occluded thrombosed vascular tree by activating the physiological level of plasminogen into plasmin.

4. Discussion

Previous works on the feeding behavior and physiology of ixodid ticks suggest that acquisition of blood-meals from mammalian hosts is modulated by a vast array of pharmacologically active biomolecules secreted from the salivary glands of these amazing tiny arthropods. Ticks' saliva is thought to efficiently manipulate the hosts' strong defense mechanisms, such as hemostasis, inflammatory reactions and immune responses that are induced against the tick during hematophagy (46, 54, 133−135). In the present study, I provide evidence that longistatin, a salivary-gland protein with two functional EF-hand Ca^{2+}-binding domains isolated from *H. longicornis* binds with fibrin and specifically activates plasminogen to its active form, plasmin. I

also demonstrate that longistatin degrades fibrinogen and is able to delay fibrin clot formation; thus, longistatin appears to be essential to keep the blood in a fluid state in the blood pool, which enables ticks to feed and replete on blood-meals from hosts.

To verify the hypothesis, several anticoagulation and fibrinolysis assays were conducted. Interestingly, I have shown that longistatin significantly extends the time of fibrin clot formation up to 90 min when fibrinogen is treated with longistatin compared with untreated fibrinogen (control), which takes only 15 min to complete fibrin clot formation. Data on fibrinogenolytic assays also support this observation that longistatin is capable of degrading the α, β and γ chains of fibrinogen in a concentration-dependent manner and completely hydrolyzes these three bands. Therefore, it may be assumed that the delay in the fibrin clot formation during *in vitro* anticoagulation assays in the presence of longistatin is due to the gradual degradation of coagulable proteins in the reaction mixture. Fibrinogenolytic activity has also been reported in tick metalloprotease isolated from *Ixodes scapularis* (136) and in several proteases identified from snake venoms (137) and spider toxins (138). Fibrinogen is the key component for the formation of cross-linked fibrin polymer. In general, after laceration of blood vessels, platelets are exposed to the subendothelial collagen and become activated and aggregated around the injuries. Then, fibrin strands, derived from cleavage of fibrinogen, intertwine about the aggregated platelets giving rigidity and stability of the initial and preliminary platelet plugs. Finally, activated factor XIII forms covalent bonds that crosslink the fibrin polymers; thus, the injured blood vessels are sealed by an extra strengthened, stable fibrin clot leading to hemostasis (46, 139, 140). Therefore, it may be predicted that fibrinogenase activity of longistatin hampers hemostasis and may facilitate hemorrhage into the blood pools from which ticks persistently feed blood-meals.

I have shown that longistatin specifically activated plasminogen in the presence of fibrin clot and cleaved it into plasmin, heavy chain (α) and light chain (β). Although plasminogen is unable to cleave fibrin clot but it has a strong affinity for fibrin. Plasminogen has a secondary

structure known as a kringle domain, which anchors plasminogen specifically to the carboxy-terminal arginine and lysine residues of the fibrin; thus, plasminogen becomes more concentrated on the surface of the clot, whenever and wherever it develops. As soon as plasminogen is converted into plasmin by its activators, it functions like a serine protease. Fibrin acts as a cofactor in the enzymatic activation reactions when plasminogen is activated by the fibrin-selective agents, like t-PA and its derivatives or staphylokinase and its derivatives. Through a highly orchestrated biochemical process, plasmin initially creates nicks on the fibrin and further digestion leads to the complete dissolution of fibrin meshwork into soluble fibrin degradation products (46, 103, 141). Results clearly demonstrate that longistatin contributes to this well-coordinated fibrinolytic pathway by activating plasminogen into plasmin. Plasminogen activators have been purified from the venomous snake, *Trimeresurus stejnegeri* (142) and from the saliva of common vampire bat, *Desmodus rotundus* (51, 143). In vampire bats, plasminogen activator is thought to be the key enzyme that plays a crucial role in the maintenance of the flow of blood during the feeding process (144) and snake-venom plasminogen activator is associated with the pathogenesis of envenomation rendering the blood incoagulable (142). Maintenance of hosts' blood fluidity at the site of biting is also very critical for the development of blood pool and subsequent blood-feeding, and eventually for the survival of ixodid ticks. From the available evidence, here I assume that fibrin-specific, plasminogen-activation-dependent thrombolytic potentiality of longistatin plays significant functional roles in the pathobiology of vector ticks through the formation of feeding lesion and by the maintenance of its homeostasis throughout the entire period of blood-feeding. Thus, longistatin helps in the successful acquisition of blood-meals and may be critical for the survival of ticks.

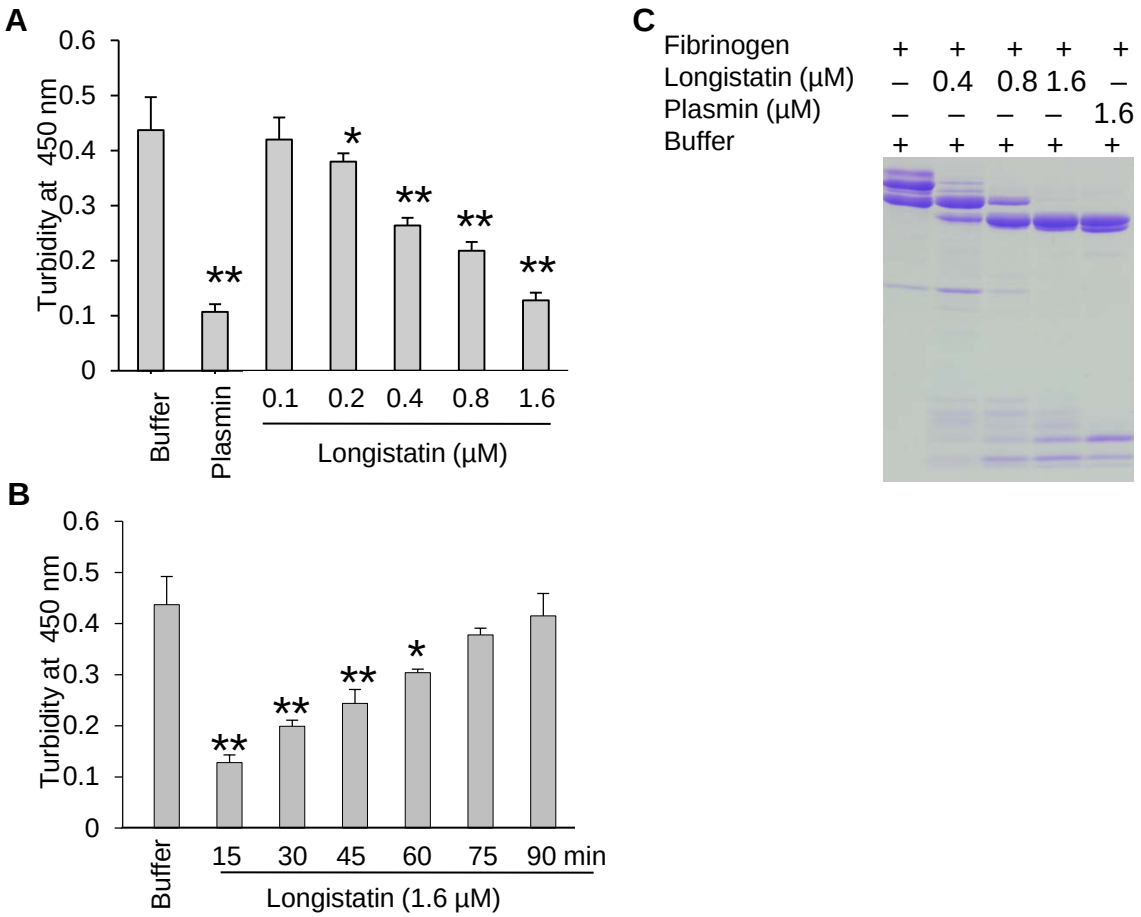

Figure 11. Anti-coagulation and fibrinogenolytic activity of longistatin. (A) Effects of longistatin on the formation of fibrin clot. Fibrinogen (7.5 mM) was pre-incubated in a buffer in the absence or presence of longistatin (0.1, 0.2, 0.4, 0.8 and 1.6 μM) or plasmin (1.6 μM) and then thrombin was added (0.10 NIH unit/μl) as described in the Materials and Methods. Clot formation was detected visually and also by determining changes in turbidity at OD_{450} using a spectrophotometer after 15 min. (B) Longistatin (1.6 μM) delayed fibrin clot formation up to 90 min. Fibrinogen was incubated in the absence or presence of longistatin (1.6 μM) following the same procedures as mentioned in A and then thrombin was added. OD_{450} was measured at 15 min intervals. (C) Fibrinogenolytic effect of longistatin. Fibrinogen (7.5 mM) was incubated in the absence or presence of longistatin (0.4, 0.8 and 1.6 μM) or plasmin (1.6 μM). Samples were collected at the indicated time period and were subjected to 12.5% SDS-PAGE analysis under reducing conditions. A gradual degradation of the α, β and γ chains of fibrinogen was detectable with the concomitant deposition of degraded products. Asterisks (*) indicate that the difference compared with the negative control group (buffer only) is significant as determined by the Student's *t*-test with unequal variance ($^{*}p<0.05$, $^{**}p<0.01$).

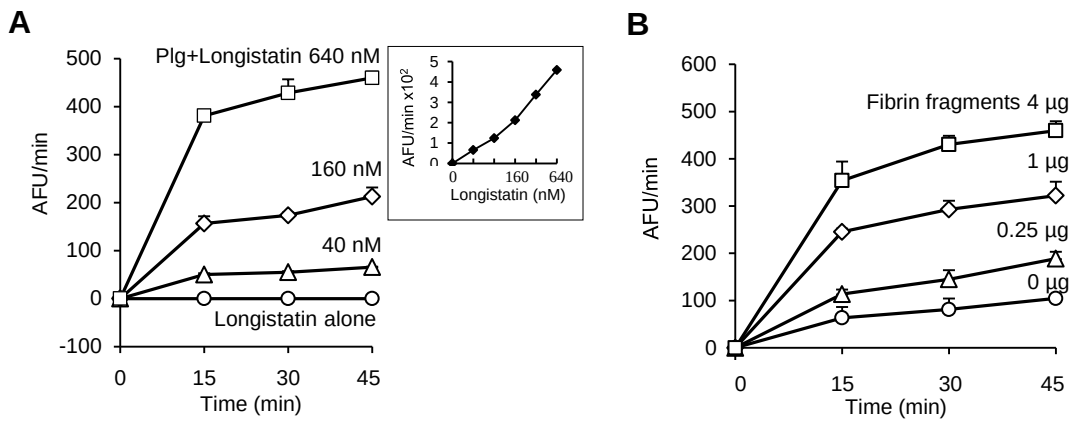

Figure 12. Plasminogen activation by longistatin. (A) Longistatin (40, 80, 160, 320 and 640 nM) was incubated without or with plasminogen (0.24 units) adding fibrin CNBr fragments (4 µg) in a total volume of 200 µl of buffer A (50 mM Tris-HCl, pH 7.5; 100 mM NaCl and 5 mM $CaCl_2$) at 25 ºC for 2 h. Then, plasmin-specific fluorogenic substrate (100 µM, final concentration) was added and substrate hydrolysis was monitored by measuring excitation and emission wavelengths of 360 nm and 460 nm, respectively, at 15 min intervals. *Inset*, initial rate of plasminogen activation at different concentrations of longistatin. (B) Effects of fibrin CNBr fragments on the activation of plasminogen by longistatin. Plasminogen (0.24 units) was incubated with longistatin (640 nM) in the absence or presence of fibrin CNBr fragments (0.25, 1 and 4 µg) as described in the Materials and Methods. All assays were performed in triplicate. AFU, arbitrary fluorescent unit.

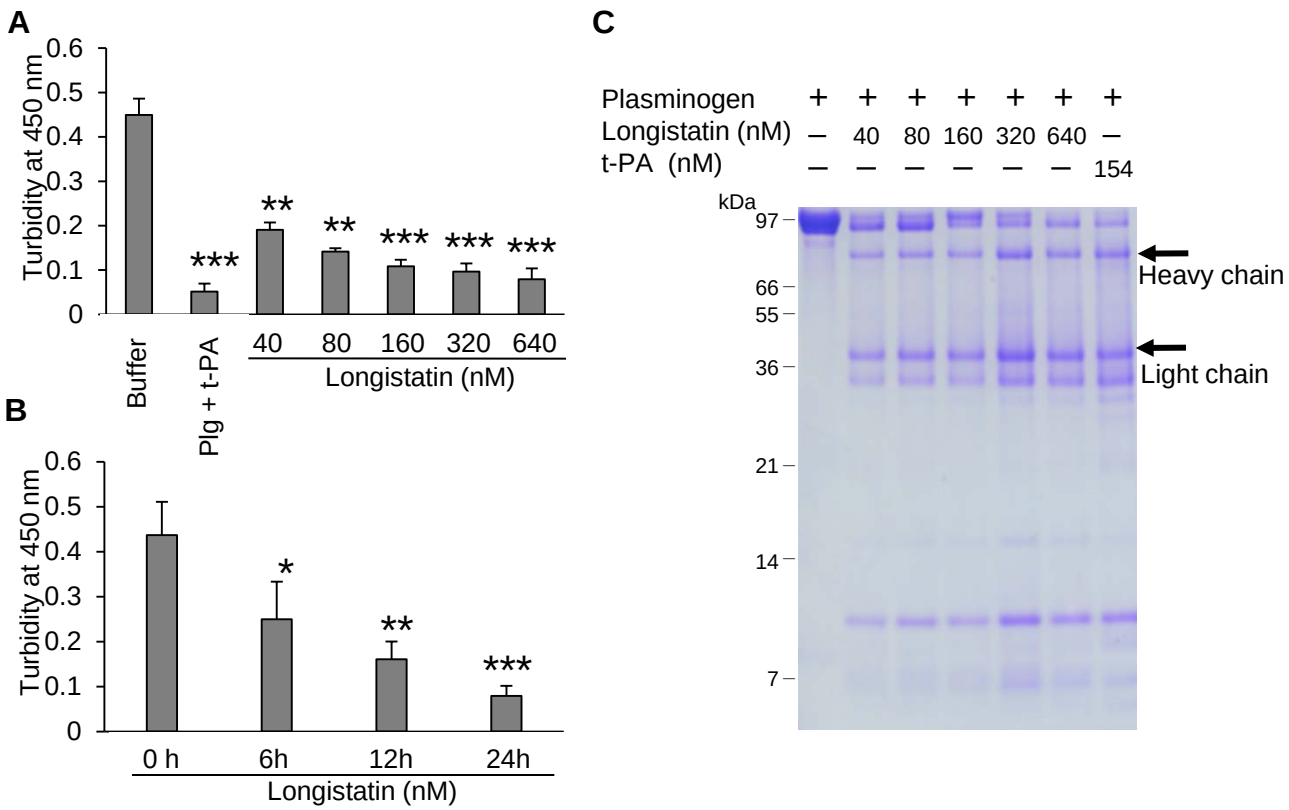

Figure 13. Longistatin induced fibrinolysis by activating plasminogen. (A) Fibrin clot was produced by incubating fibrinogen (7.5 mM) and thrombin (0.10 NIH unit/µl), and was incubated in the presence of plasminogen-t-PA/-longistatin (40, 80, 160, 320 and 640 nM) mixture or buffer only at 25 ºC for 24 h. Clot lysis was measured at OD_{450}. Plasminogen induced complete lysis of fibrin clot in the presence of 640 nM of longistatin or 154 nM of t-PA. (B) Time-dependent activation of plasminogen by longistatin with concomitant lysis of fibrin clot. (C) Cleavage of plasminogen into the heavy and light chains. Digested product of fibrin clot was electrophoresed by 12.5% SDS-PAGE under reducing conditions. Asterisks (*) indicate that the difference compared with the negative control group (buffer only) is significant as determined by the Student's *t*-test with unequal variance ($^{*}p<0.05$, $^{**}p<0.01$, $^{***}p<0.001$).

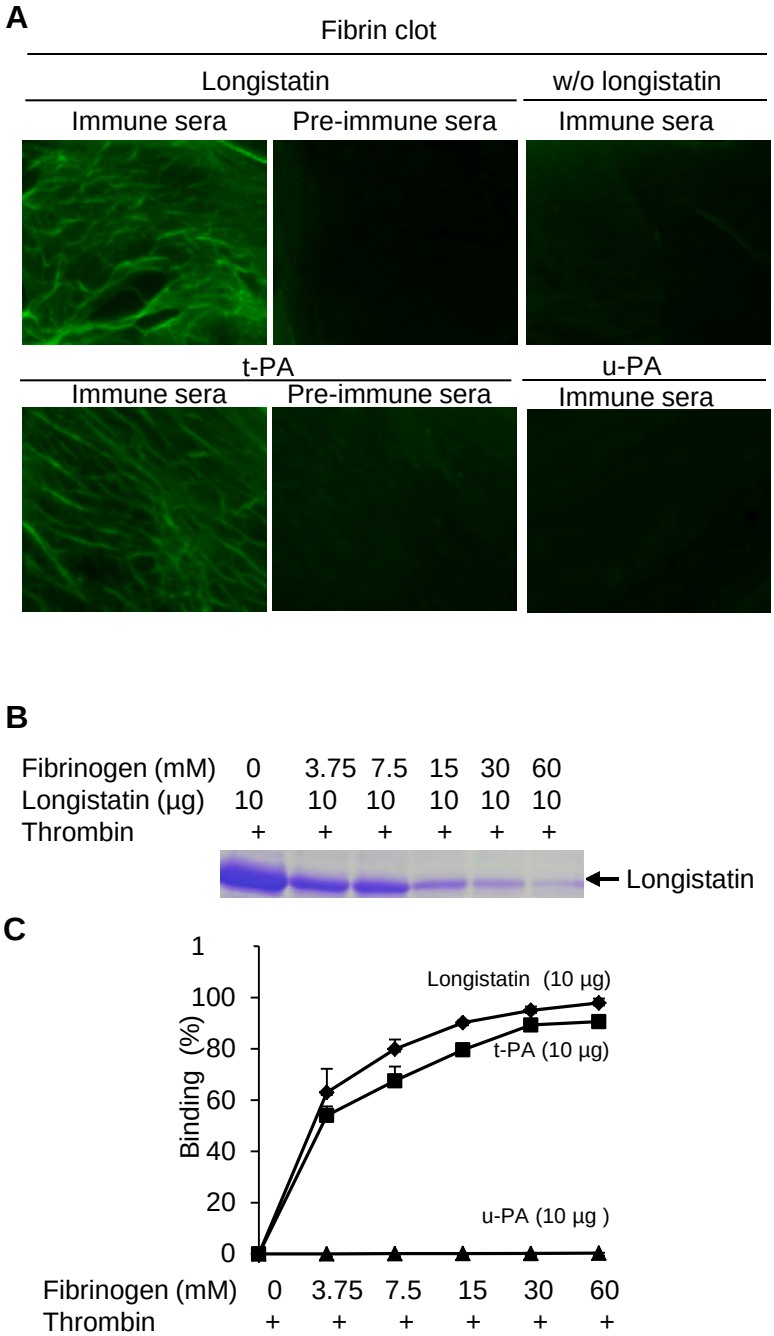

Figure 14. Binding of longistatin with fibrin clot. (A) Detection of longistatin bound on fibrin meshwork. Fibrinogen at different concentrations (3.75, 7.5, 15, 30 and 60 mM; final concentration) was mixed in the absence or presence of longistatin (10 μg) or an equal amount of t-PA or u-PA in a buffer (50 mM Tris-HCl, pH 7.5; 100 mM NaCl and 5 mM $CaCl_2$), and thrombin (0.10 NIH unit/μl) was added immediately and was incubated at 25 ºC for 1 h. The clot was treated with anti-longistatin (1: 100), anti-t-PA (1: 100), anti-u-PA (1: 20) or pre-immune sera (1: 100). Bound antibodies were detected using a green fluorescent-labeled secondary antibody (Alexa Flour® 488 goat anti-mouse IgG). (B) Supernatant was analyzed by 12.5% SDS-PAGE under reducing conditions. (C) The target protein was extracted from the supernatant and its concentration was determined using micro-BCA reagent as described in the Materials and Methods. Results were expressed as percentage of longistatin/t-PA/u-PA bound to the fibrin clot. Data represent mean±SD, n=3.

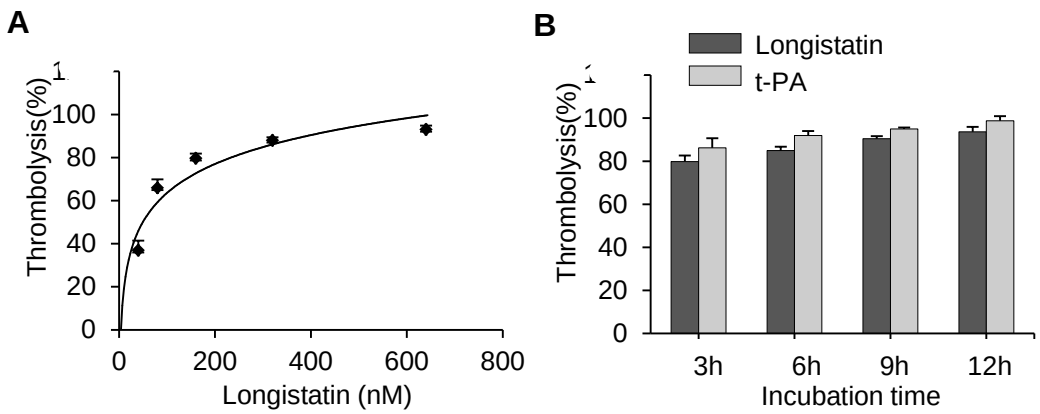

Figure 15. Lysis of platelet-rich thrombi by longistatin in dog plasma. (A) Longistatin hydrolyzes platelet-rich thrombi *ex vivo* in dog plasma. Platelet-rich clot was produced by incubating 0.2 ml of dog blood and the thrombi were treated with longistatin at various concentrations in 0.5 ml of dog plasma at 37 ºC for 12 h and weighed at the indicated period. (B) Comparison of thrombolytic activity of longistatin with that of t-PA. Thrombi were treated with longistatin (640 nM)/t-PA (154 nM) under the same *ex vivo* experimental conditions.

Table 3. Comparison of fibrin-binding parameters of longistatin with those of t-PA

Protein	**K_d (nmol/L)**	**B_{max} (µmol/L)**	**MBR[a]**
Longistatin	145.5±3.3	3.1±0.6	42.3±7.4
t-PA	159.2±7.4	1.4±0.4	19.3±4.7
	$p<0.05$	$p<0.01$	$p<0.01$

[a]Expressed as moles of longistatin/t-PA per mole of fibrin. Determined at maximum binding.

Chapter 4

Longistatin is relatively resistant to plasminogen activator inhibitor-1

1. Introduction

Thrombo-occlusive events including myocardial infarction, ischemic stroke, obstructive pulmonary disease and peripheral thromboembolism are major causes of morbidity and mortality in humans. Most countries are facing a high and increasing rate of cardiovascular diseases. In USA, heart diseases kill more people in each year than cancer does. In women, death due to cardiovascular diseases is higher than that caused by breast cancer (103, 145−151). Treatment of thrombo-occlusive diseases is one of the most challenging areas in medicine. Plasminogen activators (PAs) have great clinical significance as thrombolytic agents in the managements of cerebral and cardiac attacks (152, 153). PAs such as t-PA, u-PA and others activate plasminogen, a circulating plasma zymogen, into its active form plasmin, a powerful serine protease, which in turn dissolves thrombi and restores circulation in thrombosed vasculature; thus, rescue the affected tissues/organs from the devitalizing events of thrombosis (103, 104, 154−156). Among the PAs recommended for clinical use, t-PA is generally preferred for its relatively higher efficacy and wider safety window compared to u-PA and streptokinase. However, both t-PA and u-PA are rapidly inactivated by the fast-acting serine protease inhibitor (serpin) plasminogen activator

inhibitor-1 (PAI-1), a molecular switch of physiologic PAs, and is the major PAI in the serum (157−162). PAI-1 plays crucial roles in the regulation of PA mediated thrombolysis. PAI-1 is synthesized and secreted by a variety of cells such as endothelium, adipocytes, monocytes/macrophages, fibroblasts, cardiomyocytes, hepatocytes, smooth muscle cells, granulosa cells and megakaryocytes, and stored in the α-granules of platelets, and is released following activation of platelets (163−167). PAI-1 forms a tight complex with PAs and rapidly neutralizes them. In fact, exogenous PAs have to work after saturating the PAI-1 and other serpins present in serum that hinder thrombolytic therapy to a some extent (127, 156, 168). Therefore, development of PAI-1 resistant PA is essential for the betterment of the effective thrombolytic therapy.

In the chapter 3, I have shown that longistatin, a novel salivary gland protease from ticks, activates fibrin clot bound plasminogen; thus, induces fibrinolysis. Here, I show that longistatin is relatively resistant to SDS-treated platelet lysate. Longistatin is refractory to the inhibitory effects of activated, purified and commercially available PAI-1. Longistatin sufficiently activated plasminogen to plasmin in the presence of PAI-1 (20 nM), and completely hydrolyzed fibrin clot. Furthermore, longistatin does not form any complex with PAI-1.

2. Materials and Methods

2.1. Blood collection and preparation of plasma and serum

Blood samples were collected from fully consented healthy volunteers into EDTA-treated tubes. Platelet-rich plasma (PRP) and platelet-poor plasma (PPP) were produced following the procedures as described previously (169) with slight modifications. Briefly, PRP was produced by centrifuging blood at 100 × *g* and 23 °C for 10 min, and supernatant was collected. To prepare PPP, PRP was chilled at 4 °C for 15 min and centrifuged at 2000 × *g* and 4 °C for 30 min, and supernatant was carefully collected without disturbing the pellet. To prepare serum, 1 ml of either

whole blood, PRP or PPP was treated with 5 µl of thrombin (0.1 NIH unit/µl, Sigma) and incubated at 37 °C for 1 h. The clot was centrifuged at 10,000 × *g* and 4 °C for 30 min and supernatant was collected. Plasma and serum were stored at –20 °C until further use.

2.2. Preparation of platelet lysate

PRP (1 ml) from human blood was chilled at 4 °C for 15 min and centrifuged at 2000 × *g* and 4 °C for 30 min; then, PPP was aspirated. The pellet was extensively washed with PBS. The platelets were incubated with thrombin (0.5 U/ml, final concentration) at 37 °C for 6 h in Tyrode's buffer (pH 6.5). The platelets were sonicated with an ultrasonic processor (VP-5S, TAITEC) for 2 min on ice with 3 pauses each of 25 seconds, and centrifuged at 22,300 × *g* and 4 °C for 1 h. Supernatant was collected and treated with 0.1% SDS at 37 °C for 1 h; then, SDS was neutralized by treating with 1% Triton × 100 at 4 °C for 1 h as described previously (170). SDS-treated platelet lysate was stored at –20 °C until further use.

2.3. Treatment of longistatin with platelet lysate

An equal amount (1 µg) of longistatin, t-PA (Calbiochem) or tcu-PA (CosmoBio Co. LTD) was reacted with various amount of SDS-treated platelet lysate (0–30 µg/ml) in a total volume of 25 µl of buffer A (50 mM Tris-HCl, pH 7; 100 mM NaCl and 5 mM $CaCl_2$) at 37 °C for 15 min. Then, the mixture was immediately diluted with buffer A. Plasminogen (5 µl, 0.2 µg/µl, Sigma) was added in the reaction mixtures and incubated at 37 °C for further 1 h in the absence (incase of tcu-PA) or presence (incase of t-PA/longistatin) of soluble fibrin (8 µg/ml, Technoclone). Residual activity of the PAs was determined employing indirect fluorogenic assays using a plasmin-specific synthetic substrate (Boc-Glu-Lys-Lys-MCA, Peptide Institute). Substrate hydrolysis was monitored by measuring excitation and emission wavelengths of 360 nm and 460 nm, respectively, using a Spectra Fluor fluorometer (TECAN). Percentage of inhibition of the enzyme was calculated using the following formula:% inhibition = (1 − inhibited rate/uninhibited rate) × 100,

and IC_{50} was determined as described previously (87).

2.4. Inhibition of longistatin with PAI-1

An equal amount (1 μg) of longistatin, t-PA or u-PA was incubated with commercially available, activated PAI-1 (ITSI Bioscience, PA, USA) at various concentrations (0−90 nM) at 37 °C for different time (0−180 min) in a total volume of 25 μl of buffer A. Then the reaction mixture was immediately diluted adding buffer A and residual activity was determined using a synthetic substrate specific for t-PA/u-PA (Pyr-Gly-Arg-MCA, Peptide Institute). Substrate hydrolysis was monitored by measuring excitation and emission wavelengths of 360 nm and 460 nm, respectively, using a Spectra Fluor fluorometer (TECAN). Percentage of inhibition of the enzyme and IC_{50} were determined as described above.

2.5. Microplate clot lysis assay

Fibrin clot was produced in a 96-well plate by incubating 3 μl of fibrinogen (7.5 mM in final concentration, Sigma) and 2 μl of thrombin (0.10 NIH unit/μl, Sigma) in a total volume of 100 μl of buffer A at 37 °C for 1 h. An equal amount (1 μg) of t-PA, tcu-PA or longistatin was mixed with PAI-1 (20 nM, in final concentration) in a total volume of 90 μl of buffer A and incubated for 15 min at 37 °C. Then, plasminogen (10 μl, 0.2 μg/μl, Sigma) was mixed with each reaction mixture. The mixtures were gently added to the fibrin clot separately and incubated at 37 °C for 6 h. Only buffer A was added as a negative control and longistatin alone was used as a positive control. Lysis of fibrin clot was detected visually and also by measuring changes in turbidity at 450 nm using a spectrophotometer (TECAN) up to 6 h.

2.6. Complex formation study with active PAI-1

Commercially available, activated PAI-1 was incubated with t-PA or longistatin in an equimolar concentration (666.6 nM) in a total volume of 15 μl of buffer A at 37 °C for 10 min.

Aliquots were separated by 12.5% SDS-PAGE under reducing conditions and proteins were visualized by silver stain. Additionally, proteins were transferred onto nitrocellulose membranes and probed with either mouse anti-longistatin sera (1: 200) or mouse anti-PAI-1 sera (1: 500, AntibodyShop, Paris, France) following the same methods as described previously (77). The membranes were incubated with alkaline phosphatase-conjugated goat anti-mouse IgG (H+L) (ZYMED) for 1 h and the bound proteins were visualized with nitroblue tetrazolium/5-bromo-4-chloro-3-indolyl phosphate (BCIP/NBT, Promega).

2.7. Statistical analysis

Data were presented as mean±SD, where appropriate. Statistical significance was determined using the Student's *t* test with unequal variance.

3. Results

3.1. Longistatin is less susceptible to the inhibitory effect of activated platelet lysate

To determine the effect of platelet lysate on longistatin, I employed two-step indirect fluorogenic assays using a plasmin-specific synthetic fluorogenic substrate (Boc-Glu-Lys-Lys-MCA). In this assay, longistatin or other physiologic PAs activated plasminogen to plasmin, which in turn hydrolyzed the plasmin-specific substrate. Data revealed that longistatin was relatively less susceptible to the inhibitory effect of SDS-treated platelet lysate than physiologic PAs such as t-PA and tcu-PA. Within 15 min 30 μg/ml of activated platelet lysate almost completely inhibited the plasminogen activation potential of t-PA (98.55%) and tcu-PA (98.15%) with the estimated IC_{50} of 7.7 and 9.1 μg/ml, respectively. Whereas in the same experimental setup, the equal amount of platelet lysate caused 56.51% inhibition of longistatin showing a significantly ($p<0.01$) higher IC_{50} (20.1 μg/ml) (Figure 16), suggesting that longistatin is less susceptible to the inhibitor(s) released by activated platelets.

3.2. Longistatin is more resistant to PAI-1 than physiologic PAs

To explore the effect PAI-1 on longistatin, I conducted direct fluorogenic assays using a t-PA-/u-PA-specific synthetic fluorogenic substrate (Pyr-Gly-Arg-MCA) since longistatin also hydrolyzed the t-PA-/u-PA-specific synthetic substrate. Activated PAI-1 at 5 nM concentration inhibited only 6.34%, 8.84% and 10.75% enzymatic activity of longistatin by 5, 10 and 15 min, respectively. At the highest physiolosic concentration (20 nM), PAI-1 inhibited only 18.18%, 20.55% and 21.47% enzymatic activity of longistatin by 5, 10 and 15 min of incubation, respectively at 37 °C. Importantly, longistatin could retain its 76.73% initial activity even after very long time (3 h) of incubation with 20 nM of PAI-1 (Figure 17Ai). In contrast, in the same experimental conditions, PAI-1 almost completely inhibited t-PA and tcu-PA. PAI-1 at 5 nM inhibited 76.05%, 79.51% and 88.68% enzymatic activity of t-PA by 5, 10 and 15 min, respectively. And, PAI-1 at 20 nM concentration caused 83.95% inhibition of t-PA within 5 min of incubation at 37 °C and by 15 min it inhibited 99.17% enzymatic capability of t-PA (Figure 17Aii). PAI-1 also rapidly inactivated tcu-PA. PAI-1 at 5 nM concentration inhibited 65.46%, 74.13% and 82.4% catalytic capability of tcu-PA by 5, 10 and 15 min, respectively. PAI-1 at upper physiologic plasma level (20 nM) caused 75.71%, 93.31% and 96.84% inhibition of tcu-PA within 5, 10 and 15 min of incubation, respectively (Figure 17Aiii). To compare the inhibitory effect of the activated PAI-1 on longistatin, t-PA or tcu-PA, I also calculated IC_{50} in the same experimental settings. Estimated IC_{50} of PAI-1 for longistatin inhibition was 88.3 nM but for the inhibition of t-PA and tcu-PA the IC_{50} was 3.9 and 3.2 nM, respectively (Figure 17B), suggesting that longistatin is more resistant to PAI-1 than physiologic PAs.

3.3. Longistatin efficiently lyses fibrin clot by activating plasminogen in the presence of PAI-1

In addition to synthetic substrate hydrolysis, I conducted microplate fibrin clot lysis assays to judge the plasminogen activation and subsequent fibrinolytic potentiality of longistatin in the

presence of activated PAI-I. Longistatin in the presence of 20 nM of PAI-1 activated sufficient amount of plasminogen into plasmin which completely hydrolyzed fibrin clots produced in a 96-well plate, as it was done by longistatin in the absence of PAI-1 during the same incubation period. However, both t-PA and tcu-PA failed to activate plasminogen, and eventually to hydrolyze fibrin clot in the presence of PAI-1 even after a long time (6 h) of incubation (Figure 18). The results clearly suggest that longistatin can activate a large amount of plasminogen into plasmin, and induce robust fibrinolysis in the presence of PAI-1 at the highest physiologic level.

3.4. Longistatin does not form complex with active PAI-1

To investigate whether longistatin forms stable complex with PAI-1 or not, I incubated longistatin with activated PAI-1 in an equimolar concentration. Here, I used t-PA as a control, since t-PA produced SDS stable complex with PAI-1 in an equimolar concentration (171). After visualization of proteins with silver stain, it was observed that longistatin neither formed complex with PAI-1 nor cleaved it. In contrast, t-PA produced a stable complex with PAI-1 at the level of ~110 kDa. Furthermore, while incubated t-PA also cleaved PAI-1, which appeared at ~40 kDa (Figure 19A). To validate the data, I conducted immunoblot study using mouse anti-longistatin or mouse anti-PAI-1 antibody. However, I also could not detect longistatin-PAI-1 complex by immunoblotting but both longistatin and PAI-1 were detected individually by their own antibodies at the expected level (Figure 19B), which further reinforce the assertion that longistatin does not form any complex with PAI-1.

4. Discussion

PAI-1 is the main inhibitor of the physiologic PAs present in plasma and significantly reduces the PA-mediated thrombolysis during the conservative therapy of thrombo-occlusive disorders (156, 172−174). Therefore, PAI-1 resistant PA may be the best choice for the prompt

and efficient dissolution of thrombi and subsequent restoration of circulation to the affected tissues/organs. Here, I report on longistatin, a novel PA from the salivary glands of the hard tick, *H. longicornis*, which shows significant resistance to the activated platelet lysate and commercially available PAI-1. Importantly, longistatin does not form complex with PAI-1.

It was observed that following incubation with an amount of activated platelet lysate (SDS treated) which completely inhibited physiologic PAs such as t-PA and u-PA, longistatin significantly retained its functional activity. During thrombogenesis, thrombin causes limited cleavage of fibrinogen and produces fibrin meshwork, which entraps platelets and produces hemostatic plaque (121−124, 174). Therefore, thrombi, especially arterial thrombi, become platelet rich. PAI-1, upon production from different sources, is stored in α-granules of platelets and is released by the activated platelets during thrombi formation (165, 174). Thus, PAI-1 concentration is elevated in and around the platelet-rich thrombi and the thrombi become resistant to some extent to the PA therapy with physiologic PAs (156, 176). Longistatin exhibits significant tolerance to the activated platelet lysate, suggesting that longistatin may be resistant to the PAI-1 released by activated platelets, which is mainly responsible for the attenuation of PA-mediated fibrinolysis system.

To test the foresaid hypothesis, I treated longistatin directly with activated PAI-1 in different concentration for long period of time. It was clearly observed that longistatin exhibits significant resistance to the purified and activated human PAI-1. Generally, PAI-1 level in plasma is 5−20 nM which is sufficient to inhibit physiologic PAs and efficiently prevents the generalized activation of plasminogen (156, 176). In fact, physiologic level of t-PA is circulated as PAI-1-t-PA complex in the body; thus, PAI-1 plays crucial roles in the maintenance of homeostasis between hemostasis and fibrinolysis (163, 172, 173). During thrombogenesis, since the PAI-1 level is greatly increased, the plasminogen activation capability of exogenous PAs and subsequent thrombolysis is significantly hampered. Longistatin can tolerate ~90 nM of PAI-1, whereas t-PA

and u-PA are almost completely inhibited by 5 nM PAI-1. Furthermore, both t-PA and u-PA are rapidly (within 5−15 min) inhibited by PAI-1 (5 nM) but longistatin can tolerate the upper physiological level of PAI-1 (20 nM) for a significantly longer period of time (>3 h). Notably, longistatin completely hydrolyzed fibrin clot by activating plasminogen in the presence of an amount of active PAI-1 which completely abolished the fibrinolytic capability of t-PA and u-PA. The results clearly showed that longistatin can evade the inhibitory effects of PAI-1.

Additionally, t-PA forms an SDS-stable complex at ~110 kDa level but I could not detect any complex between PAI-1 and longistatin, which further validates the hypothesis that longistatin is resistant to the inhibitory effect of PAI-1. PAI-1 binding to the target physiologic PAs is mediated mainly by the formation of salt bridges between the series of positively charged residues (variable region 1, VR-1) in PAs with the complementary series of negatively charged residues in PAI-1. Deletion of the residues ^{296}KHRRSPG^{302} or ^{179}RHRGGS^{184}, the VR-1 of human t-PA and u-PA, respectively, renders the proteases resistant to PAI-1 inhibition. Furthermore, chicken u-PA (ch-uPA) that does not contain PAI-binding site (VR-1) is refractory to the inhibition by human PAI. VR-1 of PAs is not a general serpin binding site rather it is a specific motif of PAs for the interaction with PAI-1 (65, 127, 163). In fact, one serpin can inhibit several enzymes but each serpin is expected to have a target protease (since a particular phenotype develops due to the deficiency of a particular serpin). The ability of a serpin to neutralize a given target protease more specifically and more rapidly in a complex mixture of numerous proteases (as in plasma) depends on the interaction between one/more secondary binding site(s) of the serpins and complementary region of the proteases. For example, α_2-antiplasmin can inhibit many serine proteases but plasmin is recognized as the main target due to a lysine binding site located in the kringle 4 of plasmin to which carboxy-terminal lysines of α_2-antiplasmin interact (177−179). Similarly, the 60-loop of thrombin contributes to the specific interaction with anti-thrombin III (180). Unlike human t-PA and u-PA, longistatin does not contain a series of such positively charged residues (Chapter 1).

Therefore, substantial tolerance of longistatin to the rapid and irreversible inhibitory effect of PAI-1 is not unexpected. Collectively, the results suggest that longistatin is resistant to PAI-1 and maybe an interesting tool for the development of modern, PAI-1 resistant therapeutic agent for the efficient medication of occlusive cardiovascular events.

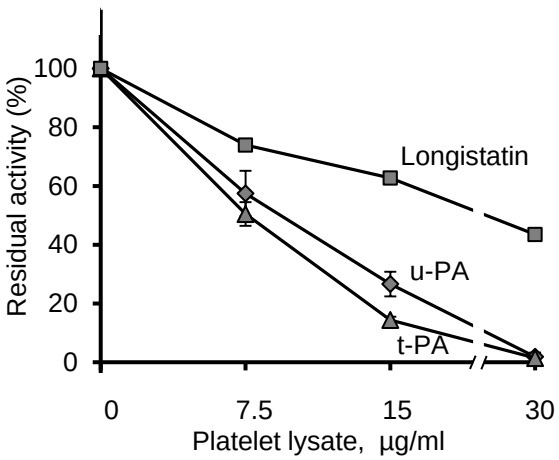

Figure 16. Effects of activated platelet lysate on longistatin. Equal amount (1 µg) of longistatin/t-PA/tcu-PA was treated with various amount of platelet lysate (0–30 µg/ml) at 37 ºC for 15 min and then diluted with buffer A (50 mM Tris-HCl, pH 7; 100 mM NaCl and 5 mM $CaCl_2$), and plasminogen (5 µl, 0.2 µg/µl) was added and incubated at 37 ºC for further 1 h in the absence (incase of u-PA) or presence (incase of t-PA/longistatin) of soluble fibrin (8 µg/ml). Residual activity of longistatin, t-PA or u-PA was determined using a plasmin-specific synthetic substrate (Boc-EKK-MCA) as detailed in the Materials and Methods.

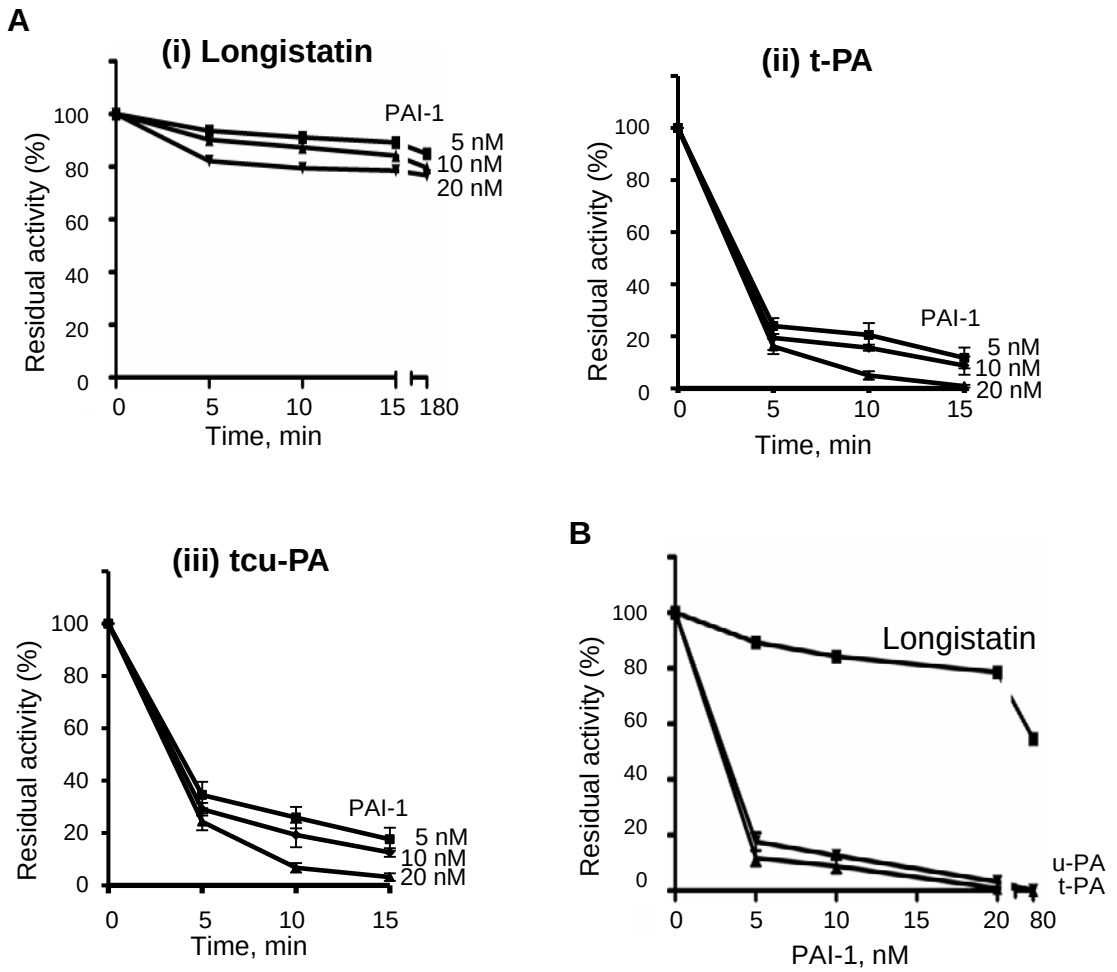

Figure 17. Effect of PAI-1 on plasmingen activators. (A) Effects of PAI-1 on plasmingen activators at different time of incubation. Logistatin (i)/t-PA (ii)/tcu-PA (iii) was incubated without or with PAI-1 (5−20 nM) at 37 ºC for different time (0−180 min) in 25 µl of buffer A (50 mM Tris-HCl, pH 7; 100 mM NaCl and 5 mM $CaCl_2$). Residual activity was determined using a synthetic substrate specific for t-PA/u-PA (Pyr-GR-MCA) as described in the Materials and Methods. (B) Comparison of inhibitory effect of PAI-1 on plasminogen activators. Logistatin, t-PA or tcu-PA was incubated without or with PAI-1 (5−80 nM) at 37 ºC for 15 min in 25 µl of buffer A. Residual activity was determined using a synthetic substrate specific for t-PA/tcu-PA (Pyr-GR-MCA) as described in the Materials and Methods.

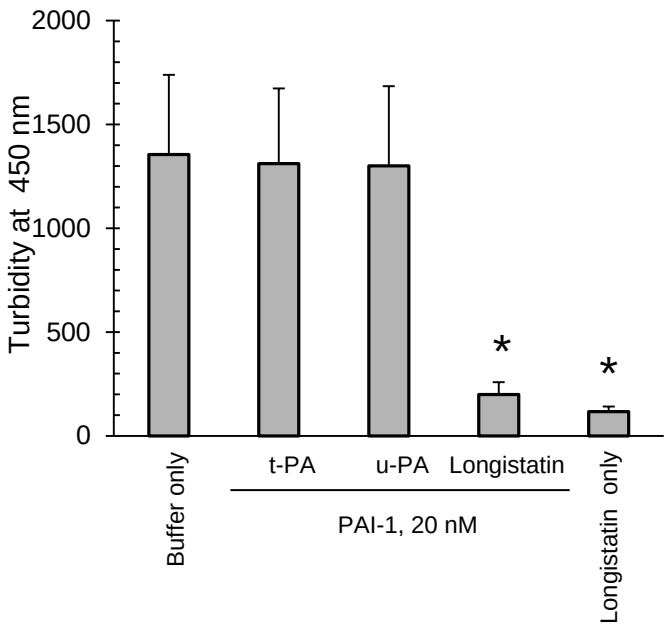

Figure 18. Fibrinolysis by longistatin in the presence of PAI-1. Fibrin clot was produced in a 96-well plate by incubating 3 µl of fibrinogen (7.5 mM, in final concentration) and 2 µl of thrombin (0.10 NIH unit/µl) in a total volume of 100 µl of buffer as described in the Materials and Methods. The same amount (1 µg) of t-PA, tcu-PA or longistatin was incubated in the absence or presence of PAI-1 (20 nM) for 15 min and then plasminogen (10 µl, 0.2 µg/µl) was added. The mixture was added to the fibrin clot and incubated at 37 ºC for further 6 h. Lysis of fibrin clot was detected as described in the Materials and Methods. Asterisks (*) indicate that the difference compared with control group is significant as determined by the Student's *t*-test with unequal variance ($^{*}p<0.01$).

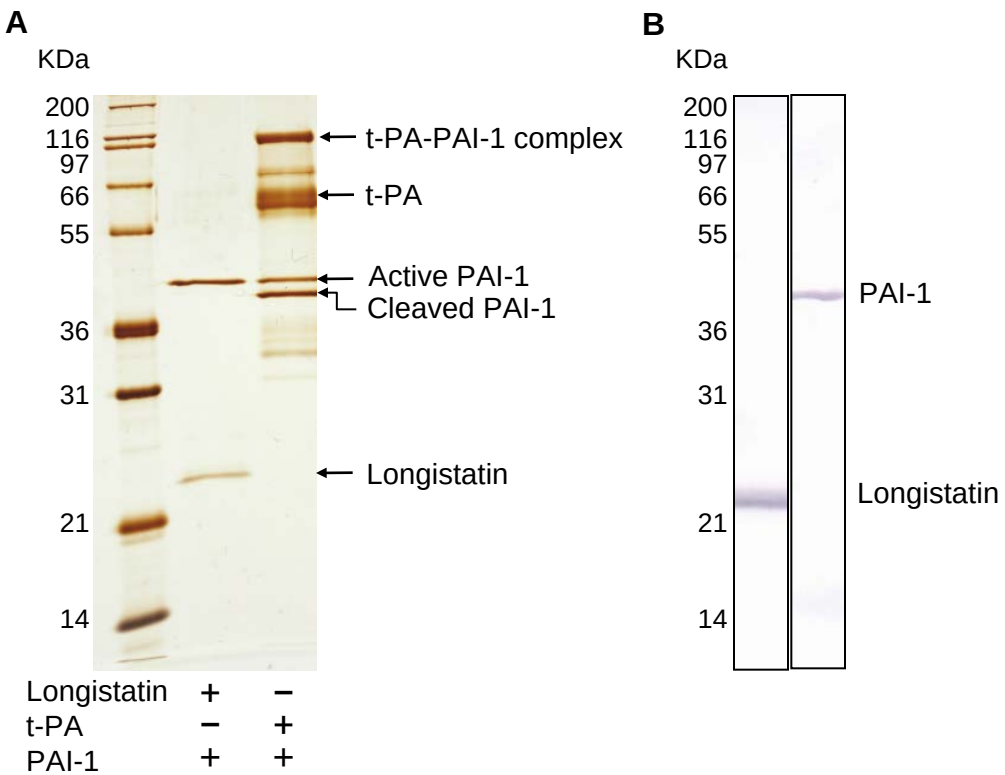

Figure 19. Detection of enzyme-PAI-1 complex. (A) Enzyme-PAI-1 complex study by silver staining. PAI-1 was incubated with longistatin or t-PA in an equimolar concentration at 37 ºC for 15 min and separated by electrophoresis using a 12.5% SDS-PAGE gel under reducing conditions. The gel was stained with silver stain. (B) Enzyme-PAI-1 complex study by immunoblotting. PAI-1 was incubated with longistatin or t-PA following the same procedures as described above and separated by electrophoresis using a 12.5% SDS-PAGE gel under reducing conditions. Proteins were transfered onto nitrocellulose membranes and probed with either mouse anti-longistatin (1: 200) or anti-PAI-1 (1: 500).

Chapter 5

Effects of longistatin on blood feeding of ticks

1. Introduction

Blood-feeding is very essential for the survival of ticks, and ticks salivary-gland derived bioactive molecules play crucial roles in the complex persistent feeding mechanisms of ticks. Development and maintenance of blood pool are very crucial for the successful feeding of blood-meals from host animals (54, 56, 87, 181, 182). Yet today, the particular molecular mechanism(s) that prevents blood coagulation and initiates fibrinolysis in the blood pool and keep blood in a fluid state is not clearly understood. From the mRNA expression profile and subsequent biochemical and functional characterization of longistatin, I have postulated that longistatin is closely linked with the feeding success of hard ticks. To judge the hypothesis, RNA interference (RNAi) technique was employed.

RNAi was discovered in the year of 1998 by injecting double-stranded RNA (dsRNA) into the nematode *Caenorhabditis elegans* (183). Since then, the technique is being used to analyze the biological function(s) of proteins in animals and plants (184−187). RNAi is used to silence genes encoding proteins in an absolutely sequence specific manner at the mRNA level, therefore, it is also known as posttranscriptional silencing of gene (56, 183). Upon introduction, the long dsRNA is processed by the RNaseIII-type enzyme, called dicer, into small interfering RNAs (siRNAs) of

about 20−25 nucleotides. Then, the siRNAs assemble into endoribonuclease-containing complexes known as RNA induced silencing complexes (RISCs) and become unwind. Then the siRNA binds to the mRNA of absolute sequence similarity and causes degradation of the target mRNA; thus, stops translation of the protein and eventually extinguishes gene function. Simplicity and specificity of the technique have made it a powerful tool for testing biological function(s) of a protein accurately in nonmodel animals (58, 183, 187, 188).

About one decade ago Aljamali et al (189) have tested the applicability and feasibility of RNAi to study the biological functions of proteins in ticks. Miyoshi et al (190) successfully used RNAi in the hard tick *H. longicornis* to analyze the function of a serine protease. Subsequently, RNAi has been used as a basic tool to study the function as well as screen vaccine or drug target molecules in tick research (56, 58, 87, 116, 191−193).

In this study, I used RNAi to validate the outlined roles of longistatin in the development and maintenance of blood pools by *H. longicornis*. By posttranscriptional scilencing of longistatin I clearly show that *longistatin*-specific gene-knockdown ticks completely lost their unique ability to create a blood pool and consequently were unable to feed and engorge on blood-meals from host animals.

2. Materials and Methods

2.1. RNA interference

I performed RNAi using dsRNA following the protocol described previously (77). The sequence coding longistatin was cloned into pBluescript II SK^+ vector in *Xho*I and *Eco*RI restriction sites. The dsRNA complementary to the *E. coli mal*E gene that encodes maltose-binding protein was used as a negative control. cDNA corresponding to *mal*E mRNA was synthesized and cloned into pBluescript II SK^+ plasmid using the primers 5′-CCGCTCGAGCGGTTATGAAAATAAAAACAGGTGCA-3′ and 5′-

GAATTCGCTTGTCCTGGAACGCTTTGTC-3′. The inserted sequences of longistatin and *mal*E were amplified by PCR using primers T7 (5′-GTAATACGACTCACTATAGGGC-3′) and CMO422 (5′-GCGTAATACGACTCACTATAGGGAACAAAAGCTGGAGCT-3′) to attach to T7 promoter recognition sites at either end. The PCR products were purified using gel extraction kit (QIAGEN). dsRNA complementary to the respective DNA inserts was synthesized by *in vitro* transcription using T7 RNA polymerase (Promega). One microgram of longistatin dsRNA (ds*longistatin*, treated group) or *mal*E dsRNA (ds*mal*E, control group) was injected into each tick through the 4th coxa. Ticks were observed in a humified incubator for 24 h at 25 °C prior to attaching them on the host for feeding. A total of 120 ticks, each of 60 in RNAi and control groups, were attached on the ear of tick-naïve rabbits. Ticks were collected at 24, 48, 72 and 96 h of feeding or after repletion. All ticks collected after they had dropped off the host following full engorgement or removed at day 6 post-attachment were weighed individually using a digital balance (Sartorius, CPA225D).

2.2. Semiquantitative RT-PCR and quantitative RT-PCR (qRT-PCR)

Salivary glands from adult ticks of both control and RNAi groups at different feeding periods (24, 48, 72, 96 h and engorged) were collected as described previously (77). Shortly after collection, salivary glands were submerged in RNA*later*®, an RNA Stabilization Reagent (QIAGEN). Total RNA was isolated using an RNeasy Mini Kit (QIAGEN) according to the manufacturer's protocol and 500 ng of total RNA was used for reverse transcription before PCR. Single-stranded cDNA was prepared using Takara RNA PCR Kit (AMV) Ver.3.0 (Takara) following the manufacturer's instructions. A series of PCRs were carried out using 500 ng of cDNA from each sample and longistatin-specific oligonucleotides (5′GCTATCTCGGCTCCTGTGTC 3′ and 5′ATCTTCGCCAGGTCCTTCTT 3′) or oligonucleotides specific for a control cDNA encoding β-actin in a final volume of 20 µl. The PCR

product was subjected to electrophoresis in 1% agarose gel. The qRT-PCR was performed in a LightCycler 1.5 instrument (Roche Instrument Centre AG, Mannheim, Germany) using LightCycler FastStart DNA Master SYBR Green I (Roche Diagnostics) following a procedure described previously (116). The reaction mixture of 20 µl contained 4 mM $MgCl_2$, 0.5 µM of each primer (forward and reverse as described above) and 2 µl (250 ng/µl) of the single-stranded DNA template. The data obtained were analyzed using LightCycler Software Version 3.5.

2.3. Immunofluorescence and histopathology

Salivary glands were collected from partially fed (96 h) adult ticks of both control and RNAi groups as described above. After collection, salivary glands were placed on slides and were fixed with 4% paraformaldehyde. Salivary glands were then permeabilized with 0.1% triton × 100 and were treated with mouse anti-longistatin sera (1: 100) overnight at 4 °C. Bound antibodies were detected using a green fluorescent-labeled secondary antibody (Alexa Flour® 488 goat anti-mouse IgG (H+L), Invitrogen). Slides were mounted with VECTASHIELD® mounting medium containing 4′,6-diamidino-2-phenylindole (DAPI, Vector Laboratories) and examined under a fluorescent microscope (Leica). In addition, thin sections were prepared from tissues collected from the feeding lesions developed on a rabbit's ear at the site of attachment of the ticks. Tissue sections were then subjected to immunofluorescent staining using mouse anti-longistatin sera as described previously (87). Rabbit's tissues were also stained with Elastica-van Gieson stain (EVGS) as described previously (194).

2.4. Immunoblot analysis

Equal numbers of adult ticks from both RNAi and control groups collected at different feeding intervals (24, 48, 72, 96 h and engorged) were dissected separately in PBS and salivary glands were isolated. Antigens were prepared as previously described (77). Equal amounts of protein (4 µg) were separated by 12.5% SDS-PAGE under reducing conditions and were

transferred onto nitrocellulose membrane. The membrane was treated with mouse anti-longistatin sera (1: 100) overnight at 4 °C. Bound antibodies were probed with alkaline phosphatase-conjugated goat anti-mouse IgG (H+L) (ZYMED). The membranes were developed with nitroblue tetrazolium/5-bromo-4-chloro-3-indolyl phosphate (BCIP/NBT, Promega).

3. Results

3.1. Injection of dslongistatin inhibits the transcription and translation of endogenous longistatin

Total RNA isolated from salivary glands of ticks of different feeding phases of both control and treated groups was analyzed by RT-PCR and qRT-PCR to demonstrate the effect of RNAi on the expression of longistatin-specific mRNA. The RT-PCR data revealed that injection of ds*longistatin* completely abolished the detectable mRNA expression corresponding to the longistatin-specific gene in ticks (Figure 20A). The qRT-PCR data also supported this finding. However, in the RNAi-treated group, longistatin-specific transcript, although very low compared to that of control, was detected in ticks at 24, 48 and 72 h of feeding only by qRT-PCR (Figure 20B). This variation in the detection of longistatin-specific mRNA by RT-PCR and qRT-PCR may be due to the sensitivity of the techniques. Furthermore, the presence of a detectable level of mRNA in the RNAi-treated group of ticks might be due to individual variations in the tick population. Here, I used pools of salivary-gland extracts, isolated from three randomly selected ticks in each feeding phase; thus, it is quite reasonable that the effects of RNAi were not exactly uniform in each and every microinjected tick. Longistatin-specific gene expression was detected in its normal pattern (Chapter 1) in ticks injected with dsRNA complementary to the gene encoding maltose-binding protein in *E. coli* (ds*mal*E) (Figures 20A and B), indicating that injection of ds*longistatin* caused disruption of longistatin-specific mRNA transcription. For *in situ* detection of the effect of RNAi on the translation of endogenous longistatin, salivary glands were collected from partially fed (96

h) ticks of both treated and control groups and were subjected to immunofluorescence staining using mouse anti-longistatin sera. Longistatin-specific reactions were almost absent in ds*longistatin*-injected ticks whereas binding of mouse anti-longistatin antibody was detected in the salivary glands of ds*mal*E-injected ticks (Figure 20C), suggesting that injection of ds*longistatin* efficiently silenced longistatin-specific mRNA expression and subsequent translation of longistatin. To further validate these results regarding *in vivo longistatin* gene silencing, I conducted Western blot analysis using salivary gland extracts collected from both treated and control ticks. Longistatin-specific bands were detected only in the salivary gland extracts of ds*mal*E-injected ticks and longistatin was upregulated with the feeding process of ticks (Figure 20D). These findings further reinforced the evidence of longistatin-specific gene silencing by ds*longistatin* injection in ticks.

3.2. RNAi-treated ticks failed to develop blood pools and were unable to feed blood-meals from hosts

All ticks microinjected with dsRNA were active and healthy during the incubation period. After placement on rabbits' ears, all ticks of both treated and control groups actively attached. However, in the ds*longistatin*-injected group, 3 (2.5%) ticks were found dead at 72 h of attachment. All ticks in the ds*mal*E-injected group reached to repletion and detached by day 6 post-attachment. Notably, ds*longistatin* injection was shown to hamper the feeding of ticks. These ticks were poorly fed and most of them failed to engorge (Figure 21A). Only two ticks (1.66%) dropped off the host following engorgement in the RNAi group. The mean body weight of the ticks collected after 6 days of feeding was significantly ($P<0.01$) lower in the RNAi-treated group (53.53±50.38 mg) than that of the control group (253.43±57.91 mg) (Figure 21B). Visible phenotypic changes were also obvious among the ticks of the treated and control groups. Ticks of the treated group, despite 6 days of feeding, were very small with a dull cuticle and devoid of normal cuticular wrinkling. In

contrast, ticks of the control group, which dropped off the host following full engorgement, were large and glossy in appearance with dorsal cuticular wrinkling (Figure 21B).

A marked difference between blood pools induced by the ticks of RNAi-treated and control groups was observed. Large blood pools were developed at the site of attachment of each tick of the control group. Grossly, blood pools were large enough with an estimated mean size of 19.53±7.85 mm^2, containing a considerable amount of exudates and blood. The affected area was cyanotic or dark bluish in color. Blood vessels in the vicinity of the blood pool were congested and distended. The surrounding area of the blood pool was markedly hyperemic. On the contrary, most of the ticks of the RNAi-treated group failed to establish a feeding lesion. Significantly ($p<0.01$) smaller blood pools (4.25±6.38 mm^2) were detected in few individual ticks. Also, no prominent gross pathological changes were detected at the site of attachment of RNAi-treated ticks (Figures 21C and D). To study the histological features, I stained the thin tissue sections of the blood pool areas with EVGS where hemorrhagic areas exhibit a bright golden yellow color. Consistently, blood pools, developed at the site of attachment of the ds*mal*E-injected ticks, showed the characteristic bright golden yellow color, implying that they were flooded with RBC. Notably, hemorrhagic changes were not detected at the biting areas of ticks of the RNAi-treated group (Figure 21E), suggesting that the *longistatin* gene plays vital roles in the formation and maintenance of a blood pool as preceded by marked hemorrhage into tick-feeding lesions. In addition, an attempt was made to detect endogenous longistatin in the feeding lesions produced by the ticks of both groups using mouse anti-longistatin sera. Longistatin-specific bright green fluorescence was detected at the well-developed blood pool areas produced by the ds*mal*E-injected ticks but no such reaction was detected at the feeding lesions induced by ds*longistatin*-injected ticks (Figure 21E), which further suggests a possible role of longistatin in the blood pool formation.

3.3. Functional implications of longistatin in blood coagulation and fibrinolysis cascades

I hypothesized that ixodid ticks synthesize longistatin and possibly other functionally related bioactive molecules to efficiently counteract host's hemostatic ability and/or to activate its own fibrinolytic machinery to create blood pools for the acquisition of blood-meals and engorgement. *In vivo* and *in vitro* data strongly support this hypothesis and that longistatin exerts its multifunctional roles both in coagulation cascades and in fibrinolytic pathways. In this study, I proposed a longistatin-induced anti-coagulation and fibrinolytic mechanism that works persistently against host's hemostatic pathways until ticks ensure full blood-meals (Figure 22).

4. Discussion

In this chapter, I show that posttranscriptional silencing of *longistatin* disrupts homeostasis of blood pools of the tick, *H. longicornis,* and the RNAi-treated ticks fail to suck sufficient amount of blood and to replete. Study revealed that injection of longistatin-specific dsRNA completely abolished the expression of longistatin-specific mRNA and subsequent synthesis of longistatin. This finding conforms to the observations of other scientists working with proteins derived from salivary glands of ticks (56, 58, 87). Salivary glands occupy the antero-lateral one-third to one-half of the tick's hemocoel and remain suspended into the tick's hemolymph (181, 195, 196). Therefore, dsRNA injected into the hemolymph through the 4th coxa can easily enter into the salivary glands. Then dsRNA enter into the cellular RNAi pathway (58) where it causes degradation of *longistatin*-specific mRNA.

The RNAi-treated ticks failed to establish blood pools and replete with blood-meals. As soon as ticks start biting, the hemostatic pathway is activated and tries to prevent bleeding and oozing from the body, intending to limit the feeding actions of ticks (46, 47, 195). Anticoagulant and/or fibrinolytic agents are then thought to be secreted by ticks and injected into the host tissues where they counteract the reactions of the coagulation cascades. It was clearly showed that

longistatin was secreted from the salivary glands and injected into the host tissues during acquisition of blood-meals. After getting entrance into the host tissues, longistatin degrades fibrinogen (Chapter 4); thus, cripples the common pathways of clotting of blood and exudates. Additionally, longistatin activates plasminogen into plasmin (Chapter 4), which causes lysis of fibrin clots and maintains the fluidity of blood in the blood pool. The RNAi data clearly shows the critical roles of longistatin in the feeding success and survival of hard ticks.

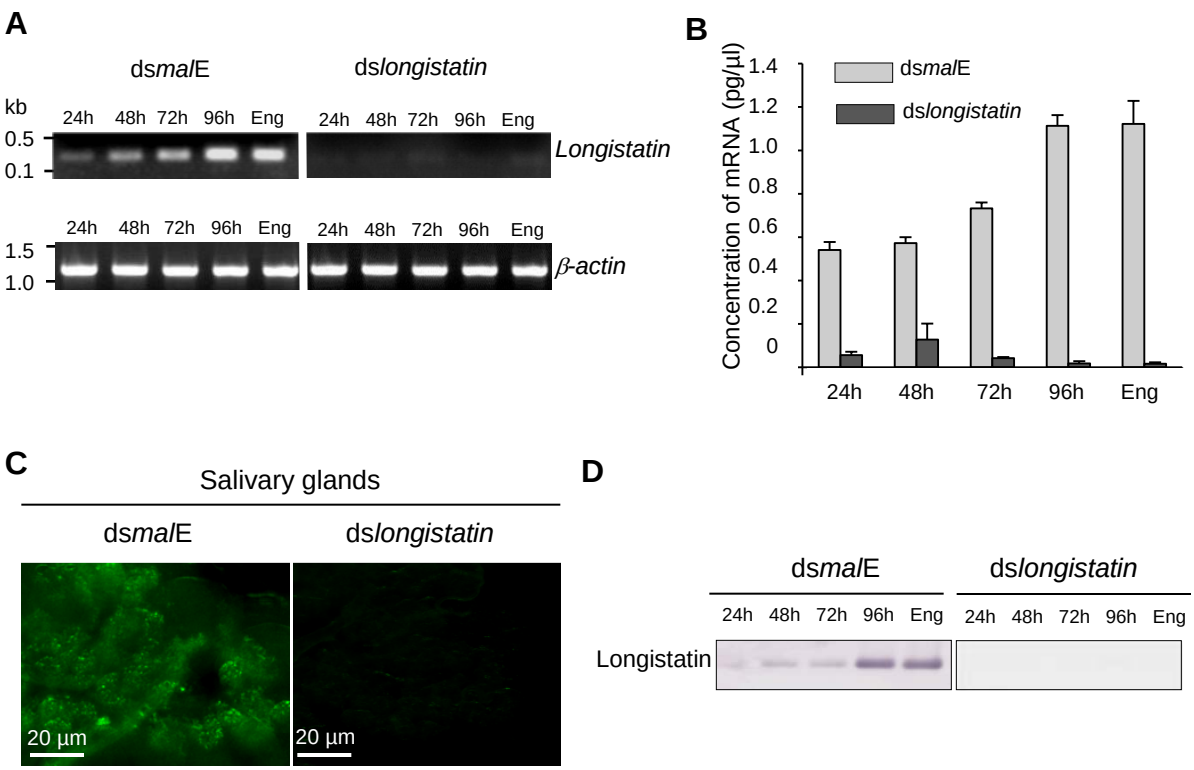

Figure 20. Post-transcriptional silencing of longistatin-specific gene in adult ticks by injecting dsRNA. (A) Semiquantitative RT-PCR analysis. One microgram of *longistatin* dsRNA was injected into the hemolymph of ticks of the RNAi-treated group. Ticks of the control group were treated with 1 µg of *mal*E dsRNA. *β-actin* was used as an internal control. Eng, engorged. (B) Quantitative RT-PCR using total RNA and primers specific for *longistatin* as in A. Eng, engorged. (C) *In situ* detection of longistatin expression in ticks' salivary glands. Salivary glands from the ticks of control and RNAi-treated groups. Endogenous longistatin was reacted with mouse anti-longistatin sera (1: 100). (D) Effect of gene silencing on longistatin translation by Western blot analysis. Salivary gland extracts were electrophoresed and transferred onto nitrocellulose membrane. Endogenous longistatin was probed with mouse anti-longistatin (1: 100). Eng, engorged.

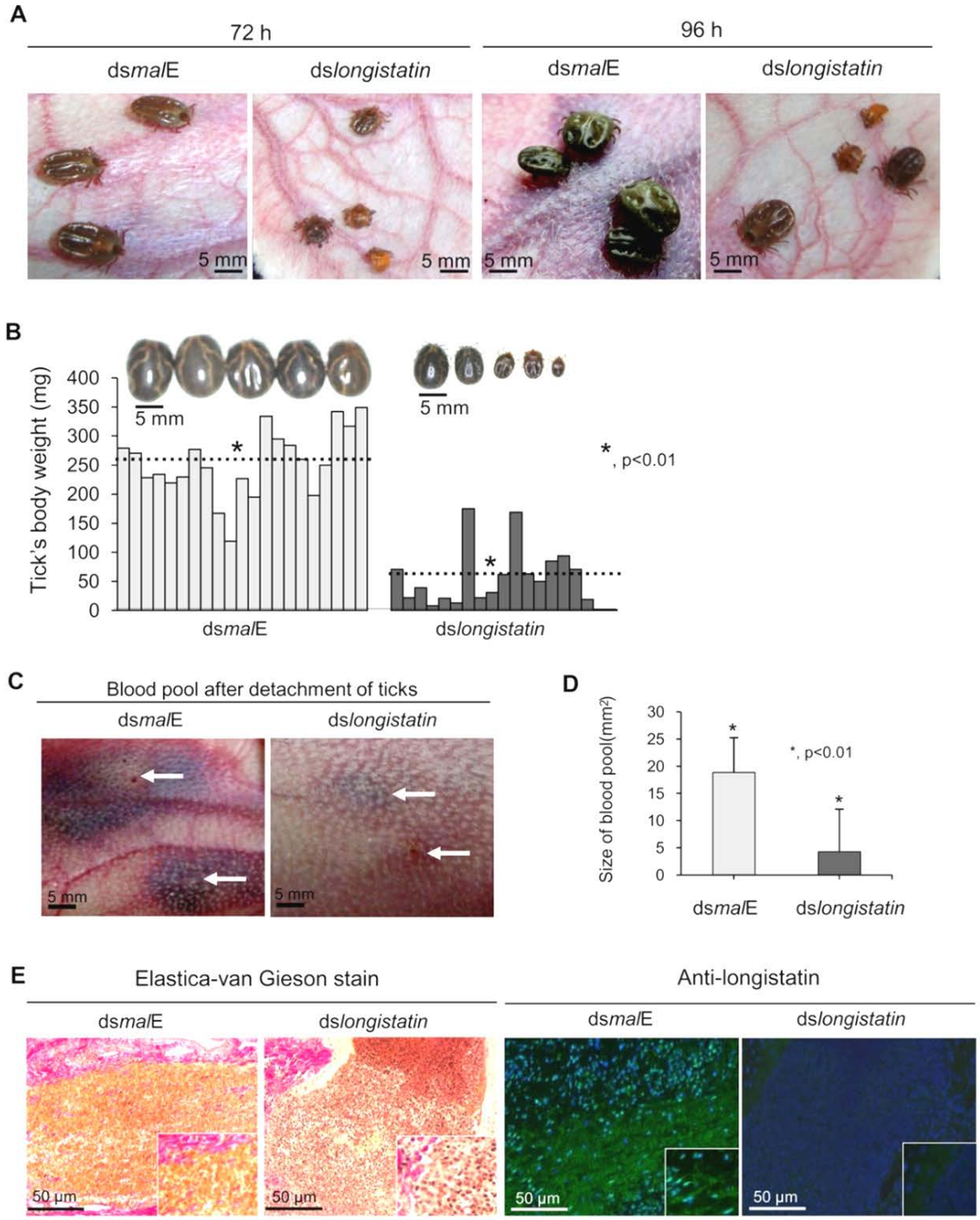

Figure 21. Effects of post-transcriptional silencing of *longistatin* gene on blood pool formation and blood feeding. (A) Impact of longistatin-specific mRNA silencing on blood-meal feeding from hosts. Adult ticks were injected with *longistatin* dsRNA or *mal*E dsRNA (1 µg/tick) and were allowed to feed on a tick-naïve rabbit. RNAi-treated ticks failed to replete. (B) Postengorgement weight was significantly ($p<0.01$) lower in the RNAi-treated group than that of the control group. Dotted lines indicate mean ± SD of body weight of ticks. (C) Effects of post-transcriptional silencing of *longistatin* gene on blood pool formation. RNAi was performed and ticks were fed in the same manner as in A. RNAi-treated ticks failed to establish a prominent blood pool. Arrows indicate site of tick attachment. (D) Blood pools were significantly ($p<0.01$) smaller in the RNAi-treated group. (E) Histopathological changes were studied using EVGS. Longistatin was detected in the feeding lesions of ticks on the host's tissues using mouse anti-longistatin sera (1: 100).

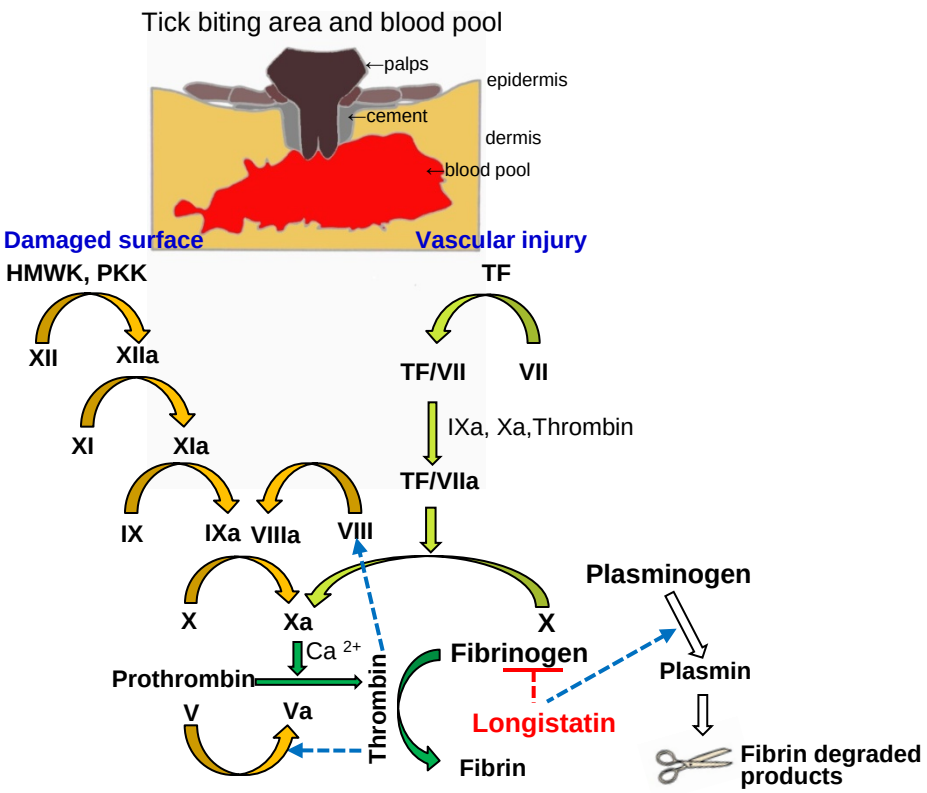

Figure 22. A schematic diagram showing roles of longistatin in blood coagulation and fibrinolysis events. In the initial phase, the tick bites and lacerates tissues at the site of attachment and damages vascular beds, which results in hemorrhage leading to the development of a blood pool. Longistatin is synthesized in and secreted from the salivary glands, and injected into the blood pool during feeding process. Longistatin degrades fibrinogen and activates plasminogen to its active form, plasmin. HMWK, high-molecular-weight kininogen; PKK, prekallikrein; TF, tissue factor. Yellow arrows, contact activation (intrinsic) pathway; olive-green arrows, tissue factor (extrinsic) pathway; green arrows, common pathway of coagulation cascade and white arrows, fibrinolytic pathway. Figure adapted from ref. (46, 103, 104).

General discussion and conclusions

Ticks are serious pests of animals and humans and serve as unique vectors of many deadly diseases. Although the tick is a temporary parasite but all of its motile lifecycle stages (eg. larvae, nymphs and adults) suck blood from various vertebrate hosts including humans (16−20). Blood-meal is very essential for almost all physiological functions of ticks including their reproductions. Ticks though can pass a long times off the hosts but ultimately unable to survive without blood-meals (33, 43). Among different types of ticks, soft ticks suck blood rapidly like the vessel feeder insects but hard ticks, the major parts of the tick fauna, acquire their blood-meal for a long time making a large blood pool under the skin and remain attached to hosts until repletion (22, 197, 198). Therefore, hard ticks have to smartly manipulate various types of host's defense mechanisms such as hemostasis, inflammations and immune responses. Among these armories of protections, hemostasis acts as a vanguard, which is initiated within few seconds against the lacerating actions of ticks (46, 54, 199). It is believed that saliva of ticks, the complex mixture of different types of bioactive molecules, counteracts successfully almost all the protective responses of hosts provoked during acquisition of blood-meals (181, 197, 199). Saliva of ticks helps to manage the strong hemostatic actions of hosts and keep the blood in a fluid state within the blood pool until a full blood-meal is ensured (46, 47). In the present study, I have selected and characterized a gene from the EST data base constructed from the salivary gland cDNA library of *H. longicornis* that encodes a protein, herein named as longistatin. I clearly showed the roles of longistatin in the wonderful

and interesting mechanisms of the development and maintenance of blood pools.

Longistatin is synthesized in, and secreted from the salivary glands of ticks. Longistatin-specific transcript was not detected in any organ except salivary glands. Expression of longistatin-specific mRNA was upregulated with the feeding processes of ticks and highly expressed at 96 h of feeding and in fully engorged tick prior to detachment from the hosts (Chapter 1). Since this is the rapid phase of feeding and at this phase blood pool contains the highest amount of unclotted blood, the functional demand of anticoagulant and/or fibrinolytic agent(s) is maximum. On the other hand, expression of longistatin-specific mRNA sharply declined in ticks as soon as they detached from the host following full engorgement, and it is quite reasonable that after repletion the salivary-anticoagulants or -fibrinolytic agents are no longer needed. Thus, it was assumed that longistatin may have some role(s) in the development and maintenance of blood pools.

Longistatin is a 17.8 kDa soluble protein and contains two EF-hand domains in the C-terminus. EF-hand domains of longistatin bind Ca^{2+}. Although Ca^{2+}-binding EF-hand proteins function within the cells but few of them are secreted and play crucial modulatory roles extracellularly (63, 70, 74). Using several independent experiments, I have clearly showed that longistatin is secreted from the salivary glands of ticks and injected into the host's tissues during acquisition of blood-meals. Longistatin does not contain canonical conserved catalytic site of serine proteases but still it functions like a serine protease and shows affinity for the amide bond of Arg. Traditional serine proteases use conserved His/Ser/Asp catalytic site to hydrolyze substrates but unconventional serine proteases do not have the conserved catalytic site. Due to different functional demand and situation present in the micro-environment of the body, proteases evolved different novel catalytic machinery and mechanism (60). Data suggest that longistatin is an atypical serine protease and is able to function in a wide range of temperature and pH. In the body, enzymes are tightly regulated by different types of activators, inhibitors or other bioactive molecules of diverse groups. Additionally, various cations play significant roles in controlling non

reversible hydrolytic cleavages of amide bonds of proteins and peptides by different classes of enzymes (63, 118, 120). I assume that Zn^{2+} act as a regulatory switch of longistatin since longistatin is potently inhibited by Zn^{2+} (Chapter 2). Although longistatin binds Ca^{2+} but the enzymatic activity of longistatin is slightly increased by Ca^{2+}.

Since longistatin is assumed to be associated with blood-feeding processes (Chapter 1), and maintenance of blood fluidity is linked with the pathogenesis blood pool (46, 47, 54) then I conducted a series of experiments using longistatin regarding hemostasis and fibrinolysis. Findings suggest that longistatin degrades fibrinogen, and activates plasminogen into plasmin. Furthermore, longistatin binds with fibrin meshwork with higher affinity than t-PA and its plasminogen activation potentiality is increased significantly in the presence of fibrin clot, suggesting that longistatin is able to potently degrade fibrin clots without causing much systemic activation of plasminogen, and simultaneously prevents further deposition of fibrin mass at the site of action in the body. Longistatin activates plasminogen bound to the surface of fibrin clots (Chapter 3). Also, longistatin potently induced thrombolysis in an *ex vivo* experimental setup. Therefore, it is quite expectable that longistatin is able to maintain the fluidity of blood within the blood pool; thus, longistatin plays critical roles in the development and maintenance of blood pool throughout the entire feeding periods of hard ticks.

Longistatin is resistant to the inhibitory effect of PAI-1 (Chapter 4). In plasma, PAI-1 is regarded as a fast-acting, specific inhibitor of physiologic PAs like t-PA and u-PA (159−162, 200). Fast and tight binding between PA and PAI-1 is mediated by the VR-1 of the activator and the complimentary region present in the PAI-1 (65, 66). However, longistatin, a novel PA from *H. longicornis*, does not have the VR-1 or a series of positive residues similar to the VR-1 of physiologic PA. Ticks and other hematophagous animals gain specific anticoagulant and/or fibrinolytic agents during their evolution to counteract the hemostatic effects of the hosts. And, during molecular evolution, a specific enzyme may change the conserved characteristics those are

present in the traditional proteases (60). Possibly, absence of VR-1 of the physiologic PAs, and canonical conserved catalytic triad of the traditional serine proteases, make longistatin a unique, unconventional serine protease that is refractory to the inhibitory effects of the PAI-1 present in the hosts' plasma and tissues. Therefore, longistatin enables ticks to evade the hemostatic as well as anti-fibrinolytic mechanisms of hosts during their complex and persistant blood-feeding processes by establishing a well defined blood pool.

To test the foresaid hypothesis, I used *in vivo* reverse genetics approach employing RNAi technique, and data clearly showed that injection of ds*longistatin* into the ticks' hemolymph completely stopped the synthesis and secretion of longistatin. The *longistatin*-knockout ticks could not establish blood pool and subsequently failed to replete with host blood, and eventually die (Chapter 5). Presently, RNAi technique is a well established technique for the screening of potential vaccine candidates or drug target molecules against different pathogens (56, 116, 117, 192, 193, 201).

In conclusion, longistatin is strictly localized in the salivary glands, secreted with saliva and injected into host tissues during acquisition of blood-meals. Longistatin possesses two canonical EF-hand Ca^{2+}-binding domains and binds Ca^{2+}. Longistatin is an atypical serine protease and is regulated by Zn^{2+}. Longistatin degrades fibrinogens and activates plasminogen. It binds with fibrin, and fibrin acts as a cofactor in the activation of plasminogen. Longistatin does not form any complex with PAI-1 and significantly resistant to the inhibitory effects of PAI-1. Ticks can not develop the blood pools, and is unable to maintain its homeostasis without longistatin. Longistatin is essential for the feeding success of hard ticks. In fact, hematophagus arthropods, including ticks, acquire anticoagulant proteins/peptides during their evolution, which play crucial roles in their feeding success. Attenuation of anti-hemostatic agents, present in their saliva, causes disruption of blood flow and blocks successful feeding of blood-meal from host animals. Therefore, these agents are considered as promising tools for the development of new generation

extermination strategies against ticks to minimize the losses caused by the blood stealing pests. Taking together, the results suggest that longistatin may be an interesting and novel candidate for the development of safe acaricide and/or effective anti-tick vaccine to control ticks and tick-borne diseases of humans and animals.

Acknowledgement

It is my immense pleasure to express my profound regards and deepest sense of gratitude to my honorable supervisor Professor Dr. Naotoshi Tsuji (Department of Global Agricultural Sciences, Graduate School of Agricultural and Life Sciences, The University of Tokyo, Tokyo, Japan) for providing me a great opportunity for the higher study. I gratefully acknowledge his cordial cooperation, scholastic guidance, constructive criticism and continuous inspirations during my entire research period. I would like express my cordial respect to him due to his patience during reviewing my dissertation critically. I would like to express my heartfelt gratitude to Professor Dr. Yasunobu Matsumoto (Department of Global Agricultural Sciences, Graduate School of Agricultural and Life Sciences, The University of Tokyo), Professor Dr. Takashi Yamakawa (Department of Global Agricultural Sciences, Graduate School of Agricultural and Life Sciences, The University of Tokyo), Professor Dr. Yoshitsugu Matsumoto (Department of Molecular Immunology, Graduate School of Agricultural and Life Sciences, The University of Tokyo) and Professor Dr. Kiyoshi Kita (Department of Biomedical Chemistry, Graduate School of Agricultural and Life Sciences, The University of Tokyo) for their great patience during reviewing my dissertation critically.

It is my great pleasure to express profound regards to Professor Dr. Kozo Fujisaki (School of Frontier Veterinary Medicine, Kagoshima University, Kagoshima, Japan) and Dr. Takashi Isobe (National Institute of Animal Health, National Agricultural and Food Research Organization, Tsukuba, Japan) for their valuable suggestion and inspirations about my research. I gratefully

acknowledge the contributions of Professor Dr. Khyrul Islam (Department of Veterinary Science, The University of Melbourne, Parkville, Victoria 3052, Australia) who has led me in the mysterious field of Molecular Parasitology. I express my heartfelt gratitude to him for his invaluable suggestions, thoughtful ideas, continuous encouragement and generous cooperation during planning and execution of my research works. I would like to convey my gratitude and acknowledgements to Dr. Takeharu Miyoshi, Dr. M. Abdul Alim, Dr. Takeshi Hatta, Dr. Matsubayashi Makoto and Dr. Kayoko Yamaji for their valuable suggestions and cordial cooperation.

I am grateful to Professor Dr. Motahar Hussain Mondal (Department of Parasitology, Bangladesh Agricultural University, Bangladesh) for his sympathy and valuable suggestion during my saty in abroad for higher study. I would like to thank Dr. Anowar Hossain (Associate Professor, Department of Biochemistry, Bangladesh Agricultural University), Dr. Golbar Hossain (Assistant Professor, Department of Pathology, Rajshahi University, Bangladesh) and Dr. Monir Hossain Mollah for the valuable discussion regarding different aspects of my research.

I sincerely acknowledge the coopration of Megumi Shimada and Masaru Kobayashi (National Institute of Animal Health, National Agricultural and Food Research Organization, Tsukuba, Japan) for their generous help in preparing histological sections.

I am grateful to my family members for their patience, cooperation, inspirations, invaluable contributions and sacrifices for me especially during my higher study.

References

1. Pound JM, George JE, Kammlah DM, Lohmeyer KH and Davey RB (2010) Evidence for role of white-tailed deer (Artiodactyla: Cervidae) in epizootiology of cattle ticks and southern cattle ticks (Acari: Ixodidae) in reinfestations along the Texas/Mexico border in south Texas: a review and update. *J Econ Entomol* 103: 211-218.
2. Dantas-Torres F (2009) Ticks on domestic animals in Pernambuco, Northeastern Brazil. *Rev Bras Parasitol Vet* 18: 22-28.
3. Jameson LJ and Medlock JM (2011) Tick surveillance in Great Britain. *Vector Borne Zoonotic Dis* 11: 403-412.
4. Jackson J, Beveridge I, Chilton NB and Andrews RH (2007) Distributions of the paralysis ticks *Ixodes cornuatus* and *Ixodes holocyclus* in south-eastern Australia. *Aust Vet J* 85: 420-424.
5. Jongejan F and Uilenberg G (2004) The global importance of ticks. *Parasitology* 129: S3-S14.
6. Ahmed J, Alp H, Aksin M and Seitzer U (2007) Current status of ticks in Asia. *Parasitol Res* 101 Suppl 2: S159-162.
7. Islam MK, Alim MA, Tsuji N and Mondal MM (2006) An investigation into the distribution, host-preference and population density of ixodid ticks affecting domestic animals in Bangladesh. *Trop Anim Health Prod* 38: 485-490.
8. Shimada Y, Beppu T, Inokuma H, Okuda M and Onishi T (2003) Ixodid tick species recovered from domestic dogs in Japan. *Med Vet Entomol* 17: 38-45.
9. Hoogstraal H, Roberts FH, Kohls GM and Tipton VJ (1968) Review of *Haemaphysalis (Kaiseriana) longicornis* Neumann (resurrected) of Australia, New Zealand, New Caledonia, Fiji, Japan, Korea, and northeastern China and USSR, and its parthogenetic and bisexual populations (Ixodoidea, Ixodidae). *J Parasitol* 54: 1197-1213.
10. Fujisaki K, Kawaju S and Kamio T (1994) The Taxonomy of the bovine *Theileria* spp. *Parasitol Today* 10: 31-33.
11. Ho T, Htwe KK, Yamasaki N, Zhang GQ, Ogawa M, Yamaguchi T, Fukushi H and Hirai K (1995) Isolation of *Coxiella burnetii* from dairy cattle and tick, and some characteristics of isolates in Japan. *Microbiol Immunol* 39: 663-671.

12. Hall-Mendelin S, Craig SB, Hall RA, O'Donoghue P, Atwell RB, Tulsiani SM and Graham GC (2011) Tick paralysis in Australia caused by *Ixodes holocyclus* Neumann. *Ann Trop Med Parasitol* 105: 95-106.
13. Diaz JH (2010) Tick paralysis in the United States. *J La State Med Soc* 162: 273-280.
14. Mans BJ, Gothe R and Neitz AWH (2004) Biochemical perspectives on paralysis and other forms of toxicoses caused by ticks. *Parasitology* 129: S95-S111.
15. Barré N and Uilenberg G (2010) Spread of parasites transported with their hosts: case study of two species of cattle tick. *Rev Sci Tech* 29: 149-160.
16. Aubry P and Geale DW (2011) A review of bovine anaplasmosis. *Transbound Emerg Dis* 58: 1-30.
17. Bhate C and Schwartz RA (2011) Lyme disease: Part I. Advances and perspectives. *J Am Acad Dermatol* 64: 619-636.
18. Florin-Christensen M and Schnittger L (2009) Piroplasmids and ticks: a long-lasting intimate relationship. *Front Biosci* 14: 3064-3073.
19. Barker SC and Murrell A (2008) Systemics and evolution of ticks with a list of valid genus and species. In: Ticks Biology, Disease and Control (eds. Bowman AS and Nuttall P). Cambridge University Press, UK. pp 1-39.
20. Anderson JF (2002) The natural history of ticks. *Med Clin North Am* 86: 205-218.
21. Murray TS and Shapiro ED (2010) Lyme disease. *Clin Lab Med* 30: 311-328.
22. Klompen H (2005) Ticks, the ixodida. In: Biology of Disease Vectors (ed. Marquardt WC). Elsevier Academic Press. London. pp 45-55.
23. Telford SR 3rd and Goethert HK (2004) Emerging tick-borne infections: rediscovered and better characterized, or truly 'new'? *Parasitology* 129: S301-327.
24. Cable RG and Leiby DA (2003) Risk and prevention of transfusion-transmitted babesiosis and other tick-borne diseases. *Curr Opin Hematol* 10: 405-411.
25. Sonenshine DE, Kocan KM and de la Fuente J (2006) Tick control: further thoughts on a research agenda. *Trends Parasitol* 22: 550-551.
26. Zaim M and Guillet P (2002) Alternative insecticides: an urgent need. *Trends Parasitol* 18: 161-163.
27. George JE, Pound JM and Davey RB (2004) Chemical control of ticks on cattle and the resistance of these parasites to acaricides. *Parasitology* 129: S353-S366.

28. Willadsen P (2006) Tick control: thoughts on a research agenda. *Vet Parasitol* 138: 161-168.
29. Willadsen P (2004) Anti-tick vaccines. *Parasitology* 129: S367-S387.
30. Dietrich M, Gómez-Díaz E and McCoy KD (2011) Worldwide distribution and diversity of seabird ticks: implications for the ecology and epidemiology of tick-borne pathogens. *Vector Borne Zoonotic Dis* 11: 453-470.
31. Dantas-Torres F, Giannelli A and Otranto D (2011) Starvation and overwinter do not affect the reproductive fitness of *Rhipicephalus sanguineus*. *Vet Parasitol* doi:10.1016/j.vetpar.2011.10.005.
32. Umemiya-Shirafuji R, Matsuo T, Liao M, Boldbaatar D, Battur B, Suzuki H and Fujisaki K (2010) Increased expression of ATG genes during nonfeeding periods in the tick *Haemaphysalis longicornis*. *Autophagy* 6: 4 473-481.
33. Randolph SE (2008) The impact of tick ecology on pathogen transmission dynamics. In: Ticks Biology, Disease and Control (eds. Bowman AS and Nuttall P). Cambridge University Press, UK. pp 40-72.
34. de la Fuente J, Manzano-Roman R, Naranjo V, Kocan KM, Zivkovic Z, Blouin EF, Canales M, Almazán C, Galindo RC, Step DL and Villar M (2010) Identification of protective antigens by RNA interference for control of the lone star tick, *Amblyomma americanum. Vaccine* 28: 1786-1795.
35. Brossard M and Wikel SK (2008) Tick immunobiology. In: Ticks Biology, Disease and Control (eds. Bowman AS and Nuttall P). Cambridge University Press, UK. pp 186-204.
36. Labuda M, Trimnell AR, Licková M, Kazimírová M, Davies GM, Lissina O, Hails RS and Nuttall PA (2006) An antivector vaccine protects against a lethal vector-borne pathogen. *PLoS Pathog* 2: e27.
37. de la Fuente J and Kocan KM (2003) Advances in the identification and characterization of protective antigens for recombinant vaccines against tick infestations. *Expert Rev Vaccines* 2: 583-593.
38. Rand KN, Moore T, Sriskantha A, Spring K, Tellam R, Willadsen P and Cobon GS (1989) Cloning and expression of a protective antigen from the cattle tick *Boophilus microplus*. *Proc Natl Acad Sci USA* 86: 9657-9661.

39. Nuttall PA, Trimnell AR, Kazimirova M and Labuda M (2006) Exposed and concealed antigens as vaccine targets for controlling ticks and tick-borne diseases. *Parasite Immunol* 28: 155-163.

40. Canales M, Almazán C, Naranjo V, Jongejan F and de la Fuente J (2009) Vaccination with recombinant *Boophilus annulatus* Bm86 ortholog protein, Ba86, protects cattle against *B. annulatus* and *B. microplus* infestations. *BMC Biotechnol* 9: 29-37.

41. Odongo D, Kamau L, Skilton R, Mwaura S, Nitsch C, Musoke A, Taracha E, Daubenberger C and Bishop R (2007) Vaccination of cattle with TickGARD induces cross-reactive antibodies binding to conserved linear peptides of Bm86 homologues in *Boophilus decoloratus*. *Vaccine* 25: 1287-1296.

42. Schuijt TJ, Hovius JW, van der Poll T, van Dam AP and Fikrig E (2011) Lyme borreliosis ccination: the facts, the challenge, the future. *Trends Parasitol* 27: 40-47.

43. Hajdusek O, Sojka D, Kopacek P, Buresova V, Franta Z, Sauman I, Winzerling J and Grubhoffer L (2009) Knockdown of proteins involved in iron metabolism limits tick reproduction and development. *Proc Natl Acad Sci USA* 106: 1033-1038.

44. Sonenshine DE (1991) Biology of Ticks. Vol 1: Oxford University Press, USA.

45. Kemp DH, Stone BF and Binnington KC (1982) Tick attachment and feeding: role of the mouthparts, feeding apparatus, salivary gland secretions, and the host response. In: Physiology of Ticks (eds. Obenchain FD and Galun R). Pergamon Press Inc., New York. pp 119-168.

46. Stark KR and James AA (1996) Anticoagulant in vector arthropods. *Parasitol Today* 12: 430-437.

47. Hovius JW, Levi M and Fikrig E (2008) Salivating for knowledge: potential pharmacological agents in tick saliva. *PLoS Med* 5: e43.

48. Cappello M, Li S, Chen X, Li CB, Harrison L, Narashimhan S, Beard CB and Aksoy S (1998) Tsetse thrombin inhibitor: blood meal-induced expression of an anticoagulant in salivary glands and gut tissue of *Glossina morsitans morsitans. Proc Natl Acad Sci USA* 95: 14290-14295.

49. Yoshida S, Sudo T, Niimi M, Tao L, Sun B, Kambayashi J, Watanabe H, Luo E and Matsuoka H (2008) Inhibition of collagen-induced platelet aggregation by anopheline antiplatelet protein, a saliva protein from a malaria vector mosquito. *Blood* 111: 2007-2014.

50. Abebe M, Cupp MS, Ramberg FB and Cupp EW (1994) Anticoagulant activity in salivary gland extracts of black flies (Diptera: Simuliidae). *J Med Entomol* 31: 908-911.
51. Friedrich T, Kröger B, Bialojan S, Lemaire HG, Höffken HW, Reuschenbach P, Otte M and Dodt J (1993) A Kazal-type inhibitor with thrombin specificity from *Rhodnius prolixus*. *J Biol Chem* 268: 16216-16222.
52. Salzet M, Chopin V, Baert J, Matias I and Malecha J (2000) Theromin, a novel leech thrombin inhibitor. *J Biol Chem* 275: 30774-30780.
53. Gardell SJ, Duong LT, Diehl RE, York JD, Hare TR, Register RB, Jacobs JW, Dixon RA and Friedman PA (1989) Isolation, characterization, and cDNA cloning of a vampire bat salivary plasminogen activator. *J Biol Chem* 264: 17947-17952.
54. Maritz-Olivier C, Stutzer C, Jongejan F, Neitz AW and Gaspar AR (2007) Tick anti-hemostatics: targets for future vaccines and therapeutics. *Trends Parasitol* 23: 397-407.
55. Koh CY, Kazimirova M, Trimnell A, Takac P, Labuda M, Nuttall PA and Kini RM (2007) Variengin, a novel fast and tight binding thrombin inhibitor from the tropical bont tick. *J Biol Chem* 282: 29101-29113.
56. Narasimhan S, Montgomery RR, DePonte K, Tschudi C, Marcantonio N, Anderson JF, Sauer JR, Cappello M, Kantor FS and Fikrig E (2004) Disruption of *Ixodes scapularis* anticoagulation by using RNA interference. *Proc Natl Acad Sci USA* 101: 1141-1146.
57. Waxman L, Smith DE, Arcuri KE and Vlasuk GP (1990) Tick anticoagulant peptide (TAP) is a novel inhibitor of blood coagulation factor Xa. *Science* 248: 593-596.
58. Ramakrishnan VG, Aljamali MN, Sauer JR and Essenberg RC (2005) Application of RNA interference in tick salivary gland research. *J Biomol Tech* 16: 297-305.
59. Wolfe MS and Kopan R (2004) Intramembrane proteolysis: theme and variations. *Science* 305: 1119-1123.
60. Ekici OD, Paetzel M and Dalbey RE (2008) Unconventional serine proteases: variations on the catalytic Ser/His/Asp triad configuration. *Protein Sci* 17: 2023-2037.
61. Carter P and Wells JA (1988) Dissecting the catalytic triad of a serine protease. *Nature* 332: 564-568.
62. Quattrocchi CC, Wannenes F, Persico AM, Ciafré SA, D'Arcangelo G, Farace MG and Keller F (2002) Reelin is a serine protease of the extracellular matrix. *J Biol Chem* 277: 303-309.

63. Tsigelny I, Shindyalov IN, Bourne PE, Südhof TC and Taylor P (2000) Common EF-hand motifs in cholinesterases and neuroligins suggest a role for Ca^{2+}-binding in cell surface associations. *Protein Sci* 9: 180-185.

64. Tallant C, Marrero A and Gomis-Rüth FX (2010) Matrix metalloproteinases: fold and function of their catalytic domains. *Biochim Biophys Acta* 1803: 20-28.

65. Sipley JD, Alexander DS, Testa JE and Quigley JP (1997) Introduction of an RRHR motif into chicken urokinase-type plasminogen activator (ch-uPA) confers sensitivity to plasminogen activator inhibitor (PAI)-1 and PAI-2 and allows ch-uPA-mediated extracellular matrix degradation to be controlled by PAI-1. *Proc Natl Acad Sci USA* 94: 2933-2938.

66. Madison EL, Goldsmith EJ, Gerard RD, Gething MJ and Sambrook JF (1989) Serpin-resistant mutants of human tissue-type plasminogen activator. *Nature* 339: 721-724.

67. Kretsinger RH and Nockolds CE (1973) Carp muscle calcium-binding protein. II. Structure determination and general description. *J Biol Chem* 248: 3313-3326.

68. Grabarek Z (2006) Structural basis for diversity of the EF-hand calcium-binding proteins. *J Mol Biol* 359: 509-525.

69. Reddy VS, Day IS, Thomas T and Reddy AS (2004) KIC, a novel Ca^{2+}-binding protein with one EF-hand motif, interacts with a microtubule motor protein and regulates trichome morphogenesis. *Plant Cell* 16: 185-200.

70. Leclerc E and Heizmann CW (2011) The importance of Ca^{2+}/Zn^{2+} signaling S100 proteins and RAGE in translational medicine. *Front Biosci* S3 3: 1232-1262.

71. Krebs J and Heizmann CW (2007) Calcium-binding proteins and the EF-hand principle. In: Calcium: a Matter of Life or Death (eds. Krebs J and Michalak M), first edition, Vol 41, Elsevier, UK. pp 51-93.

72. Lewit-Bentley A and Réty S (2000) EF-hand calcium-binding proteins. *Curr Opin Struct Biol* 10: 637-643.

73. Ikura M and Ames JB (2006) Genetic polymorphism and protein conformational plasticity in the calmodulin superfamily: two ways to promote multifunctionality. *Proc Natl Acad Sci USA* 103: 1159-1164.

74. Pottgiesser J, Maurer P, Mayer U, Nischt R, Mann K, Timpl R, Krieg T and Engel J (1994) Changes in calcium and collagen IV binding caused by mutations in the EF-hand and other

domains of extracellular matrix protein BM-40 (SPARC, osteonectin). *J Mol Biol* 238: 563-574.

75. Kahl CR and Means AR (2003) Regulation of cell cycle progression by calcium/calmodulin-dependent pathways. *Endocr Rev* 24: 719-736.
76. Berridge MJ, Bootman MD and Lipp P (1998) Calcium-a life and death signal. *Nature* 395: 645-648.
77. Alim MA, Tsuji N, Miyoshi T, Islam MK, Huang X, Motobu M and Fujusaki K (2007) Characterization of asparaginyl endopeptidase, legumain induced by blood-feeding in the ixodid tick *Haemaphysalis longicornis*. *Insect Biochem Mol Biol* 37: 911-922.
78. Boldbaatar D, Sikasunge CS, Battsetseg B, Xuan X and Fujisaki K (2006) Molecular cloning and functional characterization of an aspartic protease from the hard tick *Haemaphysalis longicornis*. *Insect Biochem Mol Biol* 36: 25-36.
79. Altschul SF, Madden TL, Schaffer AA, Zhang J, Zhang Z, Miller W and Lipman DJ (1997) Gapped BLAST and PSI-BLAST: a new generation of protein database search programs. *Nucleic Acid Res* 25: 3389-3402.
80. Benson DA, Karsch-Mizrachi I, Lipman DJ, Ostell J, Rapp BA and Wheeler DL (2002) GenBank. *Nucleic Acid Res* 30: 17-20.
81. Nielsen H, Engelbrecht J, Brunak S and Heijne G (1997) Identification of prokaryotic and eukaryotic signal peptides and prediction of their cleavage site. *Protein Eng Des Sel* 10: 1-6.
82. Wilkins MR, Lindskog I, Gasteiger E, Bairoch A, Sanchez JC, Hochstrasser DF and Appel RD (1997) Detail peptide characterization using PEPTIDE MASS-a World Wide Web accessible tool. *Electrophoresis* 18: 403-408.
83. Tsuji N, Kamio T, Isobe T and Fujisaki K (2001) Molecular characterization of a peroxiredoxin from the hard tick *Haemaphysalis longicornis. Insect Mol Biol* 10: 121-129.
84. Furuse M, Fujita K, Hiiragi T, Fujimoto K and Tsukita S (1998) Claudin-1 and -2: novel integral membrane proteins localizing at tight junctions with no sequence similarity to occludin. *J Cell Biol* 141: 1539-1550.
85. You M, Xuan X, Tsuji N, Kamio T, Igarashi I, Nagasawa H, Mikami T and Fujisaki K (2001) Molecular characterization of a troponin I-like protein from the hard tick *Haemaphysalis longicornis*. *Insect Biochem Mol Biol* 32: 67-73.

86. Miyoshi T, Tsuji N, Islam MK, Huang X, Motobu M, Alim MA and Fujisaki K (2007) Molecular and reverse genetic characterization of serine proteinase-induced hemolysis in the midgut of the ixodid tick *Haemaphysalis longicornis*. *J Insect Physiol* 53: 195-203.
87. Islam MK, Tsuji N, Miyoshi T, Alim MA, Huang X, Hatta T and Fujisaki K (2009) The Kunitz-like modulatory protein haemangin is vital for hard tick blood-feeding success. *PLoS Pathog* 5: e1000497.
88. Gariépy J and Hodges RS (1983) Primary sequence analysis and folding behavior of EF-hands in relation to the mechanism of action of troponon C and calmodulin. *FEBS Lett* 160: 1-6.
89. Zhang D, Cupp MS and Cupp EW (2002) Thrombostasin: purification, molecular cloning and expression of a novel anti-thrombin protein from horn fly saliva. *Insect Biochem Mol Biol* 32: 321-330.
90. Klee CB, Crouch TH and Krinks MH (1979) Calcineurin: a calcium- and calmodulin-binding protein of the nervous system. *Proc Natl Acad Sci USA* 76: 6270-6273.
91. Charuk JH, Pirraglia CA and Reithmeier RA (1990) Interaction of ruthenium red with Ca^{2+}-binding proteins. *Anal Biochem* 188: 123-131.
92. Francischetti IM, Mather TN and Ribeiro JM (2005) Tick saliva is a potent inhibitor of endothelial cell proliferation and angiogenesis. *Thromb Haemost* 94: 167-174.
93. Anderson JM and Valenzuela JG (2008) Tick saliva: from pharmacology and biochemistry to transcriptome analysis and functional genomics. In: Ticks Biology, Disease and Control (eds. Bowman AS and Nuttall P). Cambridge University Press, UK. pp 92-107.
94. Watterson DM, Sharief F and Vanaman TC (1980) The complete amino acid sequence of the Ca^{2+}-dependent modulator protein (calmodulin) of bovine brain. *J Biol Chem* 255: 962-975.
95. Yazawa M, Yagi K, Toda H, Kondo K, Narita K, Yamazaki R, Sobue K, Kakiuchi S, Nagao S and Nozawa Y (1981) The amino acid sequence of the *Tetrahymena* calmodulin which specifically interacts with guanylate cyclase. *Biochem Biophys Res Commun* 99: 1051-1057.
96. van Eerd JP and Takahashi K (1975) The amino acid sequence of bovine cardiac tamponin-C. Comparison with rabbit skeletal troponin-C. *Biochem Biophys Res Commun* 64: 122-127.

97. Skelton NJ, Kördel J, Akke M, Forsén S and Chazin WJ (1994) Signal transduction versus buffering activity in Ca^{2+}-binding proteins. *Nat Struct Biol* 1: 239-245.

98. Nuttall PA (1998) Displaced tick-parasite interactions at the host interface. *Parasitology* 116: 65-72.

99. Binnington KC and Kemp DH (1980) Role of tick salivary glands in feeding and disease transmission. *Adv Parasitol* 18: 315-339.

100. Guy JE, Wigren E, Svärd M, Härd T and Lindqvist Y (2008) New insights into multiple coagulation factor deficiency from the solution structure of human MCFD2. *J Mol Biol* 381: 941-955.

101. Ribeiro C, Togawa RC, Neshich IA, Mazoni I, Mancini AL, Minardi RC, da Silveira CH, Jardine JG, Santoro MM and Neshich G (2010) Analysis of binding properties and specificity through identification of the interface forming residues (IFR) for serine proteases in silico docked to different inhibitors. *BMC Struct Biol* 10: 36-48.

102. Perona JJ and Craik CS (1995) Structural basis of substrate specificity in the serine proteases. *Protein Sci* 4: 337-360.

103. Murray V, Norrving B, Sandercock PA, Terént A, Wardlaw JM and Wester P (2010) The molecular basis of thrombolysis and its clinical application in stroke. *J Intern Med* 267: 191-208.

104. Cesarman-Maus G and Hajjar KA (2005) Molecular mechanisms of fibrinolysis. *Br J Haematol* 129: 307-321.

105. Polgár L (2005) The catalytic triad of serine peptidases. *Cell Mol Life Sci* 62: 2161-2172.

106. Liu Y and Patricelli MP and Cravatt BF (1999) Activity-based protein profiling: the serine hydrolases. *Proc Natl Acad Sci USA* 96: 14694-14699.

107. Blow DM, Birktoft JJ and Hartley BS (1969) Role of a buried acid group in the mechanism of action of chymotrypsin. *Nature* 221: 337-340.

108. Wlodawer A, Li M, Dauter Z, Gustchina A, Uchida K, Oyama H, Dunn BM and Oda K (2001) Carboxyl proteinase from *Pseudomonas* defines a novel family of subtilisin-like enzymes. *Nat Struc Biol* 8: 442-446.

109. Håkansson K, Wang AH and Miller CG (2000) The structure of aspartyl dipeptidase reveals a unique fold with a Ser-His-Glu catalytic triad. *Proc Natl Acad Sci USA* 97: 14097-14102.

110. Qiu X, Culp JS, DiLella AG, Hellmig B, Hoog SS, Janson CA, Smith WW and Abdel-Meguid SS (1996) Unique fold and active site in cytomegalovirus protease. *Nature* 383: 275-279.

111. Shieh HS, Kurumbail RG, Stevens AM, Stegeman RA, Sturman EJ, Pak JY, Wittwer AJ, Palmier MO, Wiegand RC, Holwerda BC and Stallings WC (1996) Three-dimensional structure of human cytomegalovirus protease. *Nature* 383: 279-282.

112. Tong L, Qian C, Massariol MJ, Bonneau PR, Cordingley MG and Lagacé L (1996) A new serine-protease fold revealed by the crystal structure of human cytomegalovirus protease. *Nature* 383: 272-275.

113. Seemüller E, Lupas A, Stock D, Löwe J, Huber R and Baumeister W (1995) Proteasome from *Thermoplasma acidophilum*: a threonine protease. *Science* 268: 579-582.

114. Duggleby HJ, Tolley SP, Hill CP, Dodson EJ, Dodson G and Moody PC (1995) Penicillin acylase has a single-amino-acid catalytic centre. *Nature* 373: 264-268.

115. Fibla J, Atrian S and Gonzàlez-Duarte R (1993) Evidence of serine-protease activity closely associated with *Drosophila* alcohol dehydrogenase. *Eur J Biochem* 211: 357-365.

116. Tsuji N, Miyoshi T, Battsetseg B, Matsuo T, Xuan X and Fujisaki K (2008) A cysteine protease is critical for *Babesia* spp. transmission in *Haemaphysalis* ticks. *PLoS Pathog* 4: e1000062.

117. Islam MK, Miyoshi T, Kasuga-Aoki H, Isobe T, Arakawa T, Matsumoto Y and Tsuji N (2003) Inorganic pyrophosphatase in the roundworm *Ascaris* and its role in the development and molting process of the larval stage parasites. *Eur J Biochem* 270: 2814-2826.

118. Borgoño CA, Michael IP and Shaw JL (2007) Expression and functional characterization of the cancer-related serine protease, human tissue kallikrein 14. *J Biol Chem* 282: 2405-2422.

119. Spraggon G, Hornsby M, Shipway A, Tully DC, Bursulaya B, Danahay H, Harris JL and Lesley SA (2009) Active site conformational changes of prostasin provide a new mechanism of protease regulation by divalent cations. *Protein Sci* 18: 1081-1094.

120. Lövgren J, Airas K and Lilja H (1999) Enzymatic action of human glandular kallikrein 2 (hK2). Substrate specificity and regulation by Zn^{2+} and extracellular protease inhibitors. *Eur J Biochem* 262: 781-789.

121. Neyman M, Gewirtz J and Poncz M (2008) Analysis of the spatial and temporal characteristics of platelet-delivered factor VIII-based clots. *Blood* 112: 1101-1108.

122. Riddel JP Jr, Aouizerat BE, Miaskowski C and Lillicrap DP (2007) Theories of blood coagulation. *J Pediatr Oncol Nurs* 24: 123-131.

123. Byzova TV and Plow EF (1997) Networking in the hemostatic system, integrin $\alpha_{IIb}\beta_3$ binds prothrobin and influences its activation. *J Biol Chem* 272: 27183-27188.

124. Davie EW and Ratnoff OD (1964) Waterfall sequence for intrinsic blood clotting. *Science* 145: 1310-1312.

125. Collen D and Lijnen HR (2004) Tissue-type plasminogen activator: a historical perspective and personal account. *J Thromb Haemost* 2: 541-546.

126. Imura Y, Stassen JM, Kurokawa T, Iwasa S, Lijnen HR and Collen D (1992) Thrombolytic and pharmacokinetic properties of an immunoconjugate of single-chain urokinase-type plasminogen activator (u-PA) and a bispecific monoclonal antibody against fibrin and against u-PA in baboons. *Blood* 79: 2322-2329.

127. Li XK, Lijnen HR, Nelles L, Van Hoef B, Stassen JM and Collen D (1992) Biochemical and biologic properties of rt-PA del (K296-G302), a recombinant human tissue-type plasminogen activator deletion mutant resistant to plasminogen activator inhibitor-1. *Blood* 79: 417-429.

128. Siddiqi F, Odrljin TM, Fay PJ, Cox C and Francis CW (1998) Binding of tissue-plasminogen activator to fibrin: effect of ultrasound. *Blood* 91: 2019-2025.

129. Zamarron C, Lijnen HR and Collen D (1984) Kinetics of the activation of plasminogen by natural and recombinant tissue-type plasminogen activator. *J Biol Chem* 259: 2080-2083.

130. Hoylaerts M, Rijken DC, Lijnen HR and Collen D (1982) Kinetics of the activation of plasminogen by human tissue plasminogen activator. Role of fibrin. *J Biol Chem* 257: 2912-2919.

131. Wiman B (2000) The fibrinolytic enzyme system. Basic principles and links to venous and arterial thrombosis. *Hematol Oncol Clin North Am* 14: 325-338.

132. Tate KM, Higgins DL, Holmes WE, Winkler ME, Heyneker HL and Vehar GA (1987) Functional role of proteolytic cleavage at arginine-275 of human tissue plasminogen activator as assessed by site-directed mutagenesis. *Biochemistry* 26: 338-343.

133. Monteiro RQ, Rezaie AR, Ribeiro JM and Francischetti IM (2005) Ixolaris: a factor Xa heparin-binding exosite inhibitor. *J Biochem* 387: 871-877.

134. Ramamoorthi N, Narasimhan S, Pal U, Bao F, Yang XF, Fish D, Anguita J, Norgard MV, Kantor FS, Anderson JF, Koski RA and Fikrig E (2005) The Lyme disease agent exploits a tick protein to infect the mammalian host. *Nature* 436: 573-577.

135. van de Locht A, Stubbs MT, Bode W, Friedrich T, Bollschweiler C, Höffken W and Huber R (1996) The ornithodorin-thrombin crystal structure, a key to the TAP enigma? *EMBO J* 15: 6011-6017.

136. Francischetti IM, Mather TN and Ribeiro JM (2003) Cloning of a salivary gland metalloprotease and characterization of gelatinase and fibrin(ogen)lytic activities in the saliva of the Lyme disease tick vector *Ixodes scapularis*. *Biochem Biophys Res Commun* 305: 869-875.

137. Matsui T, Sakurai Y, Fujimura Y, Hayashi I, Oh-Ishi S, Suzuki M , Hamako J, Yamamoto Y, Yamazaki J, Kinoshita M and Titani K (1998) Purification and amino acid sequence of halystase from snake venom of *Agkistrodon halys blomhoffii*, a serine protease that cleaves specifically fibrinogen and kininogen. *Eur J Biochem* 252: 569-575.

138. da Silveira RB, dos Santos Filho JF, Mangili OC, Veiga SS, Gremski W, Nader HB and von Dietrich CP (2002) Identification of proteases in the extract of venom glands from brown spiders. *Toxicon* 40: 815-822.

139. Furie B and Furie BC (2005) Thrombus formation *in vivo*. *J Clin Invest* 115: 3355-3362.

140. MacFarlane RG (1964) An enzyme cascade in the blood clotting mechanism, and its function as a biochemical amplifier. *Nature* 202: 498-499.

141. Nesheim M (2003) Thrombin and fibrinolysis. *Chest* 124: 33-39.

142. Zhang Y, Wisner A, Xiong Y and Bon C (1995) A novel plasminogen activator from snake venom. Purification, characterization, and molecular cloning. *J Biol Chem* 270: 10246-10255.

143. Liberatore GT, Samson A, Bladin C, Schleuning WD and Medcalf RL (2003) Vampire bat salivary plasminogen activator (desmoteplase): a unique fibrinolytic enzyme that does not promote neurodegeneration. *Stroke* 34: 537-543.

144. Tellgren-Roth A, Dittmar K, Massey SE, Kemi C, Tellgren-Roth C, Savolainen P, Lyons LA and Liberles DA (2009) Keeping the blood flowing-plasminogen activator genes and

feeding behavior in vampire bats. *Naturwissenschaften* 96: 39-47.

145. Galati G, Gentilucci UV, Mazzarelli C, Gallo P, Grasso RF, Stellato L, Afeltra A and Picardi A (2011) Deep vein thrombosis, inferior vena cava interruption and multiple thrombophilic gene mutations. *Am J Med Sci* 342: 79-82.
146. Heidenreich PA, Trogdon JG, Khavjou OA, Butler J, Dracup K, Ezekowitz MD, Finkelstein EA, Hong Y, Johnston SC, Khera A, Lloyd-Jones DM, Nelson SA, Nichol G, Orenstein D, Wilson PW and Woo YJ (2011) Forecasting the future of cardiovascular disease in the United States: a policy statement from the American Heart Association. *Circulation* 123: 933-944.
147. Molinari AC, Saracco P, Cecinati V, Miano M, Parodi E, Grassi M, Banov L, De Mattia D and Giordano P (2011) Venous thrombosis in children: an emerging issue. *Blood Coagul Fibrinolysis* 22: 351-361.
148. Roger VL, Go AS, Lloyd-Jones DM, Adams RJ, Berry JD, Brown TM, Carnethon MR, Dai S, de Simone G, Ford ES, Fox CS, Fullerton HJ, Gillespie C, Greenlund KJ, Hailpern SM, Heit JA, Ho PM, Howard VJ, Kissela BM, Kittner SJ, Lackland DT, Lichtman JH, Lisabeth LD, Makuc DM, Marcus GM, Marelli A, Matchar DB, McDermott MM, Meigs JB, Moy CS, Mozaffarian D, Mussolino ME, Nichol G, Paynter NP, Rosamond WD, Sorlie PD, Stafford RS, Turan TN, Turner MB, Wong ND and Wylie-Rosett J (2011) Heart disease and stroke statistics-2011 update: a report from the American Heart Association. *Circulation* 123: e18-e209.
149. Baldwin K, Orr S, Briand M, Piazza C, Veydt A and McCoy S (2010) Acute ischemic stroke update. *Pharmacotherapy* 30: 493-514.
150. Houston MC (2010) The role of cellular micronutrient analysis, nutraceuticals, vitamins, antioxidants and minerals in the prevention and treatment of hypertension and cardiovascular disease. *Ther Adv Cardiovasc Dis* 4: 165-183.
151. Vanhecke TE, Miller WM, Franklin BA, Weber JE and McCullough PA (2006) Awareness, knowledge, and perception of heart disease among adolescents. *Eur J Cardiovasc Prev Rehabil* 13: 718-723.
152. Szemraj J, Walkowiak B, Kawecka I, Janiszewska G, Buczko W, Bartkowiak J and Chabielska E (2005) A new recombinant thrombolytic and antithrombotic agent with

higher fibrin affinity-a staphylokinase variant. I. *In vitro* study. *J Thromb Haemost* 3: 2156-2165.

153. Killer M, Ladurner G, Kunz AB and Kraus J (2010) Current endovascular treatment of acute stroke and future aspects. *Drug Discov Today* 15: 640-647.
154. Rijken DC and Lijnen HR (2009) New insights into the molecular mechanisms of the fibrinolytic system. *J Thromb Haemost* 7: 4-13.
155. Balsara RD and Ploplis VA (2008) Plasminogen activator inhibitor-1: the double-edged sword in apoptosis. *Thromb Haemost* 100: 1029-1036.
156. Zhu Y, Carmeliet P and Fay WP (1999) Plasminogen activator inhibitor-1 is a major determinant of arterial thrombolysis resistance. *Circulation* 99: 3050-3055.
157. Declerck PJ, Gils A and De Taeye B (2011) Use of mouse models to study plasminogen activator inhibitor-1. *Methods Enzymol* 499: 77-104.
158. Dellas C and Loskutoff DJ (2005) Historical analysis of PAI-1 from its discovery to its potential role in cell motility and disease. *Thromb Haemost* 93: 631-640.
159. Binder BR, Christ G, Gruber F, Grubic N, Hufnagl P, Krebs M, Mihaly J and Prager GW (2002) Plasminogen activator inhibitor-1: physiological and pathophysiological roles. *News Physiol Sci* 17: 56-61.
160. Deng G, Curriden SA, Wang S, Rosenberg S and Loskutoff DJ (1996) Is plasminogen activator inhibitor-1 the molecular switch that governs urokinase receptor-mediated cell adhesion and release? *J Cell Biol* 134: 1563-1571.
161. Gelehrter TD and Sznycer-Laszuk R (1986) Thrombin induction of plasminogen activator-inhibitor in cultured human endothelial cells. *J Clin Invest* 77: 165-169.
162. Krishnamurti C, Keyt B, Maglasang P and Alving BM (1996) PAI-1-resistant t-PA: low doses prevent fibrin deposition in rabbits with increased PAI-1 activity. *Blood* 87: 14-19.
163. Kruithof EK (2008) Regulation of plasminogen activator inhibitor type 1 gene expression by inflammatory mediators and statins. *Thromb Haemost* 100: 969-975.
164. Bouchard L, Vohl MC, Lebel S, Hould FS, Marceau P, Bergeron J, Pérusse L and Mauriège P (2010) Contribution of genetic and metabolic syndrome to omental adipose tissue PAI-1 gene mRNA and plasma levels in obesity. *Obes Surg* 20: 492-499.

165. Shohet RV, Spitzer S, Madison EL, Bassel-Duby R, Gething MJ and Sambrook JF (1994) Inhibitor-resistant tissue-type plasminogen activator: an improved thrombolytic agent in vitro. *Thromb Haemost* 71: 124-128.

166. Konkle BA, Schuster SJ, Kelly MD, Harjes K, Hassett DE, Bohrer M and Tavassoli M (1992) Plasminogen activator inhibitor-1 messenger RNA expression is induced in rat hepatocytes in vivo by dexamethasone. *Blood* 79: 2636-2642.

167. Reilly CF and Hutzelmann JE (1992) Plasminogen activator inhibitor-1 binds to fibrin and inhibits tissue-type plasminogen activator-mediated fibrin dissolution. *J Biol Chem* 267: 17128-17135.

168. Robbie LA, Bennett B, Keyt BA and Booth NA (2000) Effective lysis of model thrombi by a t-PA mutant (A473S) that is resistant to alpha2-antiplasmin. *Br J Haematol* 111: 517-523.

169. Erickson LA, Ginsberg MH and Loskutoff DJ (1984) Detection and partial characterization of an inhibitor of plasminogen activator in human platelets. *J Clin Invest* 74: 1465-1472.

170. Mimuro J, Schleef RR and Loskutoff DJ (1987) Extracellular matrix of cultured bovine aortic endothelial cells contains functionally active type 1 plasminogen activator inhibitor. *Blood* 70: 721-728.

171. Levin EG (1983) Latent tissue plasminogen activator produced by human endothelial cells in culture: evidence for an enzyme-inhibitor complex. *Proc Natl Acad Sci USA* 80: 6804-6808.

172. Metha R and Shapiro AD (2008) Plasminogen activator inhibitor type 1 deficiency. *Haemophilia* 14: 1255-1260.

173. Higazi AA, Ajawi F, Akkawi S, Hess E, Kuo A and Cines DB (2005) Regulation of the single-chain urokinase-urokinase receptor complex activity by plasminogen and fibrin: novel mechanism of fibrin specificity. *Blood* 105: 1021-1028.

174. Brogren H, Karlsson L, Andersson M, Wang L, Erlinge D and Jern S (2004) Platelets synthesize large amounts of active plasminogen activator inhibitor-1. *Blood* 104: 3943-3948.

175. Cilia La Corte AL, Philippou H and Ariëns RA (2011) Role of fibrin structure in thrombosis and vascular disease. *Adv Protein Chem Strucl Biol* 83: 75-127.

176. Braaten JV, Handt S, Jerome WG, Kirkpatrick J, Lewis JC and Hantgan RR (1993) Regulation of fibrinolysis by platelet-released plasminogen activator inhibitor-1: light

scattering and ultrastructural examination of lysis of a model platelet-fibrin thrombus. *Blood* 81: 1290-1299.

177. Christensen U, Bangert K and Thorsen S (1996) Reaction of human alpha2-antiplasmin and plasmin stopped-flow fluorescence kinetics. *FEBS Lett* 387: 58-62.
178. Mulichak AM, Tulinsky A and Ravichandran KG (1991) Crystal and molecular structure of human plasminogen kringle 4 refined at 1.9-A resolution. *Biochemistry* 30: 10576-10588.
179. Hortin GL, Gibson BL and Fok KF (1988) Alpha 2-antiplasmin's carboxy-terminal lysine residue is a major site of interaction with plasmin. *Biochem Biophys Res Commun* 155: 591-596.
180. Le Bonniec BF, Guinto ER and Stone SR (1995) Identification of thrombin residues that modulate its interactions with antithrombin III and alpha 1-antitrypsin. *Biochemistry* 34: 12241-12248.
181. Bowman AS and Sauer JR (2004) Tick salivary glands: function, physiology and future. *Parasitology* 129: S67-S81.
182. Sauer JR, McSwain JL, Bowman AS and Essenberg RC (1995) Tick salivary gland physiology. *Annu Rev Entomol* 40: 245-267.
183. Fire A, Xu S, Montgomery MK, Kostas SA, Driver SE and Mello CC (1998) Potent and specific genetic interference by double-stranded RNA in *Caenorhabditis elegans*. *Nature* 391: 806-811.
184. Cogoni C and Macino G (2000) Post-transcriptional gene silencing across kingdoms. *Curr Opin Genet Dev* 10: 638-643.
185. Nakano H, Amemiya S, Shiokawa K and Taira M (2000) RNA interference for the organizer-specific gene Xlim-1 in *Xenopus* embryos. *Biochem Biophys Res Commun* 274: 434-439.
186. Kennerdell JR and Carthew RW (1998) Use of dsRNA-mediated genetic interference to demonstrate that frizzled and frizzled 2 act in the wingless pathway. *Cell* 95: 1017-1026.
187. Timmons L and Fire A (1998) Specific interference by ingested dsRNA. *Nature* 395: 854.
188. Schmid A, Schindelholz B and Zinn K (2002) Combinatorial RNAi: a method for evaluating the functions of gene families in *Drosophila*. *Trends Neurosci* 25: 71-74.
189. Aljamali MN, Sauer JR and Essenberg RC (2002) RNA interference: applicability in tick research. *Exp Appl Acarol* 28: 89-96.

190. Miyoshi T, Tsuji N, Islam MK, Kamio T and Fujisaki K (2004) Gene silencing of a cubilin-related serine proteinase from the hard tick *Haemaphysalis longicornis* by RNA interference. *J Vet Med Sci* 66: 1471-1473.

191. Alim MA, Tsuji N, Miyoshi T, Islam MK, Hatta T and Fujisaki K (2009) Legumains from the hard tick *Haemaphysalis longicornis* play modulatory roles in blood-feeding and gut cellular remodelling and impact on embryogenesis. *Int J Parasitol* 39: 97-107.

192. de la Fuente J, Almazán C, Blouin EF, Naranjo V and Kocan KM (2005) RNA interference screening in ticks for identification of protective antigens. *Parasitol Res* 96: 137-141.

193. Karim S, Ramakrishnan VG, Tucker JS, Essenberg RC and Sauer JR (2004) *Amblyomma americanum* salivary glands: double-stranded RNA-mediated gene silencing of synaptobrevin homologue and inhibition of PGE2 stimulated protein secretion. *Insect Biochem Mol Biol* 34: 407-413.

194. Chino D, Fujita Y, Ishii K and Nakayama K (2003) Effects of DX-9065a, an inhibitor of factor Xa, on ellagic acid-induced plantar skin thrombosis assessed in tetrodotoxin- and N(omega)-nitro-L-arginine-treated rats. *J Pharmacol Sci* 91: 319-329.

195. Decrem Y, Rath G, Blasioli V, Cauchie P, Robert S, Beaufays J, Frère JM, Feron O, Dogné JM, Dessy C, Vanhamme L and Godfroid E (2009) Ir-CPI, a coagulation contact phase inhibitor from the tick *Ixodes ricinus*, inhibits thrombus formation without impairing hemostasis. *J Exp Med* 206: 2381-2395.

196. Šimo L, Koči J, Žitňan D and Park Y (2011) Evidence for D1 dopamine receptor activation by a paracrine signal of dopamine in tick salivary glands. *PLoS One* 6: e16158.

197. Francischetti IM, Sa-Nunes A, Mans BJ, Santos IM and Ribeiro JM (2009) The role of saliva in tick feeding. *Front Biosci* 14: 2051-2088.

198. Anderson JF and Magnarelli LA (2008) Biology of ticks. *Infect Dis Clin North Am* 22: 195-215.

199. Kopáček P, Hajdušek O, Burešová V and Daffre S (2011) Tick innate immunity. *Adv Exp Med Biol* 708: 137-136.

200. Mathiasen L, Dupont DM, Christensen A, Blouse GE, Jensen JK, Gils A, Declerck PJ, Wind T and Andreasen PA (2008) A peptide accelerating the conversion of plasminogen activator inhibitor-1 to an inactive latent state. *Mol Pharmacol* 74: 641-653.

201. Nijhof AM, Taoufik A, de la Fuente J, Kocan KM, de Vries E and Jongejan F (2007) Gene silencing of the tick protective antigens, *Bm86*, *Bm91* and *subolesin*, in the one-host tick *Boophilus microplus* by RNA interference. *Int J Parasitol* 37: 653-662.